SYNTHESIS AND CHARACTERIZATION OF VITRIMERIC MATERIALS: IMPACT OF NANOFILLER ON SELF-HEALING AND THERMOMECHANICAL PROPERTIES

A thesis submitted to the
University of Petroleum & Energy Studies

For the award of
DOCTOR OF PHILOSOPHY
in
Chemical Engineering

BY
Balaji K
January 2021

SUPERVISOR(S)
Dr. Sravendra Rana
Dr. Vijay Parthasarthy

UPES
UNIVERSITY WITH A PURPOSE

Department of Chemical Engineering
School of Engineering
University of Petroleum & Energy Studies
DEHRADUN-248007: Uttarakhand

SYNTHESIS AND CHARACTERIZATION OF VITRIMERIC MATERIALS: IMPACT OF NANOFILLER ON SELF-HEALING AND THERMOMECHANICAL PROPERTIES

A thesis submitted to the
University of Petroleum & Energy Studies

For the award of
DOCTOR OF PHILOSOPHY
in
Chemical Engineering

BY
Balaji K
(SAP ID: 500066153)

January 2021

Supervisor
Dr. Sravendra Rana
Associate Professor
Department of Chemistry
University of Petroleum & Energy Studies

Co-Supervisor
Dr. Vijay Parthasarthy
Senior Associate Professor
Department of Chemial Engineering
University of Petroleum & Energy Studies

Department of Chemical Engineering
School of Engineering
University of Petroleum & Energy Studies
DEHRADUN-248007: Uttarakhand

January 2021

DECLARATION

I declare that the thesis entitled **"Synthesis and Charcterization of Vitrimeric Materials: Impact of Nanofiller on Self-healing and Thermomechnanical Properties"** has been prepared by me under the guidance of Dr.Sravendra Rana, Associate Professor of Department of Chemistry, University of Petroleum and Energy Studies and Dr.Vijay Parthasrthy, Senior Associate Professor of Department of Chemical Engineering, University of Petroleum and Energy Studies. No part of this thesis has formed the basis for the award of any degree or fellowship previously.

Balaji K
Department of Chemical Engineering
School of Engineering
University of Petroleum and Energy Studies
Dehradun-248007, Uttarakhand, India.

DATE : 15.03.2021

UPES

UNIVERSITY WITH A PURPOSE

Great Place To Work. Certified MAR 2020–FEB 2021 INDIA

CERTIFICATE

We certify that **Balaji K** has prepared his thesis entitled "**Synthesis and Charcterization of Vitrimeric Materials: Impact of Nanofiller on Self-healing and Thermomechnanical Properties**", for the award of PhD degree of the University of Petroleum and Energy Studies, under our guidance. He has carried out the work at the Department of Chemical Engineering, University of Petroleum and Energy Studies.

Supervisor

Dr.Sravendra Rana

Associate Professor
Department of Chemistry
University of Petroleum and Energy Studies

Date: 15/03/2021

Co-Supervisor

Dr.Vijay Parthasarthy

Professor
Department of Chemical Engineering
University of Petroleum and Energy Studies

Date: 15/03/21

ABSTRACT

Vitrimers- a class of polymeric networks, those change topology above a threshold temperature have been investigated in recent years. Thermoset vitrimer materials have been fascinated many researchers widely, due to their malleability and possibility of reprocess, recycle and reuse(self-heal). An associative dynamic covalent adaptive network vitrimers with fixed crosslink density have intensified the developement of new smart materials. The inclusion of different vitrimer chemistries in thermoset materials have resulted the potential materials for recent world. However, the study of vitrimer materials with nano fillers are nascent, owing to that, the involvement of nanofillers in the vitrimer thermoset materials are inquistive by many researchers. Although, some of the extent discussed nanofiller promulgated self-healing vitrimer thermoset investigations are discussed, however, self-healing was achieved in presence of catalysts. The presence of catalyst has its own limitations (toxicity, deactivation, cost, color), while processing the materials.

Therefore, the present study is focused on the developement of catalyst free self-healing vitrimeric materials including the effect of different nanofillers on self-healing properties. Catalyst free graphene oxide (GO) promoted self-healing vitrimer nano composites were designed, where the synthesized vitrimer nano composites have demonstrated an enhanced thermomechanical properties and displayed self-healing properties via disulfide exchange based covalent adaptive network behavior. This study found that GO based nanofiller enhance the self-healing properties, including the shape memory and flexural strength of the materials. The GO induced lower glass transition was helpful to achieve low temperature self-healing: when compared to epoxy vitrimers (73% and 60% self-healing) the vitrimeric nanocomposites demonstrates a 88% and 80% self-healing for the first and second cycle, respectively.

In order to further extent their properties, disulfide exchange assisted polydimethyl siloxane (PDMS) and graphene oxide (GO) involved epoxy vitrimers were demonstrated, and exhibited a reduction in glass transition temperature and storage modulus with increase in flexural strain and a low temperature self-healing. Stress relaxation and Arrhenius study were carried out for the analysis of vitrimeric behavior, where the prepared epoxy material displays self-healing at 80 ^{0}C for 5 mins, whereas, a low temperature self-healing (60 ^{0}C) was observed for epoxy/PDMS/GO nanocomposites.

To achieve sustainable vitrimers, the involvement of bio-derived monomers or fillers are obligatory, which is helpful for ecological improvement. Thus, biomass

derived activated carbon (AC) fillers were involved in epoxy vitrimer to acquire sustainability, as well as for thermal and mechanical property modifications. Hence performed epoxy vitrimer biocomposite has demonstrated the low temperature self-healing at 70 ^{0}C for 5 mins than the pristine epoxy (80 ^{0}C for 5mins), where healing was accomplished through disulfide exchanges. Further, the examined flexural studies for healing efficiency has described the 73% and 60% (epoxy) / 85%and 70%(biocomposite) recovery after two consecutive healings. This addition of AC in epoxy vitrimer can provide beneficial pathway to attain the sustainable real time application in near future.

The already emerged vitrimer based applications (like 3D printing, adhesive, electromagnetic shield and actuator) are promising constituent to acquire further applications for real-time world. Specifically, intrinsic self-healing materials have intensively utilized in electronics field to develop the soft electronics, solid electrolytes and so on. The demonstrated self-healing solid polymer electrolytes are providing suppression over dendrites growth, although fails to withstand for thermal inflation and also exhibited poor chemical resistance, low mechanical properties. Perhaps brings up vitrimer in that system will be helpful to achieve a prominent storage devices.

ACKNOWLEDGEMENT

I would like to express my heartfelt gratitude to my supervisors Dr. Sravendra Rana and Dr. Vijay Parthasrathy, for their continuous encouragement and motivation throughout my thesis work. I am very thankful to them for presenting this promising area of research to me and for their supervision, which I have been getting all these years of my research.

In addition to my Supervisors, I would like to show gratitude to Dr. S. J. Chopra (Chancellor), Dr. Sunil Rai (Vice-Chancellor) and Dr. Kamal Bansal (Dean) at the University of Petroleum and Energy Studies for their cherished support for my research work.

I would like to express my gratitude to Dr. J. K. Pandey (Associate Dean Research) and Dr. S. M. Tauseef (Assistant Dean Research,SOE), for their support during my research.

I would like to extend my special thanks to my dear faculty colleague and friend Mr. Sanka Rama Venkata Siva Prasanna who stood with me at each phase of my work.

My sincere gratitude to Dr. Yves Leterrier and Prof. Dr. Véronique Michaud from Laboratory for Processing of Advanced Composites (LPAC), (EPFL), Lausanne, Switzerland, Prof. Wolfgang H. Binder from Institute of Chemistry, Martin Luther University Halle-Wittenberg, Germany, Dr. Gun Jin Yun, Department of Mechanical & Aerospace Engineering, Seoul National University, Korea, Dr. Anurag Srivastava from Advanced Materials Research Group, ABV - Indian Institute of Information Technology and Management, Gwalior and Prof. Nanda Gopal Sahoo (Kumaun University, Nainital) for their research collaboration.

I express my sincere gratitude to my family for all their love, encouragement and support. My heartfelt thanks to my lovable friends, who all stood as backbone for my every footsteps.

I would like to acknowledge in-house Central Instrumentation Centre (CIC) and Composite Lab facility; where I have carried out my research work. I also thank lab technicians Mr. Charu Pant, Dr. Devendra Rawat and Mr. Anuj Kumar.

I would like to express my gratitude to R&D Department and SRE Department for their support. I also thank Ms. Rakhi Ruhal, Mr. Amit Pandey and Team R&D. My special thanks to Science and Engineering Research Board (SERB-DST), Government of India (Grant No. ECR/2016/001355) for financial assistance over entire research period. Finally, a gratitude to all my dear colleagues for their continuous help and support.

TABLE OF CONTENTS

ABBREVATIONS

AC	Activated Carbon
ADCAN	Associative Dynamic Covalent Adaptive Networks
AFD	2-Aminophenyl Disulfide
BCC	Bis(6-Membered Cyclic Carbonate)
BD	1,4 Butanediol
CNT	Carbon Nanotube
DCAN	Dynamic Covalent Adaptive Networks
DDCAN	Disassociative Dynamic Covalent Adaptive Networks
DETA	Diethylenetriamine
DGEBA	Diglycidyl Ether Bisphenol A
DMA	Dynamic Mechanical Analysis
DSC	Differential Scanning Calorimeter
$\mathbf{E}_a$	Activation Energy
ENR	Epoxidized Natural Rubber
EPR	Electron Paramagnetic Resonance
FTIR	Fourier Transform Infrared Spectroscopy
GLYMO	(3-glycidyloxypropyl)trimethoxysilane
GO	Graphene Oxide
HBE	Hyperbrached Epoxy
HRTEM	HighResolution Transmission Electron Microscopy
IR	Infrared
PDMS	Polydimethylsiloxane
PFPE-VU	Perfluoropolyether Vinylogous Urethane
PTIL	Poly(1,2,3-triazolium ionic liquid)
RAFT	Reversible Addition Fragmentation Chain Transfer
TA	Thermal Analysis
TEMPO	2,2,6,6- tetramethyl-piperidinyl-1-oxyl
THF	Tetrahydrofuran
TREN	Tris(2-aminoethyl)amine
UV–Vis	Ultraviolet–Visible spectroscopy
XRD	X-ray Diffraction Spectroscopy

List of Figures

List of Tables

CHAPTER 1: INTRODUCTION

1.1 Self-healing materials

The era of self-healing materials are gradually settling in where man-made materials can putback their structural satbility in case of material fracture. For instance, the macro and micro fracture in structural materials can close up on solitarily without any external influence and the scratches on cars can seal up with a complete restoration of the shiny appearance of the car as it was before the damage. The whole concept of self-healing materials was stimulated by nature in view of the way customary healing of wounds and injury occur in living species. Ultimately, with time, practically all materials undergo natural or artificial degradation and deterioration, and in the case of constructed materials the prolonged degradation provides rise to microcracks that promotes material breakdown hence making repair crucial in order to enhance the reliability and lifespan of the materials The focus of self-healing materials has been on polymers and polymer composites with these materials assuming industrial dimensions and also finding relevance in everyday life. Polymer-based self-healing materials exhibit additional properties which corrects traditional defects in polymers, polymer composites. These additional properties which self-healing materials exhibits are:

i) Their capability to automatically heal the damage par of materials multiples times

ii) Their capability to heal defects regardless of the sizes

iii) Their ability to exhibit better or equal performance behaviour when compared with their traditional counterpart at a lower cost which makes them economically more preferred [1].

Self-healing materials can be typically classified into two main groups: intrinsic and extrinsic self-healing materials [2]. These materials primarily differ in their mechanisms as well as their chemistries [3–5]. The extrinsic self-healing materials requires the implanting of healing agent filled microcapsules or vascular networks in a matrix system [6]. The capsule integrated self- healing system (It can delivers required healing agent via the break of capsule),

and microvascular network systems are the mechanisms often performed in the development of extrinsic self-healing materials. The different polymerization techniques [7] and polymers, have been utilized to produce the microcapsules and to prepare the shell walls [8–12]. In the development of microcapsule involved self-healing materials, a few important factors are carefully considered, summarized in Table 1.1. Meanwhile, the microencapsulation technique distinctly affects from two major limitation than others, such as (i) the price of catalyst, especially Grubbs' catalyst, (ii) the action of self-healing is irreversible, suggested healing can happen once and even there is subsequent cracks on the earlier healed region, healing would not occur due to the quantity of the healing agent is utilized in the formerly healed place. In spite of that, various reviews have been published with recommended solutions to overcome these snags [12–14].

A prominent solution to overcome the difficulty of diminutive supply of a healing agent in capsule based self-healing concept is the approach based on microvascular networks exemplified, which was eventually explored by White et al. [12, 15] The fundamental motivation of this approach is the dependence of the centralized network, where the polymeric materials can flow continuously and distributes effectively in the damaged matrix. Because of the difficulty of fabricating synthetic materials with microvascular networks, this approach was rarely applied for practical applications. On the other hand, intrinsic self-healing materials are based on dynamic covalent interactions and non-covalent chemistries as described by Wang et al. [16]. The dynamic bonding interactions utilizes the radical exchange reaction, Diels-Alder reaction, dynamic amine bond formation, and trans-esterification reaction to mention but a few [17–22]. On the contrary, the non-covalent bonding reaction approach is based on numerous techniques in addition to $\pi - \pi$ stacking, hydrogen bonding, host-guest interaction [23, 24]. It is important to state that a number of external factors comprising pH change, temperature, pressure, light or oxygen can trigger the re-formation of the chemical bonds in intrinsic self-healing materials. However, the non-covalent adaptive bond interactions can lead to lower mechanical properties due to their weaker bonding energies (typically 1-5 kcal/mol) [25], in comparison to the covalent bond energy ($\approx$50-150 kcal/mol) [26].

1.2 Vitrimers

Recently established vitrimer concept represents an important contribution to improve the lifetime and recycling of thermoset-systems. The concept of As-

Table 1.1: Vital parameters for developing capsule-based self-healing materials

Parameters	**Influencing factors**
Microcapsule	Healing agent should be inside to the polymer shell wall. Close proximity of the microcapsule to the catalyst. Longer self-life of the microcapsule. Frail shell wall to increase rupture. Very strong interfacial interaction between the microcapsule shell wall and the polymer matrix. Compatibility with the dispersion polymer medium.
Monomer	Liquid monomer which can flow to the area of the cracked plan till capillary action. Less volatile to allow adequate time for polymerization.
Catalysts	Dissolve in matrix. The absence of agglomeration with the polymer matrix. Stability during processing. Economic.
Polymerization	Must be rapid. Stress relaxation and no stress encouraged shrinkage. Low temperature polymerization.
Coatings	Less effect on the physicomechanical properties of the matrix due to the incorporation of the microcapsules. The thickness of the coatings must be greater than the microcapsule size. Affordable manufacturing process.
Healing	Must be rapid. Several times.

sociative Dynamic Covalent Adaptive Networks (ADCAN), based on thermoset vitrimers, demonstrates a high level of stress relaxation, shape memory and self-healing properties. In such a "vitrimer" the dynamically fixed crosslink density allows to reprocess the material without loss of macroscopic properties based

on a temperature dependent associative exchange. The overall reprocessing can be achieved by purely associative bond-exchange, controlled by kinetic profile, adjustable, via the used catalysts. Due to their high mechanical properties, thermal stability, resistance to chemicals and environmental stress, thermosetting polymeric materials are intensively focused by researchers over the past few years [27–30], and have been involved in many applications, such as high-performance materials for aircrafts, protective coatings, wind turbines and other areas [31–33]. However the inherent irreversible crosslinking in thermosets naturally restricts flow, bond exchange, and malleability, both required for reprocessing or self-healing [34–36]. Thus conventional thermosetting materials are susceptible to failure after fracture or damage during service, leading to a sharp decrease in their sustainability, safety, and lifetime [37, 38].

The exploration of recyclable and healable thermosetting polymeric materials is in high demand as these materials would allow to overcome not only difficulties connected to damage diagnosis, but also include appropriate interventions to restore (and subsequently) recycle the material functionality [39–42]. To improve the lifetime, safety, and environmental impact of man-made materials great attention has therefore been paid for developing the recycling and self-healing polymeric materials [43, 44]. Different concepts to generate materials that are able to repair autonomically [45] or via an external stimuli such as heat [46], light [47], or pressure, have been designed [42] using of various approaches such as capsule based covalent systems [48]. To achieve recyclable and self-healing in thermosetting materials, non-covalent bonds like hydrogen bonds [34,49], $\pi - \pi$ stacking [24] and metal-ligand bonds [23] were introduced in thermosetting matrix. However, the non-covalent adaptive bond interactions can lead to lower mechanical properties due to their weaker bonding energies (typically 1-5 kcal/mol) [25], in comparison to the covalent bond energy ($\approx$50-150 kcal/mol) [26].

A new paradigm dynamic covalent adaptive network (DCAN) has been introduced in thermoset material [50], helpful to enhance repairing ability of thermosets via dissociative and associative distinctive exchange pathways(Figure 1) [51]. In case of dissociative dynamic covalent adaptive networks (DDCAN) the dynamic bonds can exchange even in highly crosslinked networks, such as in thermosetting materials, where the decrease in crosslinking density is proportional to the loss in network connectivity (Figure 1.1 (A)), observed in step by step breaking and reformation of bonds [52, 53]. As an example, Wudl and coworkers [54] have developed a re-processable and self-mendable thermosetting

material based on a thermo-reversible Diels-Alder reaction, where furan and maleimide moieties are detached at high temperature and again reformed to the bicyclic Diels-Alder-product at lower temperature. Various other chemistries have also been investigated to heal thermosetting polymers, where (crosslinking density) drops nonlinearly with increasing temperature, leading to significant changes in the flow of the material, which can reverse upon subsequent cooling, in turn regaining material strength [55, 56].

An associative dynamic covalent adaptive network (ADCAN) displays a more fixed crosslink density during bond exchange, as observed during breaking and reformation of bonds (Figure 1.1 (B)). This concurrent dynamic exchanges results in a minimal change in macromolecular structure during their bond exchanges (due to the fixed crosslink density), whereas DDCAN exchanges display a maximum change in macromolecular structure while bond exchanges [51]. In 2005, the first ADCAN, based on reversible addition fragmentation chain transfer (RAFT) reaction was observed in thiol-ene monomer units, taking place via the introduction of allyl sulphide moieties [57]. An associative dynamic covalent adaptive network in thermosetting polymers was designed by Leibler and co-workers in 2011 [56]. In this study an epoxy network was transformed into a "vitrimer" exploiting a transesterification mechanism, where the observed dynamic exchanges resembles a vitreous silica like behaviour, terming the resulting material as "vitrimer" [56, 58].

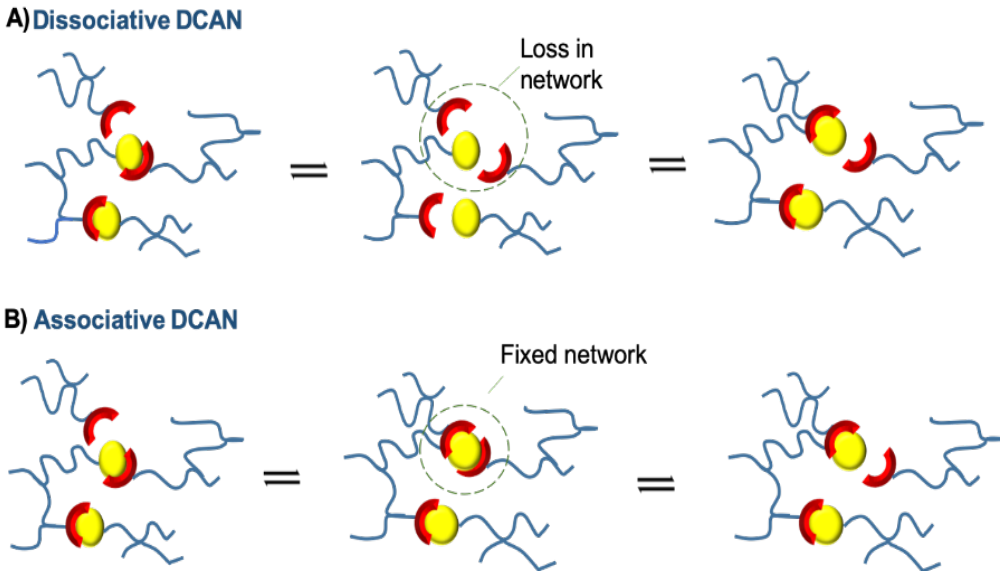

Figure 1.1: (A) Dissociative exchange and (B) Associative exchange in dynamic covalent adaptive networks

The rearrangement process of vitrimers could be controlled between two temperature ranges, including the glass transition temperature (T_g) and the topology freezing point temperature (T_v). This remarkable associative covalent adaptive network formation of vitrimers is eminently suitable for a variety of fields, including transport industries, defence industries, civil engineering, electronics [59, 60]. A covalent bond exchange mechanism and glass forming ability was demonstrated through a patchy particle model, where free energy between particles (phase behaviour) was calculated via Wertheim thermodynamic perturbation theory including its validation with computer simulations [61]. In addition molecular dynamics simulations for vitrimer particle model had elucidated the swap driven exchange during their restructuring, and conforms the fixed network integrity of vitrimer material through a theoretical bond swapping algorithm [62].

1.3 Characteristics of vitrimers

Vitrimers are distinguished according to their temperature dependent viscoelastic behaviours, as the covalent exchange rate is related to the transition temperature. Generally, thermoplastic materials and dissociative CAN's change their topology gradually while heating above the glass transition temperature (T_g), macroscopically in line with a William-Landel-Ferry (WLF) behaviour. However, the additionally introduced dynamic (covalent) bond introduces an additional, temperature-dependent (Arrhenius-type) behaviour, where viscosity gets controlled by chemical exchange reactions [52]. Due to this controlled viscosity behaviour, vitrimers allow processing in a wide temperature range without loss in network integrity, whereas thermoplastic materials and dissociative CAN's exhibit a significant drop in viscosity as well as crosslink density while increasing the temperature [63]. In case of thermoplastic polymeric materials, the transition from solid to rubbery (Figure 1.2 (a)) is described by T_g, whereas, a new temperature transition range is introduced to identify the viscoelastic phase transitions in vitrimers, termed as the topology freezing point temperature (T_v). The position of T_v was situated between the phase transition of viscoelastic solids to viscoelastic liquids, and this transition temperature was chosen at the point where viscosity reaches 10^{12} Pa.s [64, 65]. Thus, the vitrimer T_v has an upper and lower temperature range, where slow and fast exchange reaction is observed at below and above T_v, respectively. Studies found that the exchange in vitrimer topology initiates when it crosses T_g and increases steadily once it reaches the T_v. This different temperature dependent characteristic behaviour can be deter-

mined in view of the T_v position in vitrimer materials. Vitrimer characteristics have been therefore categorized into two pathways. In a first case, T_v is situated above T_g, whereas in another case T_v situated well below the T_g. In both the cases dynamic covalent bond exchange takes place after T_g, whereas in the first case it behaves like a viscoelastic solid or rubbery till it reaches to T_v, hence flowing like a viscoelastic liquid with Arrhenius behavior after it has reached T_v (Figure 1.2 (b)).

In case T_v is situated below the T_g, chain mobility is frozen (till reaches T_g) due to zero segmental motions [53], and after crossing $T_{g,}$ bond exchange happens in an uncontrolled manner for a certain period via William-Landel-Ferry (WLF) behaviour However, eventually it follows Arrhenius behaviour (Figure 1.2 (c)). The material topology freezing point temperature could be analysed via dilatometry or stress relaxation experiments, and the hypothesis $T_g > T_v$ has extrapolated with the help of Arrhenius equation (1) [66]and Maxwell equation (4) (Figure 1.3) [52, 67, 68]. As an example, the often topology freezing point epoxy graphene vitrimer temperature was analysed through dilatometry (Figure 1.2 (d,e)). The so obtained phase transitions, amorphous I, II and III are helpful to understand the temperature dependent viscosity drop with a fixed crosslink density. In each region, material viscosity is reducing continuously, and sudden drops in amorphous II region, denoted as T_v [69]. Thermosetting vitrimeric materials release their strain with time (relaxation time) [70–73], however, the stress relaxation behaviour cannot be identified in a general thermosetting materials [74, 75]. To find out the activation energy (E_a), stress relaxation time ($\ln(\tau^*)$) vs temperature(1000/T) graph has been plotted (equation 2). The determined activation energy (E_a) of material describes the least energy to start the reaction [76].

$$\tau^* = \tau_0 exp(E_a/RT) \tag{1}$$

After natural logarithm on both sides, the equation (1) becomes,

$$ln(\tau^*) = ln(\tau_0) + (E_a/RT) \tag{2}$$

From the above equations, τ^* = Relaxation time; τ_0 = Characteristic relaxation time; E_a = Activation Energy; R = Gas constant; T = Temperature. Henceforth, the material's topology transition temperature of the vitrimer, T_v can be calculated with the help of Maxwell (3) and the Arrhenius (2) equations,

$$\eta = G * (\tau^*) \tag{3}$$

From the equation, η = Viscosity; G = Shear viscosity modulus.

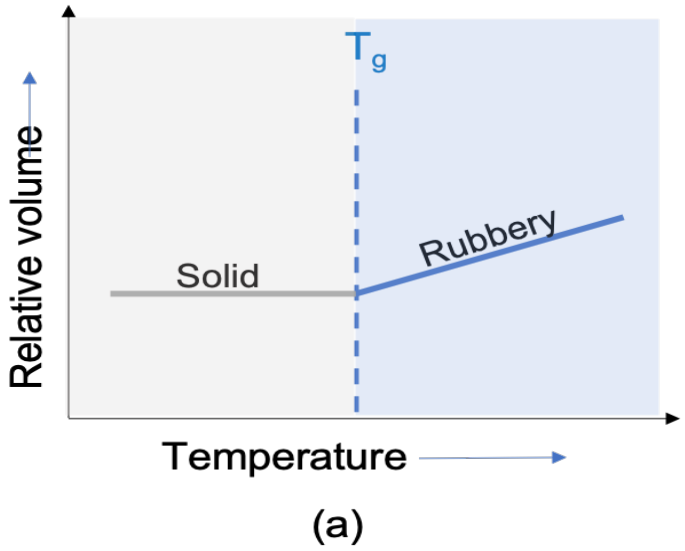

(a)

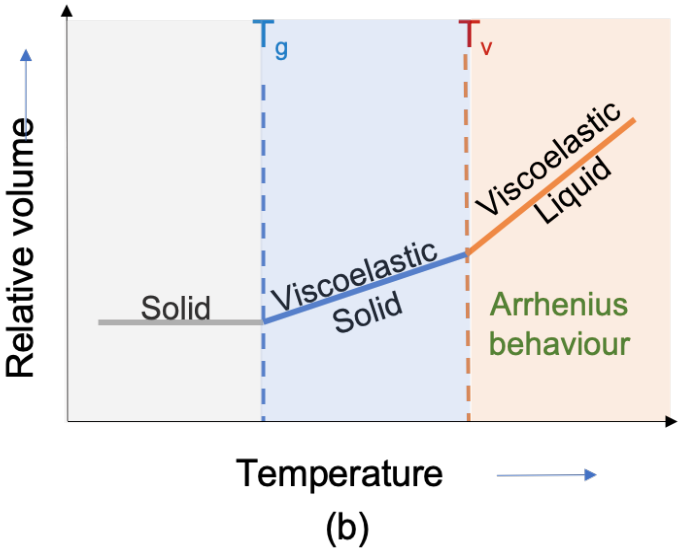

(b)

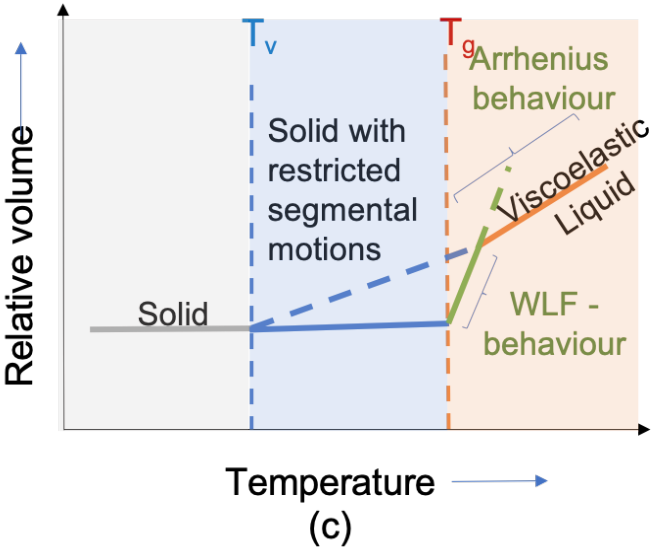

(c)

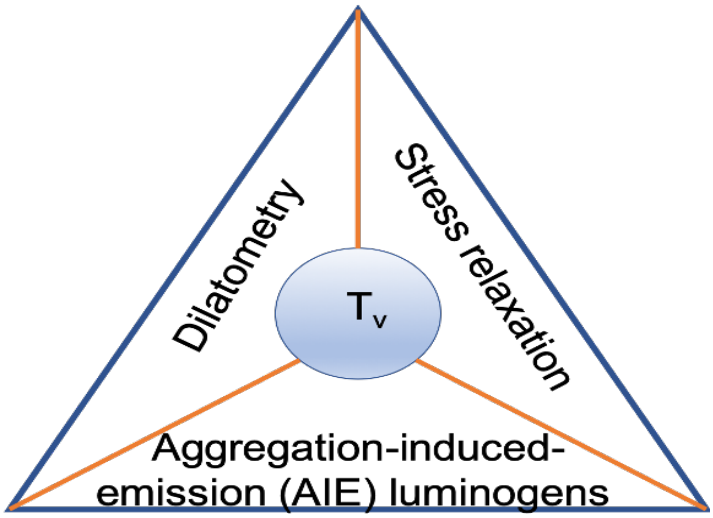

(d)

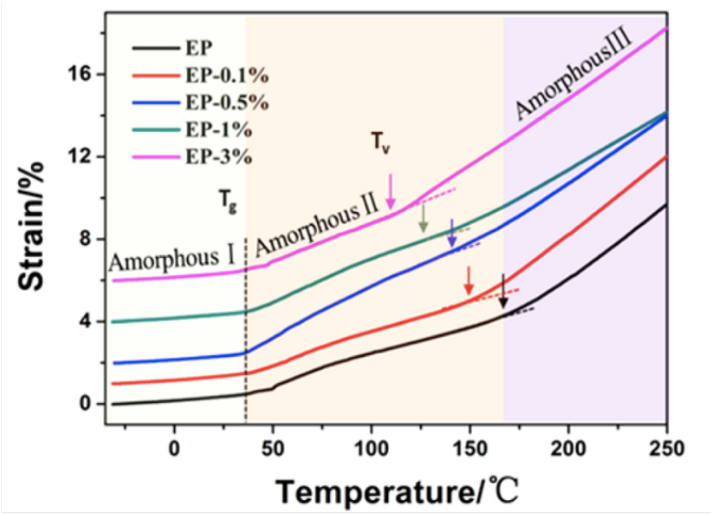

(e)

Figure 1.2: (a) Thermoplastic and dissociative covalent material phase transitions. Thermosetting vitrimer following (b) T_g below T_v and (c) T_v above T_g (d) Different characterization techniques to find T_v(e) Dilatometry experiments of graphene-vitrimers

In case of Maxwell equation (3), an arbitrary value of viscosity has been taken as 10^{12}Pa s and the shear viscosity modulus is substituted to identify the relaxation time (τ^*). This observed relaxation time was substituted in equation (2) to find T_v [59]. For instance, fully bio-based polyimine vitrimer stress relaxation (temperature range from 40 ^{0}C to 80 ^{0}C) and Arrhenius plotted graph (ln(τ^*) vs 1000/T) with trendline equation (Figure 1.3 (a,b)), allows to identify the activation energy (E_a= 64 KJ/mol) and the T_v (-58.3 ^{0}C) through Maxwell equation [76].

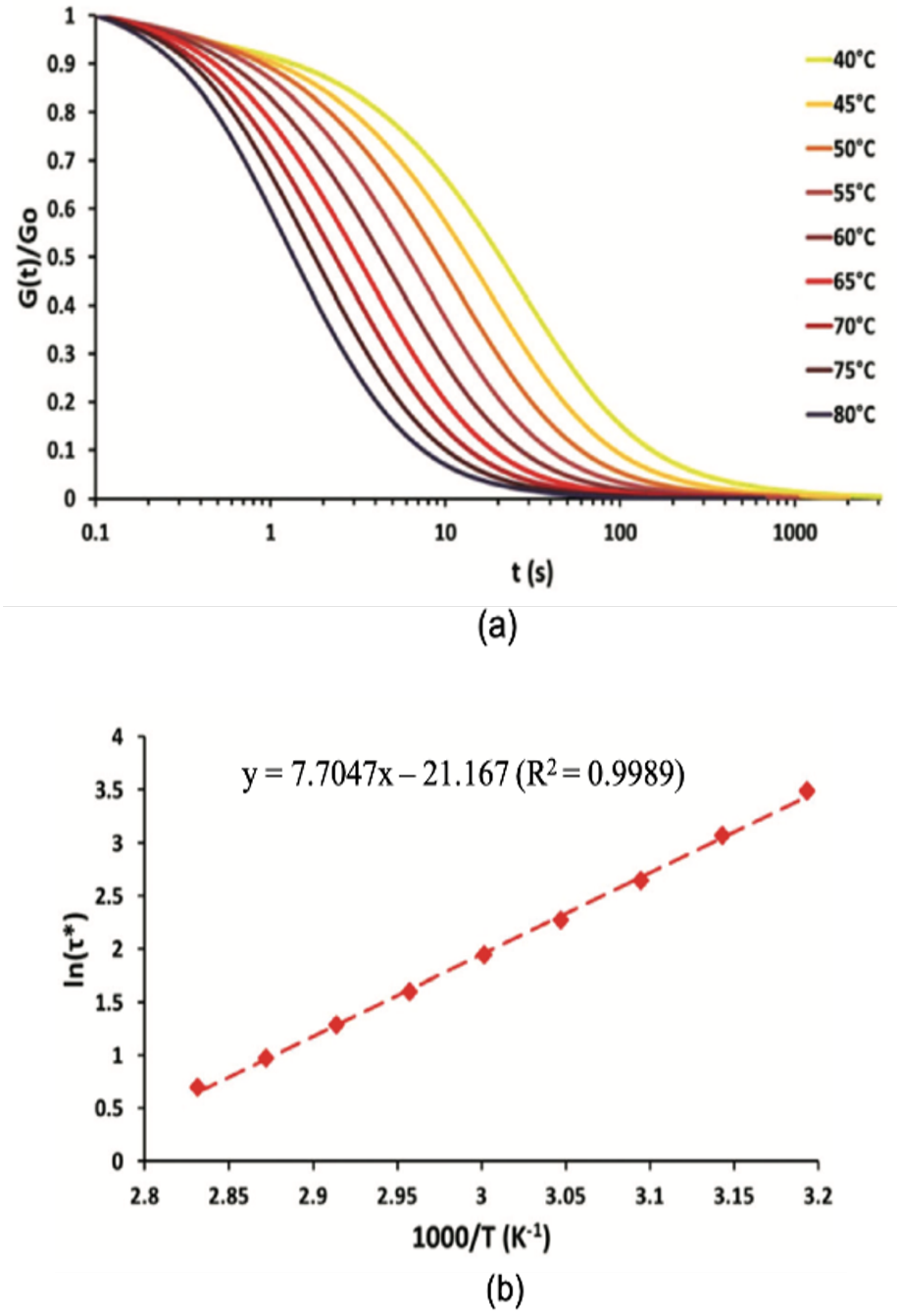

Figure 1.3: Polyimine vitrimer stress relaxation graphs (40 ^{0}C to 80 ^{0}C) (a) stress relaxation graph (b) Arrhenius plotted graph [76]

Recently, Yan ji and coworkers has demonstrated a method of aggregation-induced-emission (AIE) luminogens in vitrimer to find T_v in static condition without any external force, which was different from the above-mentioned dynamic characterizations (Dilatometry and stress relaxation). This technique requires doping of AIE fluorescent molecules in the vitrimer network, where the fluorescence of AIE luminogens changes below and above T_v [77].

1.4 Motivation

In recent years, the explained mechanism (ADCAN) has effectively involved in various thermoset materials, to attain the vitrimeric behaviour. However, nanofiller promoted thermoset vitrimer based self-healing nanocomposites have demonstrated at seldom manner. Even that reported studies are most often described the high temperature healing with moderate mechanical properties. Furthermore, bio filler involvement in vitrimer system has meagrely investigated. Owing to these reasons, this work mainly focuses to develop the catalyst free vitrimer system with different nano and bio fillers.

1.5 Objectives

An associative covalent adaptive network (ADCAN) rearrangement occurs thermally during the crack propagation in epoxy vitrimer-graphene oxide nanocomposite material. To effectuate the strategy, following are the main objectives:

- Development of catalyst free self-healing epoxy vitrimer
- Impregnation of graphene oxide in vitrimer to enhance their properties
- Optimization of nano-filler content and evaluate the mechanical properties of developed self-healing material
- Incorporation of bio derived activated carbon fillers in epoxy vitrimer to develop a sustainable self-healing material

CHAPTER 2: LITERATURE REVIEW

Vitrimeric materials have been synthesized through many different chemist-ries including an efficient covalent bond exchange behaviour. In many cases the presence of a catalyst can modulates the exchange process. Therefore, some studies report on a catalyst free mechanism, whereas the same chemistry displays a different material property in the presence of an added catalyst system (Figure 2.1). Herein, we summarize the chemistries (catalyst dependent and independent) used for the design of ADCAN based thermosetting polymers and tabulated their healing conditions (Table 1).

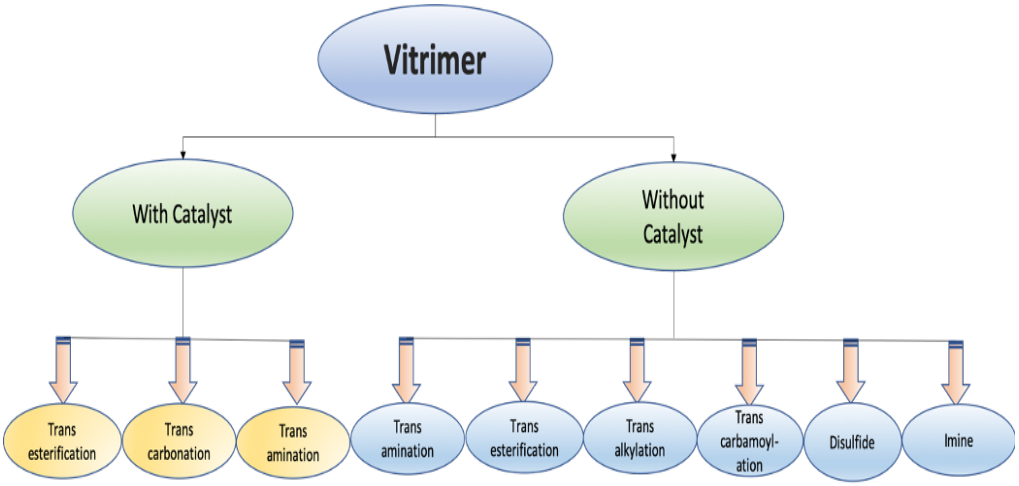

Figure 2.1: Overview of involved chemistries in vitrimer

2.1 Catalyst based mechanisms

2.1.1 Transesterification

Transesterification is a process of interchanging an ester with an alcohol in the presence of different acid/base catalysts [78].The foremost vitrimer material has been developed with a simple carboxylate transesterification reaction by Leibler and coworkers [18], where the authors used the associative exchange without depolymerization in both, hard and elastomeric materials. Initially elastomeric epoxy-resins were prepared through a classical chemistry relying on DGEBA and tricarboxylic acids. The transesterification process in the material has been

effectively controlled by a zinc acetate [$Zn(Ac)_2$] catalyst. A hard epoxy-resin was prepared through diglycidyl ether bisphenol A (DGEBA) and glutaric anhydridein presence of zinc acetyl acetonate [$Zn(Ac\ Ac)_2$] catalyst. The resulting stress relaxation and Arrhenius dependent activation energy were almost similar for both, an elastomeric and the hard network, where the obtained activation energies were 80 kJ/mol and 88 kJ/mol, respectively. Then effect of silica nanoparticles incorporation into an epoxy matrix was also investigated, where the study found that the presence of silica in the polymer matrix enhanced the modulus due to interfacial bond interactions among silica particles and epoxy matrix. However, poor silica particles dispersion infringes their mechanical properties, whereas the surface-modification of the nanofillers was helpful to enhance their dispersion. The resulting relaxation time for (3-glycidyloxypropyl) trimethoxysilane (GLYMO) silica within the matrix was lower than the bare silica-nanoparticles of similar sizes [79]. To understand the impact of the catalyst on the exchange kinetics, bio based epoxy vitrimers were prepared with conventional zinc acetyl-acetonate ($Zn(AcAc)_2$)catalyst. The study found that higher catalyst-loadings exhibited a faster relaxation, investigated through the stress relaxation behaviour [80]. Different amine catalysed, covalently bonded epoxy networks (tertiary amine e.g. tributylamine; secondary amine e.g. dibutylamine; and primary amine e.g. butylamine) were investigated for transesterification exchange, where different network structures and transesterification rates were observed with respect to the used amine and its concentration. The study found that, compared to primary and secondary amines, a tertiary amine catalyst induced vitrimeric behaviour within the epoxy vitrimer with an activation energy of 93.6 kJ/mol, leading to a repairable temperature of 160 ^{0}C and improved healing properties [81].

Theoretical and computational studies were found advantageous to understand the vitrimer dynamic covalent exchanges [61], and the performed molecular dynamics were helpful to perceive the fixed crosslink density during the bond exchanges [62]. Further some theoretical studies were investigated to understand transesterification reaction with their thermomechanical behaviour. Hence for the performed vitrimer blend (hard-anhydride and soft-acid involved epoxy), a multibranch thermoviscoelastic model was employed (Figure 2.2 (a-c)), where the vitrimer blends designability were investigated via the parametric studies. It was demonstrated that the capability of increasing the room-temperature modulus during the reduction of rubbery modulus, as tuned the crosslink density/or the rigidity/flexibility of the entire network, thus generates vitrimers with good

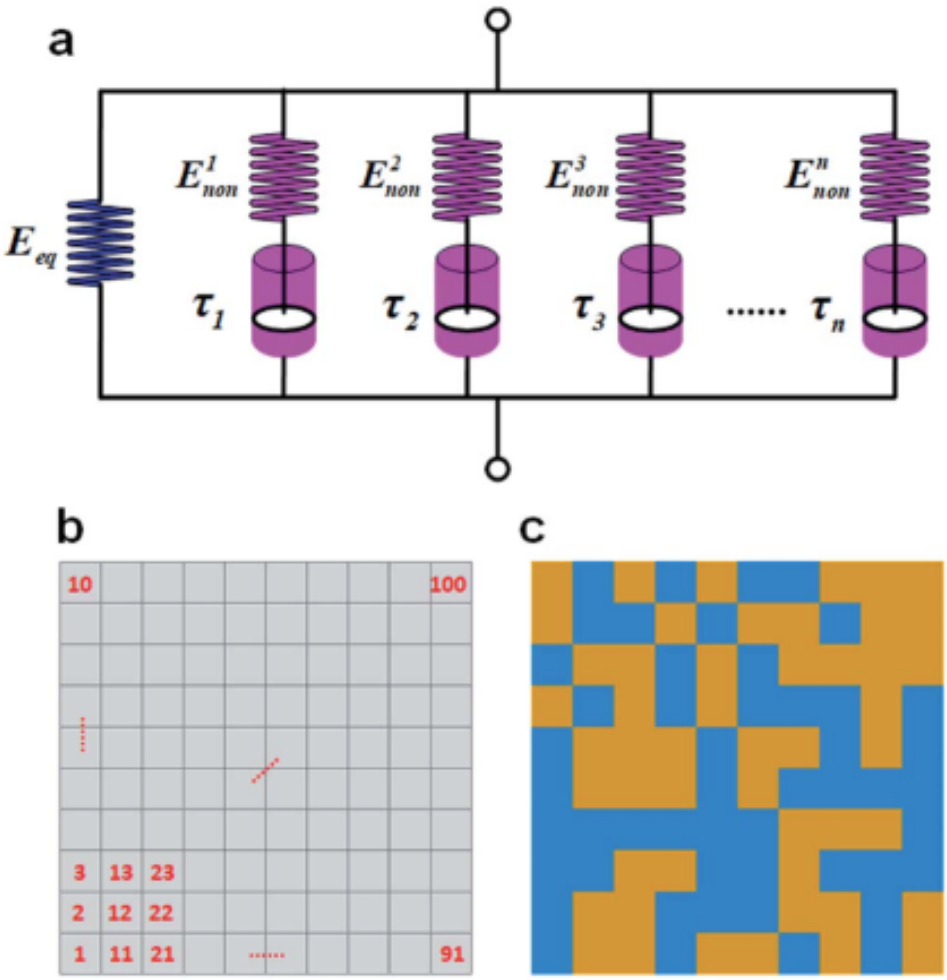

Figure 2.2: (a) Thermoviscoelastic multibranch model (b) Representative volume element (RVE) division (c) Material assignment for volume element(Orange- hard; Blue- soft) [82]

miscibility by decreasing the difference in glass transition temperature and broaden the loss factor (tan δ) curve. The evaluation of the computational model was determined by the agreement towards experimental and theoretical prognosis (thermomechanical properties) of recycled vitrimer blends with different compositions [82].

2.1.2 Transcarbonation

Catalyst promoted transcarbonation exchange has been studied for polycarbonate materials, where the polycarbonate vitrimers were synthesized through bis(6-membered cyclic carbonate) (bCC) and 1,4-butanediol (BD) in the presence of a Ti(IV) alkoxide catalyst (Figure 2.3 (a)). The catalyst promotes transcarbonation exchange rate significantly at elevated temperatures (Figure 2.3 (b)), where

three different catalyst loaded samples were analysed through stress relaxation rates and the resulting change in relaxation is shown in Figure 2.3 (b). Reprocessing of the so obtained vitrimer is possible at 140 ^{0}C, reaching more than 71% recovery in plateau storage modulus and tensile strength [73].

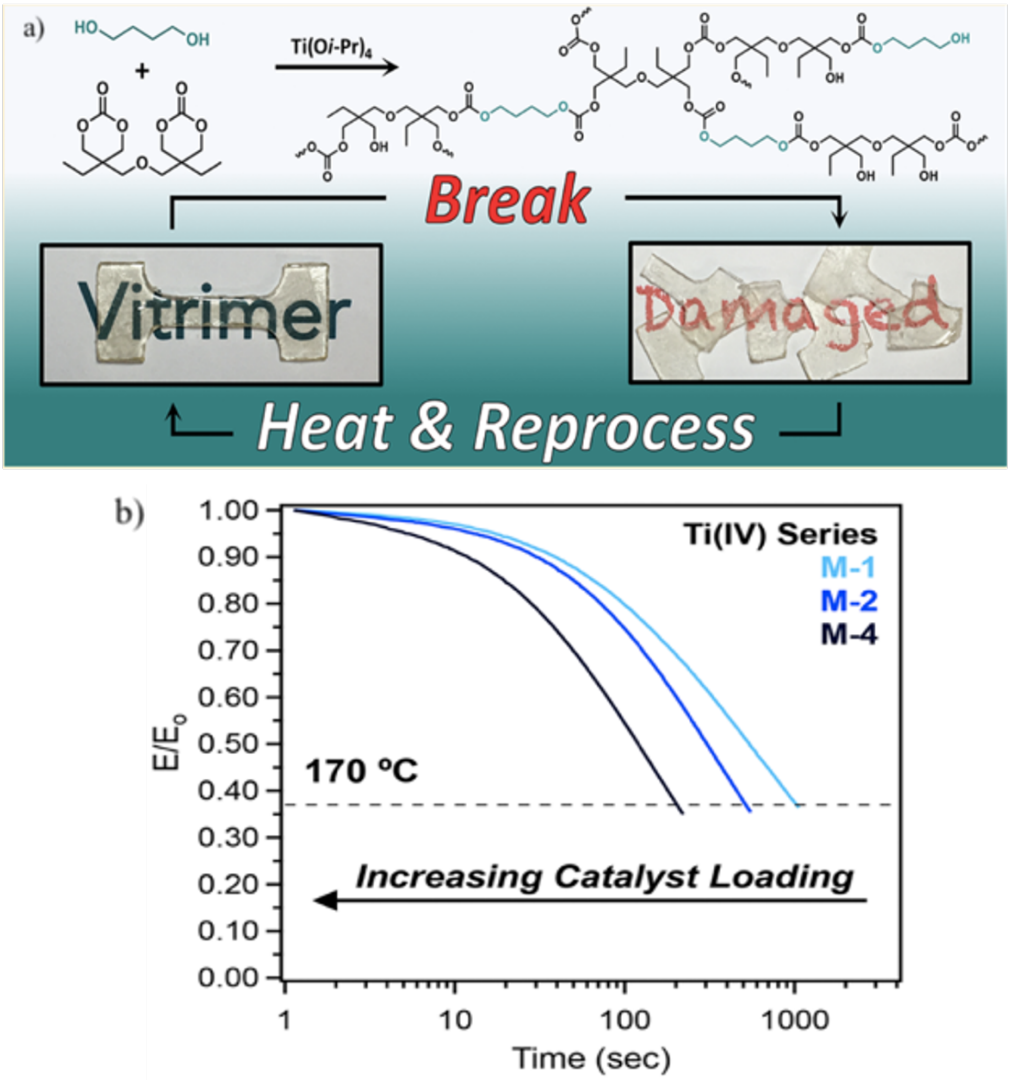

Figure 2.3: (a) Formulation of polycarbonate vitrimer and reprocessing. (b) M-1, M-2 and M-4 denoted medium with catalyst content 1%, 2%, and 4% respectively [73]

2.1.3 Transamination

Transamination is an exchange reaction where the transfer of amino groups is taking place towards a ketoacid. Vinylogous urethane vitrimer transamination exchange can be conducted without catalyst, or under addition of acid and base additives to change the exchange kinetics. The tuning of vinylogous urethane viscous flow happens by general acid/base catalysis of Bronsted- or Lewis acids,

strongly reducing the exchange reaction activation energy (45 kJ/mol). The report found that the generated Lewis acid based protonic species were efficient in enhancing the chain exchange via proton transfer in the vitrimeric materials [63]. An Al_2O_3 (AT1)-catalyst promoted vinylogous urethane-based polydimethylsiloxane vitrimer was reported, where bond exchanges with prominent mechanical properties take place. The effect of neutral, acid and base filler catalyst in transamination exchanges were analysed through relaxation times, where higher stress relaxation time for the neutral catalyst was observed in comparison to the acid catalyst loaded samples. The study found that the acidic and base catalysts slightly tuned the relaxation time, postulated as a reduced chain mobility. A certain filler influence in activation energy was also observed, where the activation energies for pristine, neutral filler, acidic and basic fillers containing PDMS were 149 ± 16 kJ/mol, 146 ± 2 kJ/mol, 129 ± 24 kJ/mol, and 115 ± 17 kJ/mol, respectively. This change of activation energy was observed due the filler matrix interaction, where acidic and basic based fillers exhibited stronger interaction than the neutral filler, and thus these acidic and basic fillers are helpful to enhance the mechanical strength of the developed materials. The incorporation of fillers enhances the mechanical properties, decreases the soluble fraction, preserves processability and, depending on the concentration of filler added, follows the possibility to be recycled, without lack of properties [83].

2.2 Catalyst free mechanisms

Generally, catalyst-based reactions promote the chain exchanges in vitrimeric materials, however, any some cases failure drastic inhibition in chain exchange. Therefore, several investigations were performed in the absence of catalysts, where the catalyst free vitrimers resulted in an optimized exchange efficiency, discussed together with the required reprocessing conditions.

2.2.1 Transamination

A catalyst free vinylogous urethane vitrimer material was developed through trans amination exchange and the obtained stress relaxation rate was competitively lower compared to the respective catalyst supported systems. The vinylogous urethane vitrimers were synthesised through condensation reaction between acetoacetates and amines, where the excess of amine in the network enhances transamination reaction. The excess amine in the network was acquired through a stochiometric increment of amine monomer and the resulting activation energy 59 ± 6 KJ/mol has determined for faster exchange reaction, with

an effective reprocessing achieved at 150 ^{0}C within 30 mins [52]. The vinylogous urethane catalyst-free transamination exchange was efficiently involved in fluorinated polymers, and the reported perfluoropolyether vinylogous urethane (PFPE-VU) vitrimer exhibits a dual viscosity behaviour depending on their temperature, 60 kJ/mol and 130 kJ/mol activation energies obtaining for low and high temperature respectively. This dual activation energy was extrapolated due to the presence of excess amines in the network, where lower barrier exchanges (Iminium pathway) reaction occurred at lower temperature, whereas higher barrier exchanges (Michael pathway) were executed at high temperature. An excess primary amine involvement in PFPE-VU vitrimer resulted in a change of exchange kinetics and mechanical properties. Observing a dual activation energy was observed only in excess amine network. The efficient reprocessing of PFPE-VU was possible at 150 ^{0}C within 5mins, and the reprocessed sample demonstrates a 95% recovery in its mechanical properties [67].

2.2.2 Transesterification

Recently, catalyst free transesterification reactions were observed in a succinic hydride cured hyperbranched epoxy (HBE) network, where dynamic chain exchanges in the epoxy network was observed due to the abundant hydroxyl groups (Figure 2.4).

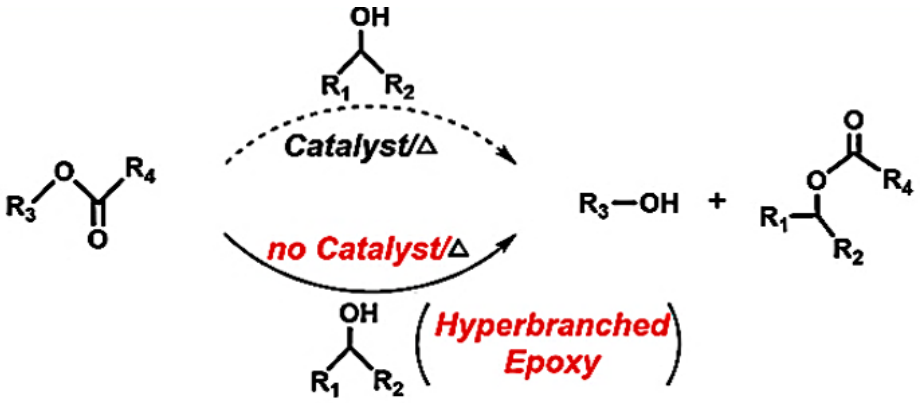

Figure 2.4: Schematic Illustration of transesterification in hyperbranched epoxy (HBE) [84]

The excess of hydroxyl groups in HBE network act as reacting moieties, demonstrating high catalytic properties for exchange reaction. Thus, the observed relaxation rate was faster compared to catalyst-based transesterification reactions, in line with an observed activation energy of 29.5 kJ/mol, which is lower than the earlier reported values. Based on the HBE molecular weight, proper-

ties like tensile strength, elastic modulus and glass transition temperature was changed evidently. The performed vitrimer material displayed self-healing and self-welding properties like conventional catalyst involved vitrimer material. Further, HBE vitrimer was applied as a coating material on metal plate, where it demonstrates excellent hardness and self-adhesion properties. Interestingly, HBE coated metal plates were scratched and healed at 150 ^{0}C for 1h, and exhibited a prevailed electrolyte erosion protection after healing [84].

2.2.3 Disulfide linkages

Disulfide exchange promoted epoxy vitrimers were prepared through a diglycidyl ether of bisphenol A (DGEBA) and 4-aminophenyl disulfide (AFD) (Figure 2.5 (a)), where the disulfide exchange mechanism [85–92] achieves chain exchanges in epoxy with a fixed crosslink density. Due to the rapid relaxation rate a comparatively lower activation energy (55 kJ/mol) was observed and the extrapolated T_v was about -13 ^{0}C. However, reprocessing of the material requires a temperature of almost 200 ^{0}C due to its higher T_g. Furthermore, fiber reinforcement has been performed and their repair/reprocess ability was effectively investigated. The 4-aminophenyl disulfide crosslinked epoxy vitrimer system was identified as comparably simple and efficient [93], additionally displaying transient mechanochromism (Figure 2.5 (b)) [72]. Bio-based disulfide epoxy materials displaying an exchange mechanism were prepared using isosorbide-derived epoxy and disulfide containing aromatic diamines as crosslinker. The reported biobased epoxy vitrimer displays a similar healing mechanism as discussed before, however, with the advantage of using natural resources as components. However, the isosorbide-derived epoxy, showed a moderate activation energy of 106 kJ/mol among reported vitrimer materials, and exhibits a lower T_g (40.6 ^{0}C) and T_v (31.3 ^{0}C), being helpful to achieve an efficient reprocessing at 100 ^{0}C [71].

Recently a disulfide network was introduced into a polyhydroxy urethane (PHU) vitrimer, and the reported PHU vitrimer demonstrates reprocessability via transcarbamoylation exchange at 150 ^{0}C. A PHU-disulfide vitrimer was prepared using bis cyclic carbonate(bcc) and cystamine with tris(2-aminoethyl) amine (TREN) as crosslinker. The study found that a high cystamine concentration results in a lower activation energy (62 kJ/mol) and a lower relaxation time. The reprocessing temperature and time (150 ^{0}C, 30 min) [94] both were lower than in the rigid amine based PHUs (160 ^{0}C, 240-480 min). We recently have developed a catalyst free graphene oxide (GO) promoted self-healing vitrimer nanocom-

posites, where the synthesized vitrimer nanocomposites displays self-healing properties via disulfide exchange based on a covalent adaptive network at 80 ^{0}C for 5mins, and extrapolated $T_v$was 19 ^{0}C. This study found that graphene oxide based nanofiller is helpful to enhance the flexural strength of the material, where percentage of GO incorporation plays a key role for achieving the mechanical and flexural strength. The study has also found that more than one percent of nanofiller exhibited a reduction in flexural strength, due to their agglomeration in epoxy matrix. An efficient self-healing of the material was demonstrated even at low temperature, due to the presence of GO, where speed of chain exchanges had been increased (due to the free volume between GO and matrix) and hence 88% and 80% self-healing for the first and second cycles respectively was achieved [95].

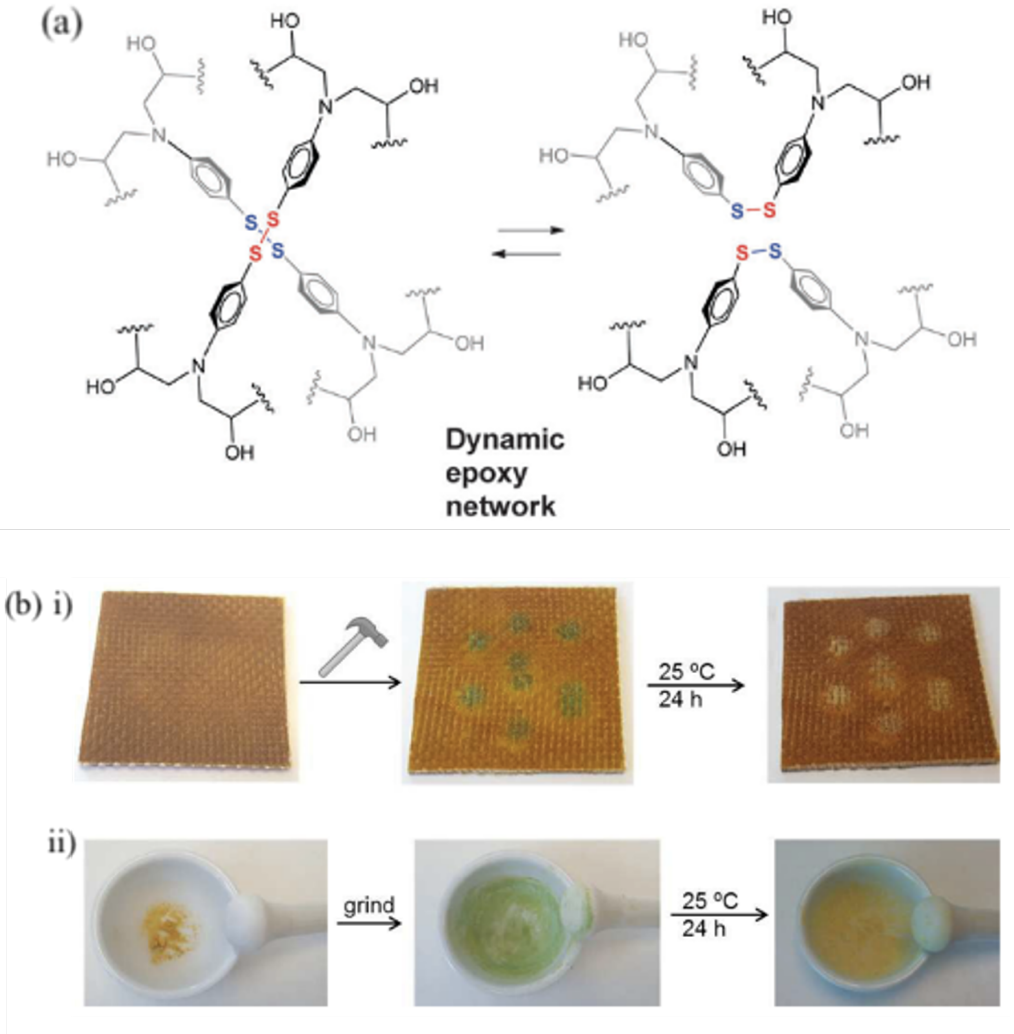

Figure 2.5: (a) A dynamic epoxy network with included dislufides (b) i)Hammer hitted ii) Mortar grinded epoxy(p-EPO)-glass fiber composite [72]

2.2.4 Transalkylation

Drockenmuller and coworkers have developed a poly (1,2,3-triazolium ionic liquid) (PTILs) vitrimer with the help of an α-azide-ω-alkyne monomer and a 1,6-dibromohexane difunctional cross-linker, where the involved crosslinker behaves as a quaternization agent. The kinetic of exchange is initiated and terminated via nucleophilic attack of the counter anion and the triazole to the alkyl halides, resulting in a rapid attachment and detachment via dissociative exchange. The slower relaxation rate and the comparably high activation energy (149 kJ/mol) describes a moderate rate of chain exchanges. However, the extrapolated T_v (98 ^{0}C) was higher than the T_g (-11 ^{0}C), thus efficient reprocessing was achieved at 170 ^{0}C under 200 kPa pressure [96]. Furthermore, investigations were carried out on the same networks to tune their viscosity, allowing to modulate flow by control of the monomer and crosslinker ratios. The performed different concentrations ratio results in a progressive change in activation energy (140–162 kJ/mol), and the observed flow was widely tuned through the used counter anions [97]. Recently, transalkylation promoted poly(thioether) vitrimer networks were developed by photoinduced thiol-ene reactions. The analysed exchange reaction activation energy (108 ± 4 kJ/mol) was lower than the conventional PTIL network activation energy, and chain exchanges in the network results in a fixed crosslink density, where efficient reprocessing was enabled at 160 ^{0}C within 45 mins [98].

2.2.5 Transcarbamoylation

Transcarbamoylation reactions can be promoted under both, strain and temperature, where strain accumulates on the nitrogen lone pair conjugated to the carbonyl groups, promoting the exchange process in the so strained material. A catalyst free vitrimer polyhydroxy urethane (PHU) was prepared starting from a bis (six membered) cyclic carbonate and triamine. Vitrimer reprocessing is promoted by the applied mechanical stress including temperature and pressure, where arbitrary shapes were achieved by heating the material at 160 ^{0}C at 4 MPa pressure for 8 hours. The stress relaxation has been characterized by Arrhenius activation energy, and the obtained energy (111 ± 10 kJ/mol) was much lower than the model PHU compounds (trimethylene carbonate and butylamine involved) activation energy (148 ± 7 kJ/mol) [70]. The demonstrated networks show large variances in the Arrhenius activation energy (99- 136 kJ/mol), depending on their network structure. The study suggests that transcarbamoylation has affected by chemical and mechanical effects like change in chemical com-

position and repeated reprocessing. Owing to this, crosslink density has varied in the material, and it changes the relaxation time and activation energy accordingly, affected. Hence, all crosslinked polyhydroxyurethanes developed from six-membered cyclic carbonates describe mechanical properties typical of thermoset polymers, however, recovers 80% of their pristine sample tensile properties at elevated temperature [99].

2.2.6 Imine exchange

Imine chemistry (Schiff base chemistry) promoted reversible polymer network exchange reactions have been reported very often [100–105]. Recently m-xylylene diamine, terephthaldehyde, and tris (2-aminoethyl) amine based vitrimeric polyimine network has been reported [106]. The introduction of imine chemistry based vitrimer was commenced to enrich the mechanical and thermal properties of diamine and dialdehyde monomer involved polyimine networks, reported earlier by Zhang et al. [107] The conjugated polyimine vitrimer resulted in a satisfactory glass transition (T_g= 102 ^{0}C), storage modulus (1.58 GPa), stress at break (49 MPa(dry sample) and 32 MPa(wet sample)), T_v (56.5 ^{0}C) and activation energy (E_a= 79.65 KJ/mol). The position of T_v below T_g helps to achieve the faster relaxation at high temperatures, as well as exhibited efficient healing at 110 ^{0}C (within 30mins), and then solvent assisted reprocessing was demonstrated at 80 ^{0}C for 24 h with ethylenediamine [106], The same polyimine network was investigated with m-xylylenediamine dimer instead of m-xylylene diamine, leading to an enhanced flexibility, recyclability and processability of the developed materials. However, besides a lower temperature healing, a change in glass transition temperature (T_g= 72 ^{0}C), storage modulus (0.85 GPa) stress at break (45 MPa(dry sample) and 27 MPa(wet sample)) were observed [108]. A, fully bio-based vitrimer (100%renewable carbon) was prepared with fructose derived furan dialdehyde and bio-based diamine/triamine which were acquired from fatty acids. The performed bio-based polyimine vitrimer established fast stress relaxation even at room temperature, and observed T_g (-10 ^{0}C) was higher than the extrapolated T_v (-60 ^{0}C), hence exhibited a lower activation energy (64 kJ/mol) [76].

2.3 Self-healing and shape memory properties

The combination of self-healing [36] properties and vitrimers follows a similar concept, although at different activation-temperatures. Both rely on the reversible exchange of components on the nanoscale, induced by dynamic (chem-

ical or supramolecular) bonds. Whereas true "self"-healing [34] can only be achieved via considerably weak bonds, usually those where the activation energies are situated close to $\sim$ kT (thermal energy at room temperature), also depending on the presence of micro- and nanophases within the material [3, 109, 110], vitrimers normally require temperatures of $100\ ^0$C or more to be remended. Thus, a combination of both properties is attractive in material science, as they lead to an increased lifecycle of the material, both improving sustainability. Thermoset vitrimers healing properties in some context e.g. photo weldable epoxy carbon nanotube composite vitrimeric materials were reported with transesterification reaction of diepoxy and dicarboxylic acid.The involvement of carbon nanomaterials not only affects the material core transesterification chemical reactions, but also facilitates the heat energy from absorbed light. The time span of incident illumination acts a major factor in the healing time (Figure 2.6 (a)). Illumination with 15.2 W.cm^{-2} of an incident IR light irradiation for 10 s results in a 5 MPa stress break strength, while increased illumination times of 30s exhibited an original sample like mechanical strength (nearly 100$\%$) with a 20 MPa strength (Figure 2.6 (b)). Even direct heat (180 ^{0}C, for 10 mins) yielded a comparatively lower strength, due to their meagre heal ability(Figure 2.6 (c)) [111].

The self-healing ability of transesterification promoted conventional and hyperbranched epoxy (HBE) vitrimer networks was investigated with and without catalyst respectively. Eventually, significant healing was observed in the catalyst free HBE network at 150 ^{0}C for 90 mins, whereas at same conditions, only 30$\%$ crack healing was observed in the catalyst involved conventional epoxy network. Hence the faster healing behaviour of the HBE vitrimer was attained due to the presence of abundant hydroxyl groups in the network, which were acted as reacting moiety as well as catalyst for transesterification reaction [84]. Due to the higher T_g, self-healing effectively occurred at high temperature under slight pressure [112]. Furthermore, 2,2,6,6- tetramethyl-piperidinyl-1-oxyl radical (TEMPO) oxidized cellulose nanocrystals (TOCNs) crosslinker used epoxidized nature rubber (ENR) demonstrates the healing as well as TOCNs works as a reinforcing agent of the matrix. The observed healing efficiency 85$\%$was acquired through transesterification exchange reaction, achieved at 160 ^{0}C for 3h [113]. Photothermal properties for vitrimers containing nanofillers (0.5 wt$\%$ of polydopamine coated gold nanospheres) was also tested, where gold nanospheres were incorporated in epoxy vitrimers. The incorporation of gold nanospheres has been commenced an infrared laser (IR=3.5 W/cm^{2}for 120 s)

induced healing due to their tremendous photo thermal effect, which resulted a significant healing efficiency and hence subsequently investigated material healing at 180 ^{0}C for 10 min resulted a poor healing efficiency.

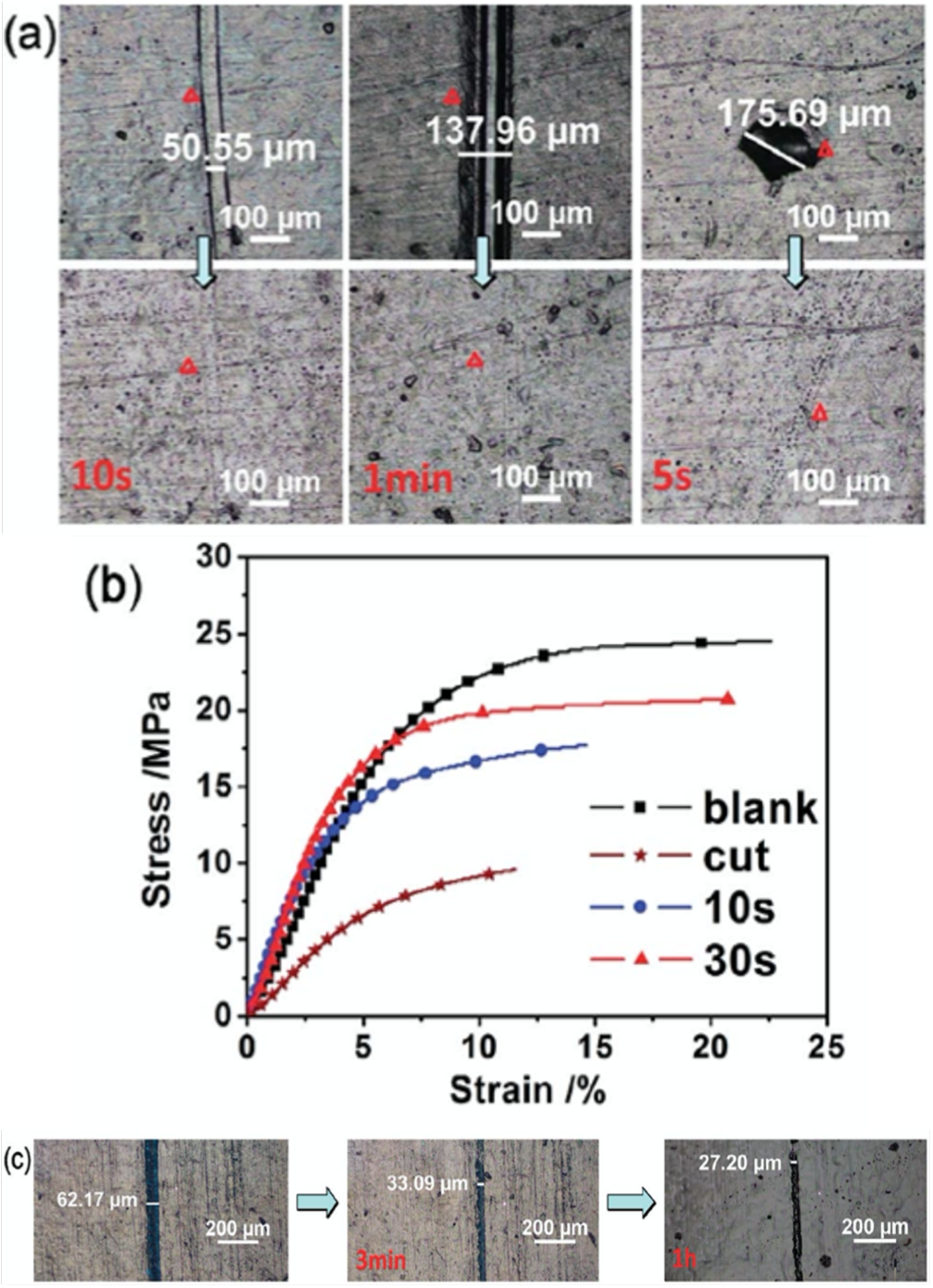

Figure 2.6: (a) Vitrimer-CNT light induced healing (b) Stress–strain graphs for different time healed samples (c) Healing of the samole at 180 ^{0}C [111]

However, agglomeration of gold nanospheres was observed and this disadvantage has been overcome by using polydopamine modified gold nanospheres,

where dispersion of the nanoparticles within the epoxy matrix is enhanced [114]. Henceforth, silica nanofillers impregnated epoxy was reported and their exchange reaction was designed via the disulfide exchange mechanism. To reduce the agglomeration while dispersion, a different functionalizations were introduced in the silica particles which increase their steric stabilization. From the performed unmodified, thiol-modified and epoxide-modified silica NPs containing epoxy networks, a healing efficiency at 180 ^{0}C [115]of up to 80 $\%$ was observed.

The combination of shape memory-properties is also attractive. Thus graphene-based dual triggered shape memory vitrimer nanocomposites were reported with transesterification chemistry. An overall shape memory had been observed in the presence of temperature and NIR light irradiation, whereas pristine epoxy networks have not persisted high shape memory effect under NIR light. However, graphene containing epoxy (1 wt$\%$) demonstrates an efficient shape memory under NIR irradiation, as graphene transforms the IR-radiation into heat , taken up from the irradiation [116]. A temperature dependent shape memory behaviour was observed for biobased epoxy vitrimers, where shape memory behaviour was observed at 80 ^{0}C(40s-55s) via the disulfide exchange mechanism [71]. Recently, UV cured epoxy vitrimer materials were reported based on the transesterification exchange reaction, and a shape memory effect was described through a conventional four step procedures: (1) heating up the system, (2) loading at the rubbery temperature, (3) cooling to a glassy state while holding the stress constant, and (4) unloading respectively [117]. Furthermore, epoxy liquid crystal elastomeric (LCE) vitrimers are discussed with covalent exchange network bonds, promoted through catalyst (triazabicyclodecene based transesterification reaction) where it allows to remould, realign and reprocess.

Permanent network involved epoxy LCEs does not exhibit shape memory behaviour like vitrimer systems, and the performed shape memory behaviour of the vitrimer material was commenced on or above their phase transition temperature (T_i=130 ^{0}C), which is above the glass transition temperature (T_g=50 ^{0}C) [118]. CNT based transesterification reaction promoted liquid crystalline elastomeric vitrimers (CNT-xLCE) demonstrated the light induced 3D structures [69]. A similar kind of transesterification promoted adaptable LCE vitrimers were synthesized via thiol-acrylate Michael-addition reaction, and this material demonstratess a low temperature shape memory effect (80 ^{0}C) [119]. When subject to various external stimuli the LCE based materials are explored to prepare multifunctional devices including artificial muscles. A disulfide ex-

change based LCE with reprocess able and self-healing ability is reported. The material can be reprogrammed from the poly-domain state to mono-domain state with external stimuli (heating or UV illumination) [120].

Table 2.1: overview of different vitrimer materials and their healing conditions

Mechanism	**Material**	**T_g**	**Healing conditions**	η	**Strength**	**Ref.**
Trans estrification	Biobased triepoxy	187 ^{0}C	220 ^{0}C and slight pressure	90%	[a]62.8–69.2 MPa	[112]
	Epoxy with tertiary amine	130 ^{0}C	160 ^{0}C, 3h	57%	[a]0.461 MPa	[81]
	Amino-capped aniline trimer liquid crystalline	58 ^{0}C	IR laser	100%	[b]20-22 MPa	[121]
	Epoxy with Polydopamine-modified gold nanospheres	42 ^{0}C	Light, 120mins	90-100%	[b]25MPa	[122]
Trans alkylation	poly(1,2,3-triazolium ionic liquid)	-8 ^{0}C - 23 ^{0}C	——	——	[f]15MPa	[97]
	poly(thioether)	-20 ^{0}C	160 ^{0}C, 45mins	100%	[f]80MPa	[98]
Disulfide	Epoxy with silica nano particles	151 ^{0}C -155^{0}C	180 ^{0}C, 30-120 mins	36.8-78.1%	[c]764±8	[115]
	Polyhydroxy urethane	66 ^{0}C	150 ^{0}C, 5-10MPa for 30mins	65%	[a]35MPa	[94]
	Epoxy with FRP	127 ^{0}C	200 ^{0}C, 100bar for 5mins	——	[d]242-292MPa	[123]
	Polycarbonate	19 ^{0}C - 34 ^{0}C	160 ^{0}C, 5-10MPa	64-80%	[c]7± 1MPa	[73]

Trans amination	Poly(vinylogous urethane)	87 ^{0}C	150 ^{0}C, 30mins	100%	^{e}2*10^3 MPa	[52]
Trans carbamoylation	Polyhydroxy urethane	54 ^{0}C	160 ^{0}C, 4MPa for 8hours	76%	^{e}2.2 ± 0.4 GPa	[70]

T_g- Glass transition temperature; η-Healing efficiency; a- Tensile strength; b- Stress-strain; c- Tensile modulus; d- Compression strength; e- Young modulus; f- Storage modulus.

Summary

An ADCAN contained thermoset vitrimer material all are having the ability to reprocess in certain physical conditions, however, self-healing behaviour of vitrimer has discussed sporadically, and from the above-mentioned chemistries, some of that was performed with absence of catalyst. Hence, very few studies were investigated the nanofillers (especially carbon based nanofillers) involved vitrimer material and their properties. The malleability of thermoset epoxy material, as well as shape memory behaviour at lower temperature has not explored. Therefore, to the best of knowledge catalyst free disulfide promoted self-healing epoxy vitrimer nanocomposite with shape memory behaviour has not been explained yet.

CHAPTER 3: DEVELOPMENT OF EPOXY/ GRAPHENE OXIDE VITRIMER NANOCOMPOSITE

3.1 Introduction

A covalent exchange studies had been done in thermoset material through different mechanisms like Diels- Alder chemistry [124–126], transesterification [59, 81, 127], transalkylation [128], trans amination [52], disulfide [129], often requires a catalyst. However, some disulfide exchange studies were reported without catalyst [123], where exchanges have been promoted through metathesis [130] or radical mediated exchanges [131]. The disulfide exchange mechanism is simple and efficient in many polymer networks, promoting exchange at lower temperature [91]. Hence the improvement of mechanical properties in polymers have been attained by addition of carbon nanomaterials [116, 132], especially the incorporation of GO has demonstrated a good impact in mechanical properties of polymeric networks [133–135].

Herein, we explore a robust approach to prepare a catalyst free graphene oxide promoted self-healing epoxy vitrimer nanocomposites. The synthesized nanocomposites demonstrate self-healing properties via disulfide exchange based covalent adaptive network behavior [131], where aromatic disulfide hardeners promote the radical mediated exchanges to effectuate the bond exchange in such vitrimer [123]. This study found that GO based nanofiller is helpful to enhance the self-healing properties including the shape memory and flexural strength of the materials. The GO endorsed lower glass transition was helpful to achieve a low temperature self-healing, where compared to epoxy vitrimers (73% and 60% self-healing) the vitrimeric nanocomposites demonstrates a 88% and 80% self-healing for the first and second cycle, respectively.

3.2 Materials and Methods

Bisphenol A diglicidyl ether (BADGE) (340.41 g/mol) resin and 2-Aminophenyl

disulfide (AFD) (248.37 g/mol)/ Diethylenetriamine (DETA) (103.17 g/mol) hardener was purchased from sigma-aldrich. The graphene oxide sheets prepared from graphite flakes, which was purchased readily from sigma-aldrich.

3.3 Preparation of epoxy nancomposite

Hummers method was followed to synthesis graphene oxide (GO) sheets [136]. The sulfuric acid (23ml) was added in the mixture of graphite flakes (1g) and sodium nitrate ($NaNO_3$) (0.5g) at 0 ^{0}C (ice bath). After 10 -15 mins, the Potassium permanganate ($KMnO_4$) (3mg) was slowly addedin the reaction mixture at 20 ^{0}C, then it was allowed at 35 ^{0}C for 7h.

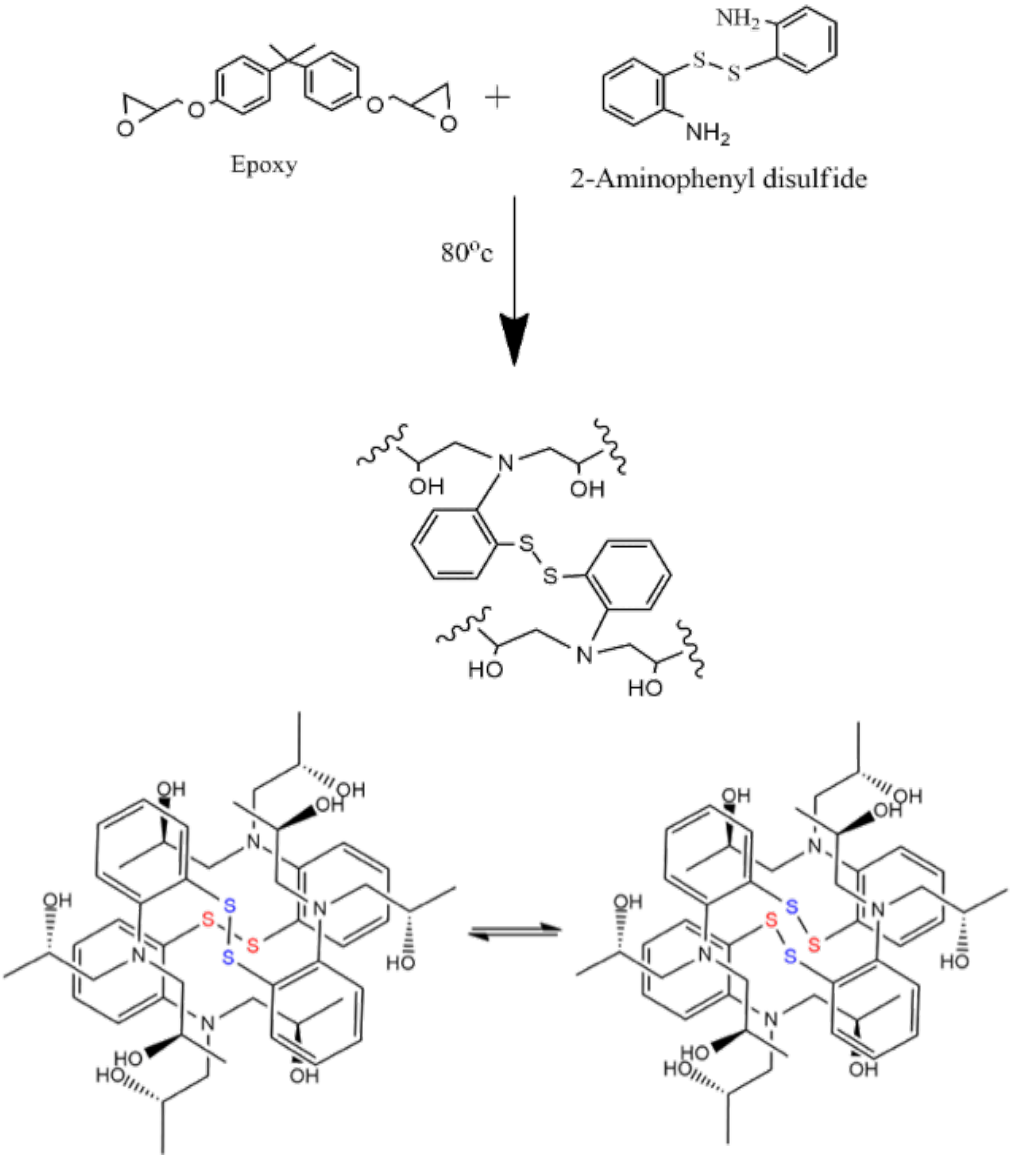

Figure 3.1: Synthesis and chemical structure of epoxy networks

Furthermore, Potassium permanganate ($KMnO_4$) (3g) was added slowly in the reaction and it was stirred at 35 ^{0}C for 10-12h. Then after, reaction mixture was cooled at room temperature and then cold water (133 ml) was added with 30% hydrogen peroxide(H_2O_2) (3ml). Finally, after certain time precipitated layer was washed with ethanol, HCl and water 3 times respectively by centrifuge. The synthesized GO (300 mg) was dispersed in 20 mL ethanol and ultrasonicated for 30 mins. The obtained GO solution was immediately added in the Bisphenol A diglicidyl ether resin and stirred vigorously. The different percentage of GO suspended solution added epoxy resin were named as EP- x% (x= 0,0.1,0.2,0.5,1,2), where 'x' denotes the GO weight percentage(Table A1). Furthermore, the mixture was heated at 80 ^{0}C and degassed under vacuum, till ethanol evaporation. After that, stoichiometric ratio of hardener (2-Aminophenyl disulfide (AFD)) was mixed and stirred for 15 min at same temperature (Figure 4.1).
Subsequently, the degassed mixture was poured into a silicon mould and cured in an oven at 150 ^{0}C for 5 h. For studying the impact of AFD on self-healing, Bisphenol A diglicidyl ether resin based reference specimen were also prepared using diethylenetriamine (DETA) as a hardener as per earlier reported method [137, 138]. To access the GO effects, reference pristine (R-Epoxy) and GO nanofiller impregnated epoxy (R-Epoxy-1%) nanocomposites were also prepared.

3.4 Characterization techniques

X-Ray Diffraction spectroscopy was analyzed through D8 ADVANCE ECO – Bruker to identify the graphene oxide. Spectro Photo meter UV-Vis (LAMDA 35, Perkin Elmer) spectra was recorded to address the GO in epoxy. The curing was observed through FT-IR (Frontier FT-IR/FIR, Perkin Elmer) spectra analysis. Graphene oxide dispersion in epoxy matrix was studied through HR-TEM, JEM 2100F, JEOL. The glass transition temperature was characterized through differential scanning calorimetry (DSC) experiments and also through TA-Q400em dimensional change experiments. Perkin Elmer differential scanning calorimeter (DSC-7) was performed at temperature range from 30 ^{0}C to 220 ^{0}C using 19.8mL/min nitrogen purge gas flow with 3bar pressure. In TA-Q400em, three-point bending test was performed to address the storage modulus, loss modulus, stress relaxation and stress-strain behavior of the rectangular specimens (15*5*0.5 mm). All dimensional change, storage modulus and loss modulus experiments were performed through temperature ranges from 40 ^{0}C to 120 ^{0}C using heating rates of 10 ^{0}C/min with 50mL/min nitrogen purge gas

flow and 0.02N force. In stress relaxation study, $1*10^{-3}$ N preloaded force applied to straighten the specimen. During test, required temperature and 1%strain was applied, then relaxation modulus was evaluated with respect to time. Stress-strain experiments were performed in strain ramp mode with 0.02N force and evaluated strain at 40 ^{0}C isothermal temperature.

3.5 Results and Discussions

The synthesized GO was analyzed through x-ray diffraction spectroscopy (XRD), to determine the interlayer distance between graphite layers. Hence the obtained graphite peak (26^0) has denoted the lower space between their interlayer, however, the performed oxidation process has shifted the graphite peak to 12.18^0 (Figure 3.2), where that represents the GO formation. Thus, resulted peak has described the larger distant between the graphite layer after oxidation, due to their chemical heterogeneity [139, 140].

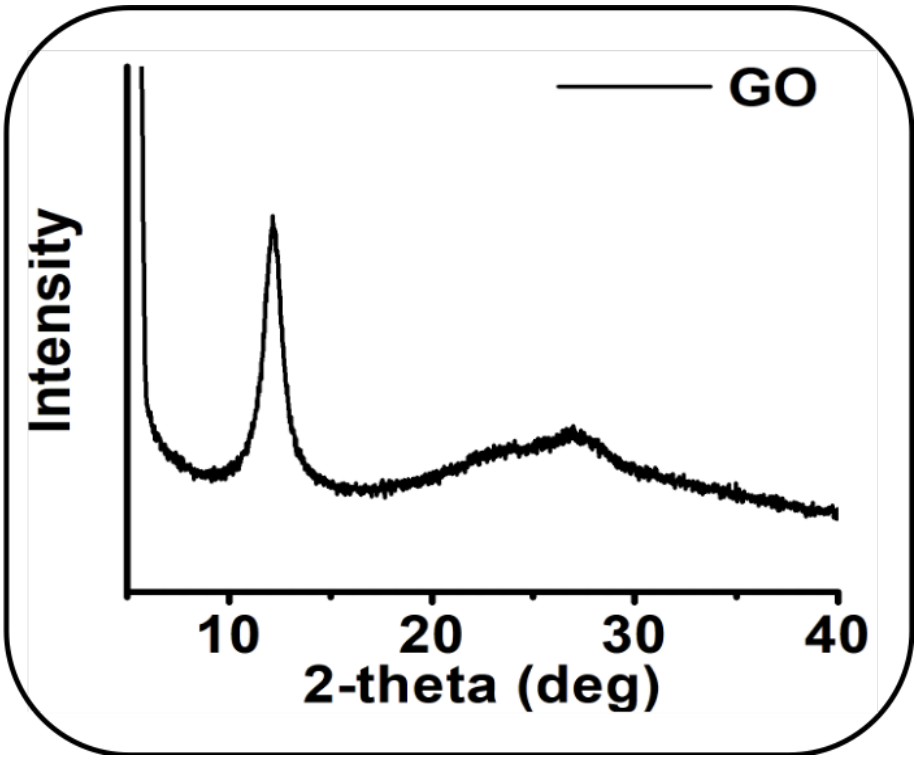

Figure 3.2: X-Ray Diffraction spectroscopy analysis for graphene oxide

An ethanol dispersed fine grinded vitrimer nanocomposite has evaluated through ultraviolet spectroscopy (UV) to observe the presence of GO in epoxy vitrimer composite. The absorbance peak at 221 nm witnessed the presence of GO in epoxy composite. The attained UV results for epoxy, GO and epoxy-GO composites had plotted together in Figure 3.3. Epoxy curing was investigated with

respect of time via FTIR, and after 5 hours declination of oxirane rings (at 914 cm^{-1}) was held as constant, and thus confirms the epoxy curing completion (Figure 3.4).

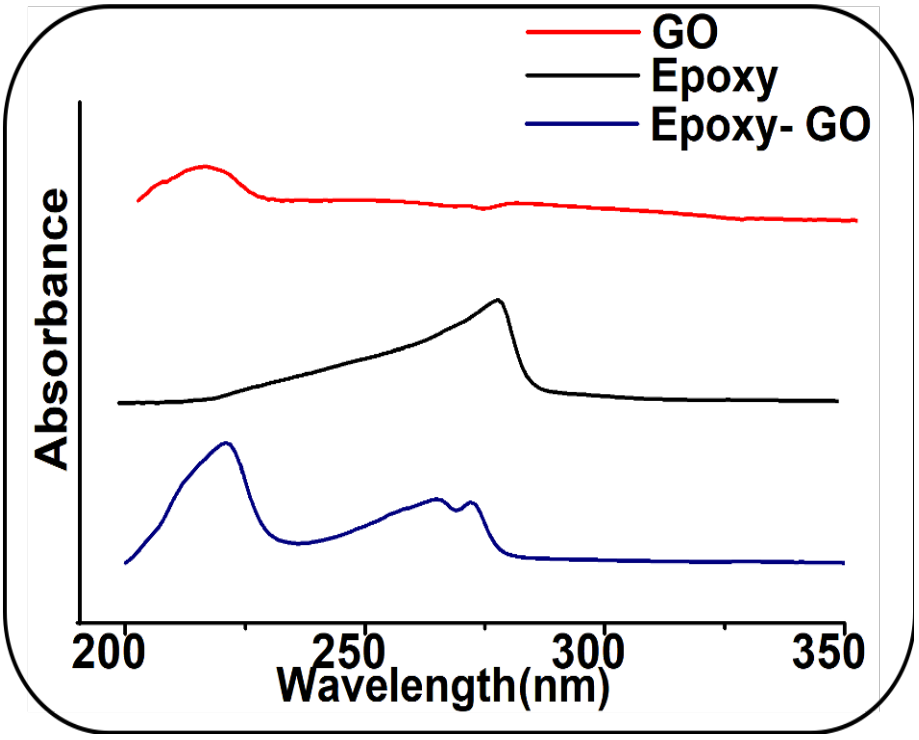

Figure 3.3: UV spectrum for GO, epoxy, and epoxy GO nanocomposite

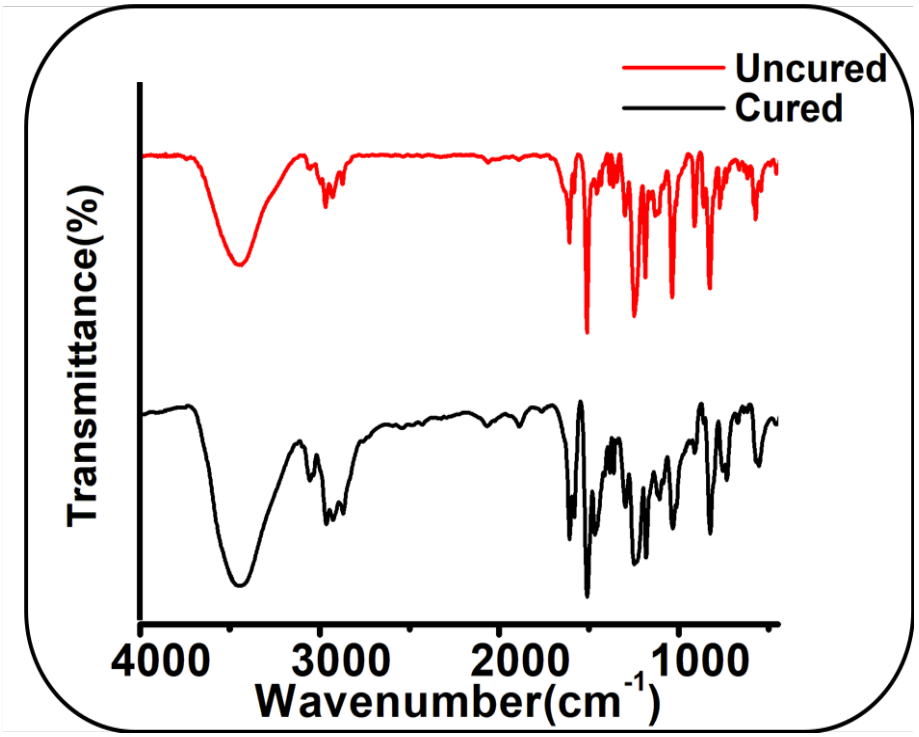

Figure 3.4: FTIR spectrum for uncured and cured EP-1%

Based on FTIR results, cured pristine and GO involved samples have demonstrated the same stretches with an imperceptible change in the hydroxyl group region ($\sim$3400 cm^{-1}). The increased hydroxyl region has determined the performed epoxy was reacted with amine groups, also with the small amount of hydroxyl groups. Due to this, the hydroxyl group interaction between GO and epoxy have been expected; altogether, the minimal hydroxyl groups of GO could be reacted with the epoxy [141]. Furthermore, epoxy curing fulfilment was verified through THF solvent swelling test, as shown Figure 3.5. After 10 mins vigorous stirring cured epoxy was not dissolved whereas, a fully dissolved solution was obtained for uncured epoxy.

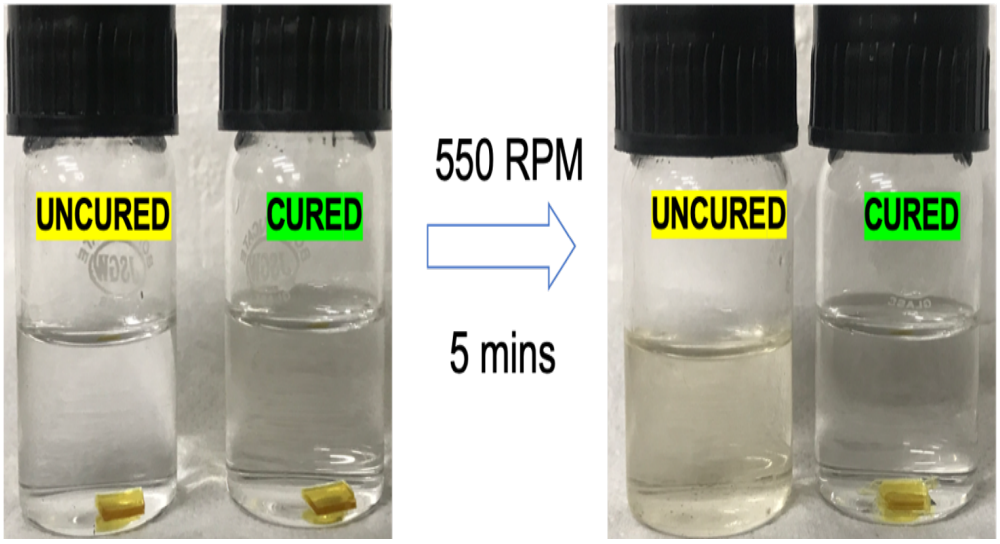

Figure 3.5: Photographs of uncured EP-1% and cured EP-1% in THF solvent to prevail the solubility differences

To analyze the glass transition (T_g) thermal properties of pristine epoxy and nanocomposites have been studied (Table 3.1).

Table 3.1: Thermal properties of epoxy GO vitrimer nanocomposites

EP-x%	Tg (^{0}C) (DMA)	Tg (^{0}C)(DSC)
EP-pristine	64	62
EP-0.1	62	59
EP-0.2	59	57
EP-0.5	56	54
EP-1	53	48
EP-3	56	52
R-Epoxy	69	67
R-Epoxy-1	58	55

The performed TA Q-400em is helpful to acquire the T_g from their temperature

modified dimension changes(Figure A1). While increasing GO content in the matrix, the chain mobility increases due to poor interface interaction between epoxy and the GO, and thus poor interaction exhibits a free volume between the filler and matrix. Therefore, polymer chains near the interface moves freely into the free volume and thus resulted an increment in chain mobility and decrease in T_g [142]. However, an addition more than 1% GO increases the T_g, which could be due to the agglomeration of GO in epoxy and vitrimer matrix [143, 144]. The obtained lower T_g is helpful to achieve a low temperature self-healing and shape memory properties. Therefore, further study was focused for the nanocomposites containing maximum 1 wt% GO in matrix. DSC investigations (Figure 3.6) were also carried out and a similar trend in T_g was observed with minor difference with the data obtained via TMA.

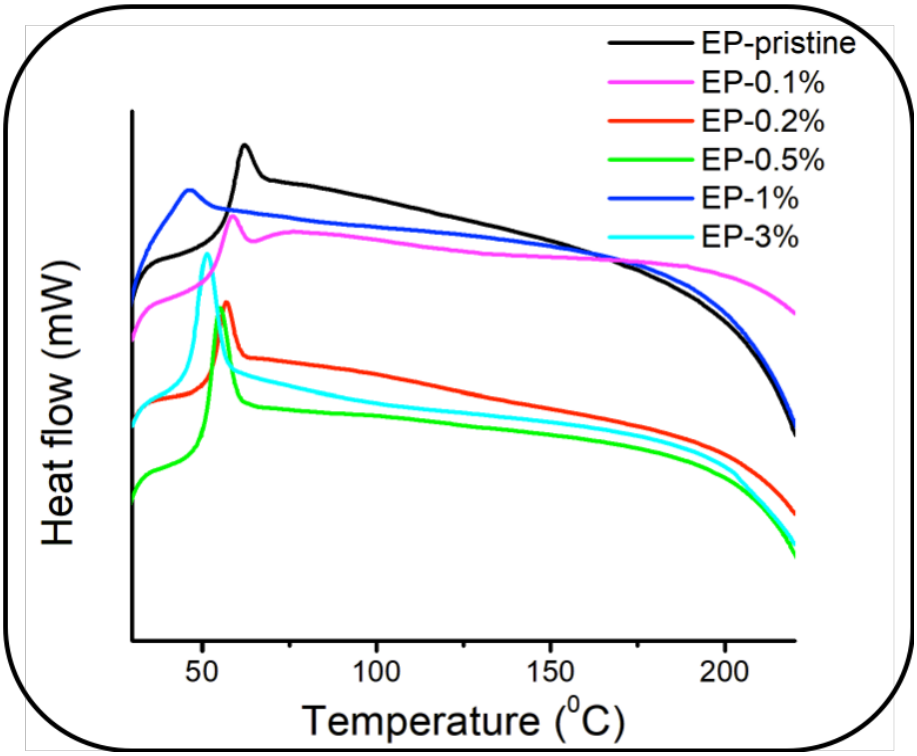

Figure 3.6: DSC results of EP-pristine and EP-x% nanocomposites

The dispersibility of the graphene oxide nanosheets was analyzed using optical microscopy, where a homogeneous dispersion of graphene oxide nanosheets was obtained. The indicated optical images are helpful to capture a large area (1 cm scale bar) (Figure 3.7 (a, b)), where we could not observe any kind of bundles (due to graphene agglomeration). However, TEM image further supports the uniform dispersion of nanofillers in epoxy matrix (small scale;100 nm) with higher resolution) (Figure 3.7 (c)).The images show an excellent dispersion of GO nanosheets in epoxy vitrimer matrix (EP-1%).

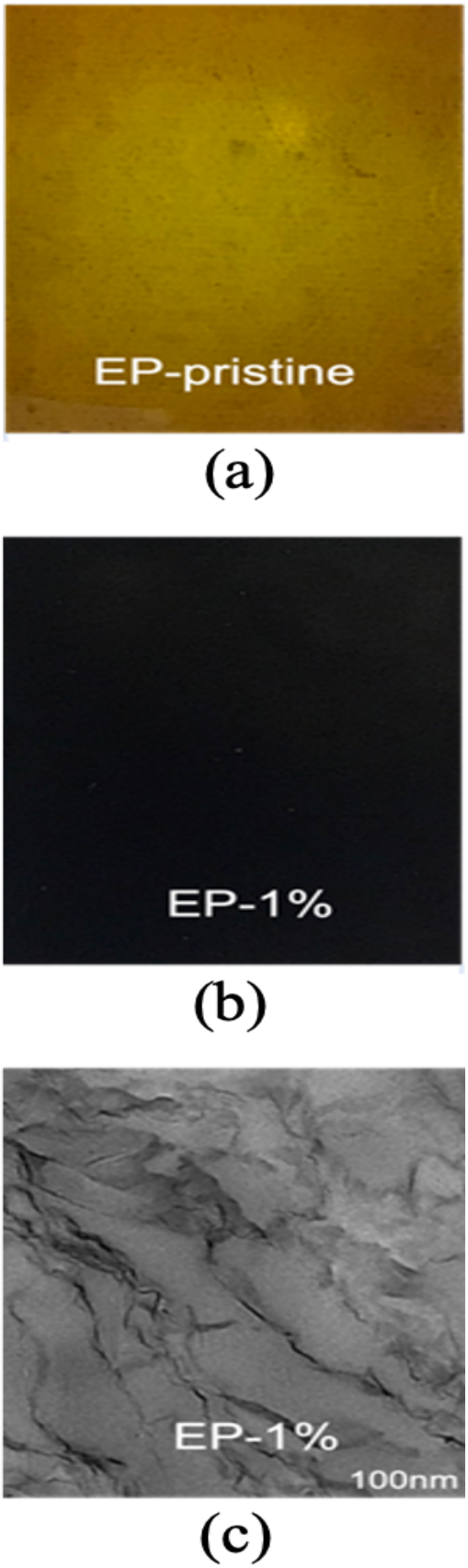

Figure 3.7: Optical image of (a) EP-pristine and (b) EP-1% (c) TEM image of epoxy vitrimer GO nanocomposites (EP-1%)

To understand the nano filler influences on the mechanical behaviour of the prepared epoxy vitrimer, a dynamic three-point bending test was carried out. Furthermore, DETA cured pristine and GO involved epoxy was investigated to validate the changes in mechanical properties with vitrimer epoxy and hence attained results were tabulated in Table 3.2(shown in Figure A2). The temperature dependent viscoelastic behavior of the epoxy vitrimer material was addressed from the storage (E') and loss (E") modulus. The results show high storage modulus (52.2 GPa) at 40 ^{0}C for high GO containing sample (EP-1%). A gradual increase of storage modulus according to the nanofiller was observed in (Figure 3.8 (a)) and attained values are tabulated in Table 3.2.

Table 3.2: Mechanical properties for different epoxy/GO nanocomposites

EP-x%	Storage modulus (GPa)	Flexural strength (MPa)	Flexural strain (mm/mm)
EP-Pristine	39.7	17.9	0.058
EP-0.5	43.7	18.17	0.055
EP-1	52.2	19.2	0.054
R-Epoxy	42.8	18.3	0.055
R-Epoxy-1	53.9	20.1	0.051

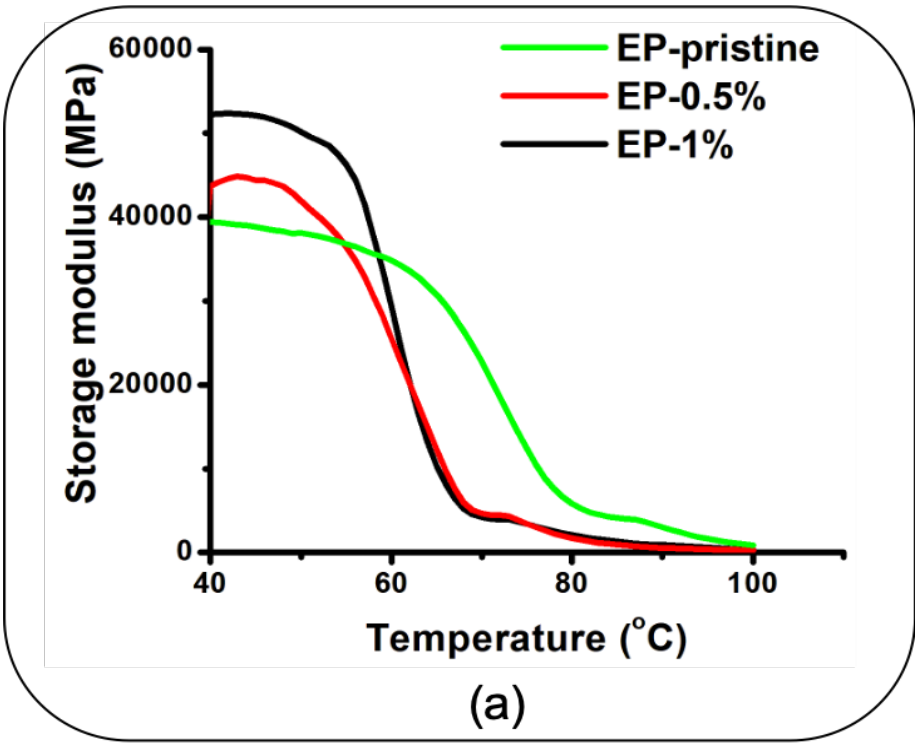

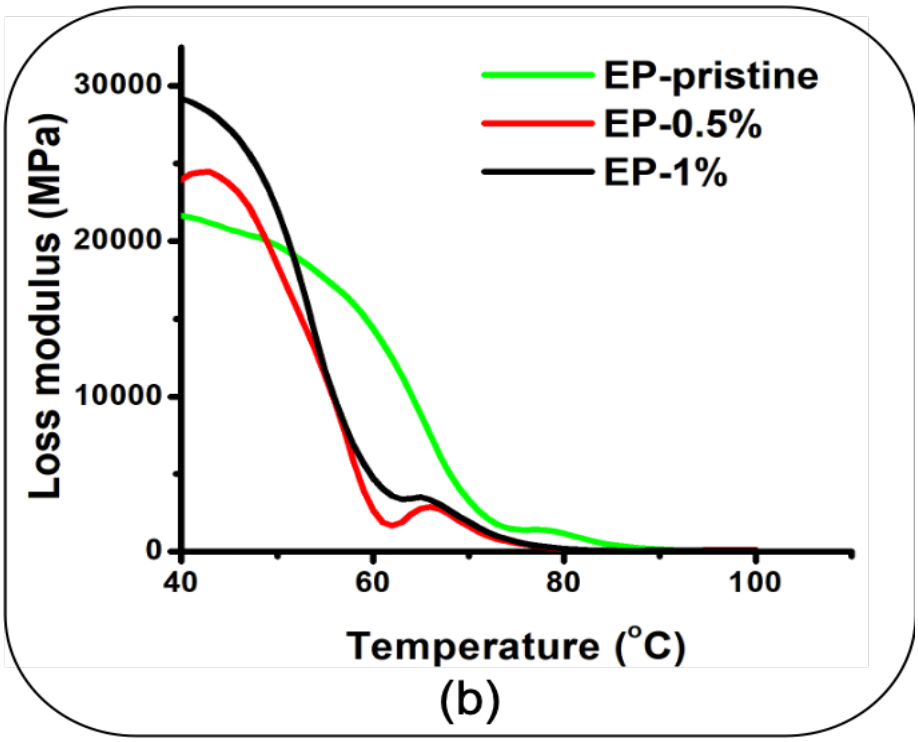

Figure 3.8: (a)storage modulus (b)loss modulus

The increment in modulus could be due to the presence of GO wavy topology, where it has been helpful to achieve the efficient intercalate interlocking with polymer matrix and modulus changes [144]. Furthermore, the loss modulus (E") (Figure 3.8 (b)) witness the viscoelasticity of the material through E'>E" behavior. Stress-strain relationship of vitrimer nanocomposites have identified through same three-point bending test with force ramp mode at 40 ^{0}C. The analyzed flexural stress-strain behaviors of EP-pristine, EP-0.5% and EP-1% have been plotted in Figure 3.9 (a), where higher flexural strength was obtained for sample EP-1% compared to EP-Pristine and EP-0.5%, and the resulted flexural strengths for EP-0.5% and EP-1% were 1.1% and 7.1% higher than the EP-pristine samples (Table 3.2). The reduction in strain-at -break was helpful to determine the stiffness increment of nanocomposites [133].Fracture toughness reduction also affirmed the flexural modulus augmentation and resulted flexural modulus had been increased to 0-9.4% with the involvement of GO nanofillers.

Compared to EP-0.5% and EP-1%, a 1.4%and 9.4% lower in flexural modulus was obtained for the pristine epoxy sample. The nanofiller based difference in flexural strength and flexural modulus are detailed in Figure 3.9 (b). And different flexural studied values (strength and strain at break) of conventional and vitrimer epoxy networks are tabulated in Table 3.2. The conventional epoxy

networks (R-Epoxy and R-Epoxy-1%) have resulted a greater mechanical properties than the AFD cured vitrimer epoxy network, which could be due to the stronger bonding strength and higher crosslink density of aliphatic amines [145].

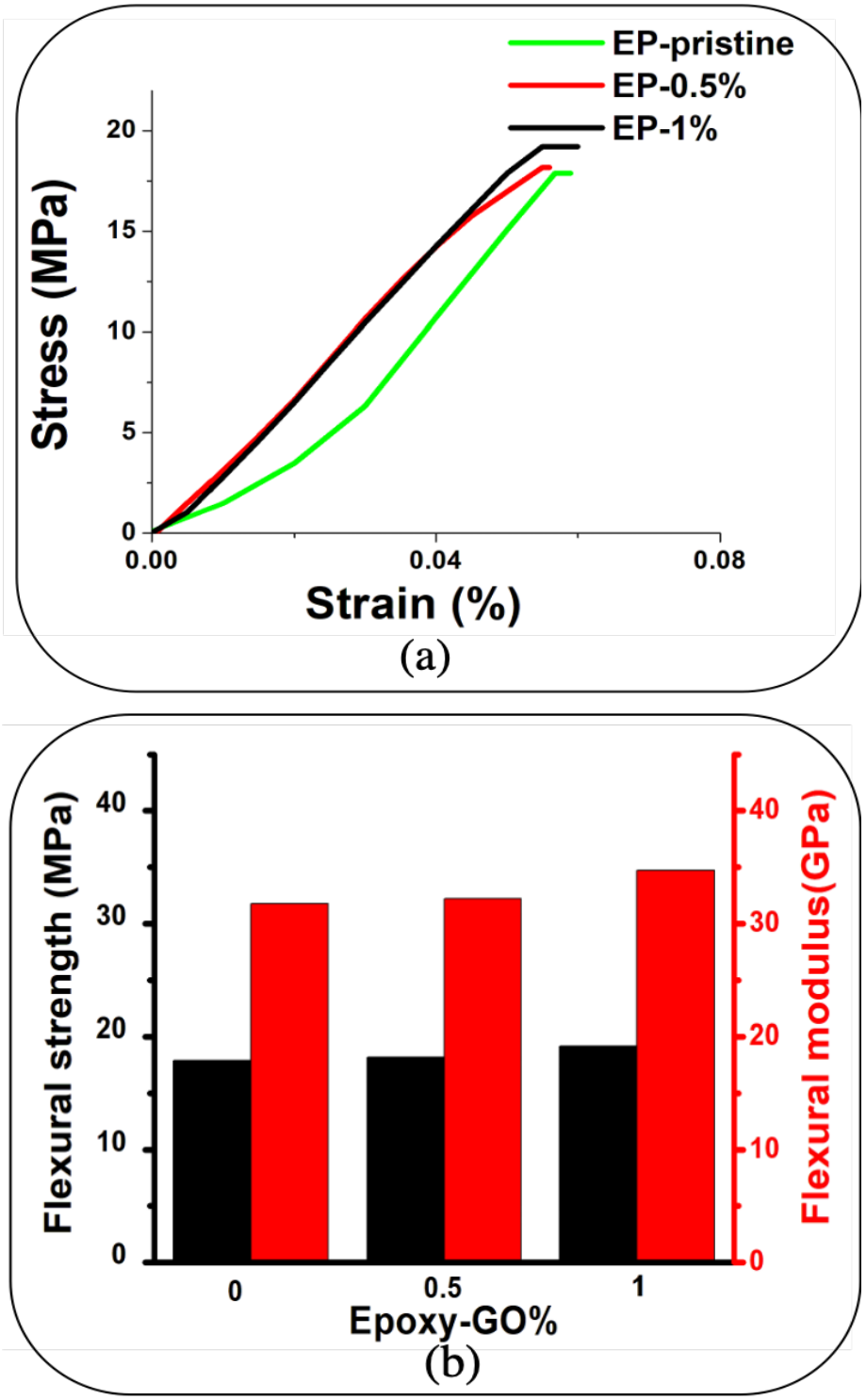

Figure 3.9: (a) Stress-strain relationship between different epoxy vitrimer nanocomposites (b) Flexural strength and flexural modulus of nanocomposites

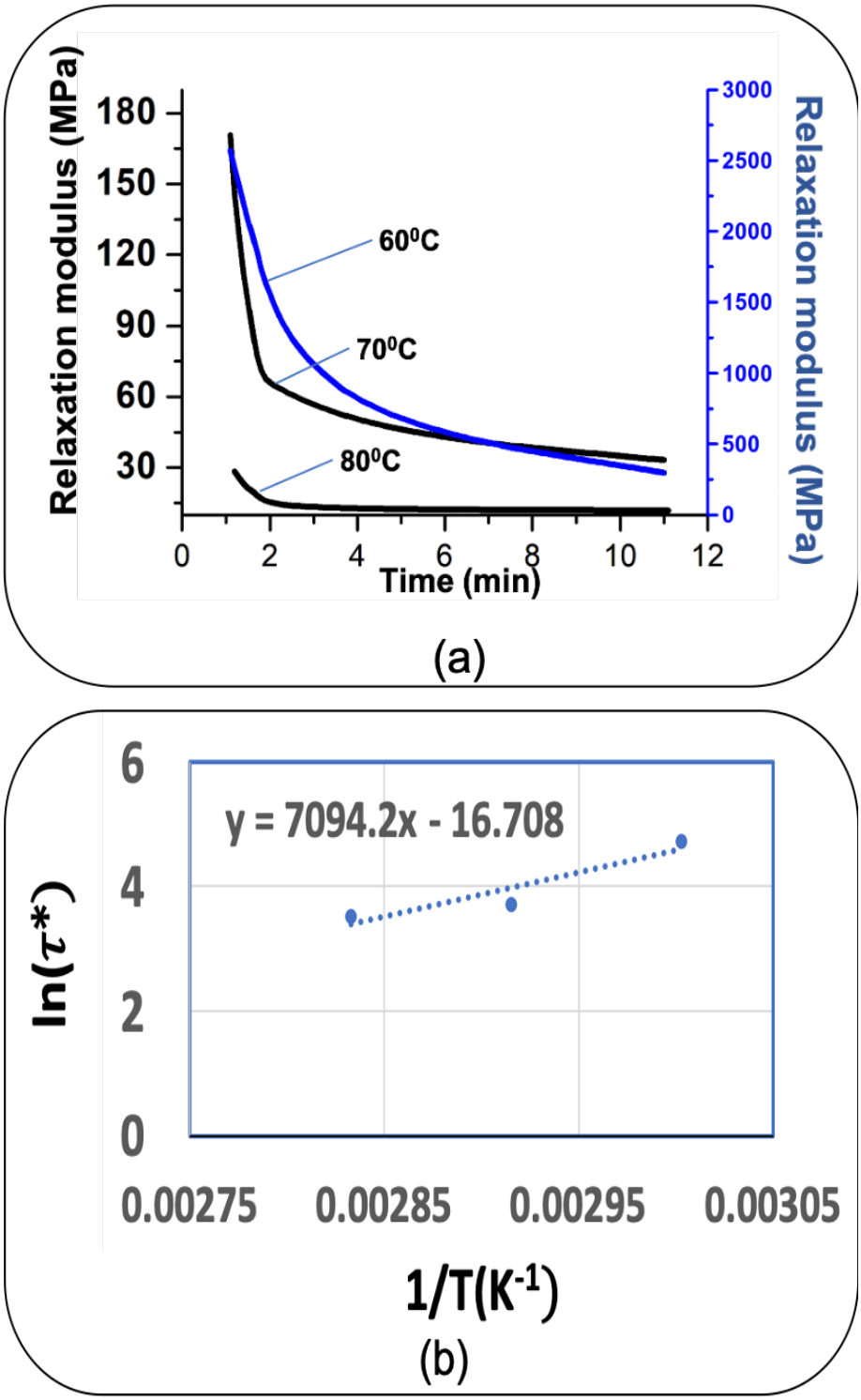

Figure 3.10: (a) Stress relaxation analysis in different temperature for pristine epoxy vitrimer (b) Arrhenius plotted graph for epoxy vitrimer

Vitrimer behavior of the epoxy nanocomposites has been confirmed through stress relaxation analysis, which tends to evaluate the relaxation modulus of malleable material [146] and resulted time dependent relaxation modulus has

been plotted according to their temperature determined results (Figure 3.10 (a)). The prevailed high relaxation rates represent a rapid disulfide exchanges in the material. The relaxation time decreases with respect of temperature, and reduction in time describes the faster disulfide exchange [71].

$$y = 7094.2x - 16.708$$

Which corresponds to : $\ln(\tau^*) = E_a/R\ (1/T) + \ln(\tau_0)$

$$\ln(\tau^*) = 7094.2 * 1/T - 16.708$$

$$E_a/R = 7094.2$$

$$\mathbf{E_a = 7094.2 * 8.314 = 59\ kJ/mol}$$

$$\eta = G.\ \tau^*$$

G- Shear viscosity modulus;

Relation between shear modulus and tensile modulus,

$$G = E'/\ 2(1+\upsilon)$$

Generally, υ- Poisson's ratio is 0.5 for rubbery materials.

So , $G=1504/3= 501MPa$ (or) $501*10^6$ Pa

$$\tau^*= 10^{12}/(501*10^6) = 1996\ s.$$

$$\ln(\tau^*) = \ln(1996) = 7.59.$$

Equation obtained from Arrhenius law:

$$\ln(\tau^*) = 7094.2x - 16.708$$

$$x=1/T= (\ln(\tau^*)+16.708)/7094.2 =0.003426$$

So, $T= 1/0.003426$

$$\mathbf{T_v=292\ K\ (or)\ 19^0C}$$

Here stress relaxation test was performed for EP-pristine The performed temperature ranges 60 ^{0}C, 70 ^{0}C and 80 ^{0}C have been resulted a relaxation times 112.8 s, 40.8 s and 34 s respectively. The obtained results suggest a fast exchange reaction after T_g and rapid relaxation of applied stress. Hence, obtained results were plotted in Arrhenius equation (4) (Figure 3.10 (b)), and obtained a low activation energy (E_a = 59/KJ mol-1) [70, 147].

$$\tau^* = \tau_0 exp(E_a/RT) \tag{4}$$

Generally material topology transition change temperature has been considered when viscosity crossed 10^{12} Pa.s [74]. According to this conventional consideration, extrapolated topology freezing transition temperature (T_v) was 19 ^{0}C, calculated using Maxwell's and Arrhenius equation. Self-healing behavior was investigated for the prepared samples at the temperature value of 80 ^{0}C, however reference samples (R-Epoxy and R-Epoxy-1%) have not demonstrated a self-healing behavior. The healing for vitrimer could be due to their disulfide mediated radical exchanges [123]. A low temperature self-healing (60 ^{0}C for 5mins) was obtained for the sample EP-1% (Figure 3.11).

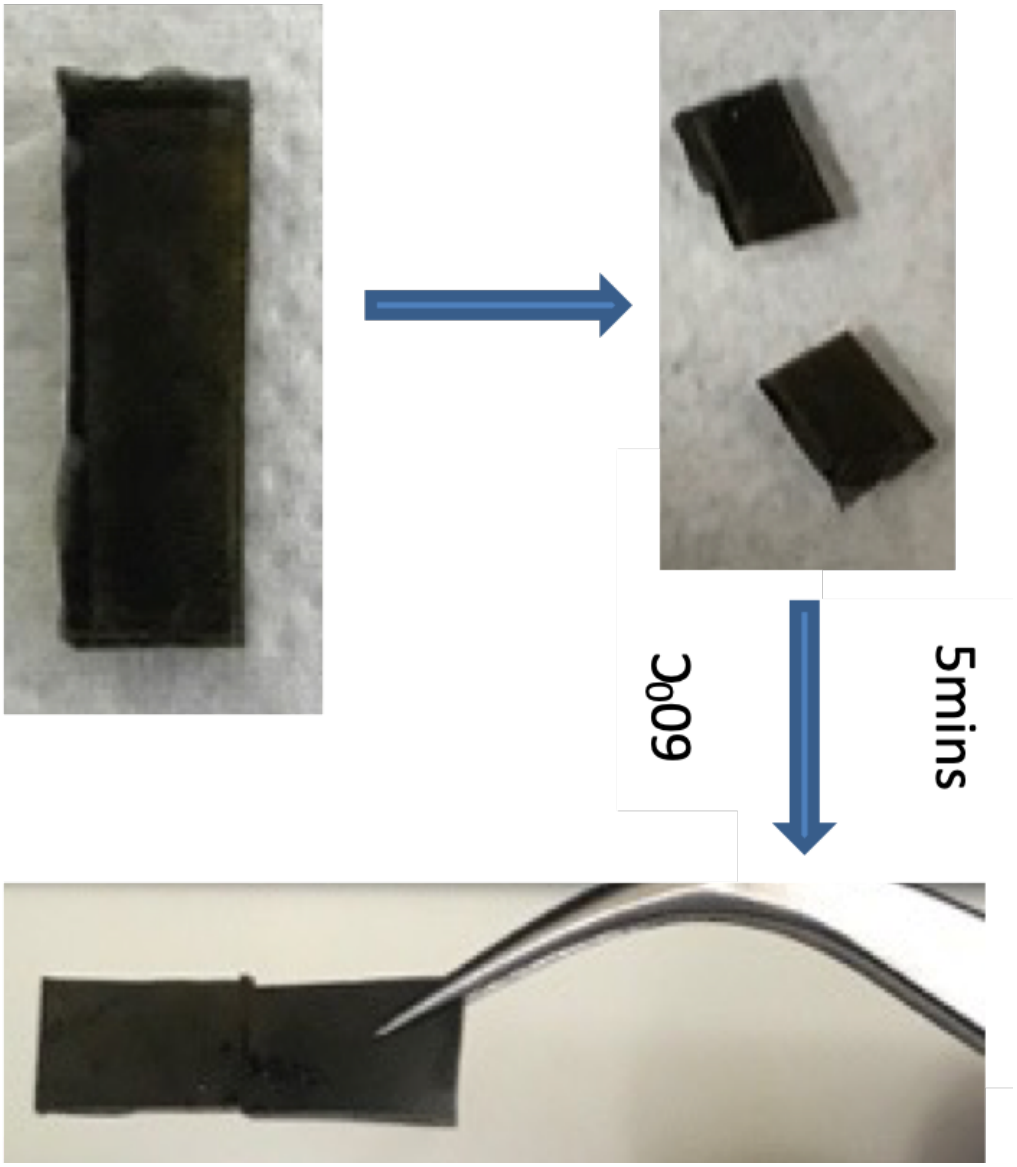

Figure 3.11: Optical images of uncutted, cutted and healed EP-1% specimen

Thus obtained self-healing temperature is related to the GO content, helpful to reduce the T_g [144], as discussed earlier using DSC data. The temperature extension after T_g merely tends the chain mobility, owing to this, GO fillers were effectively contributed to attain the low temperature healing.

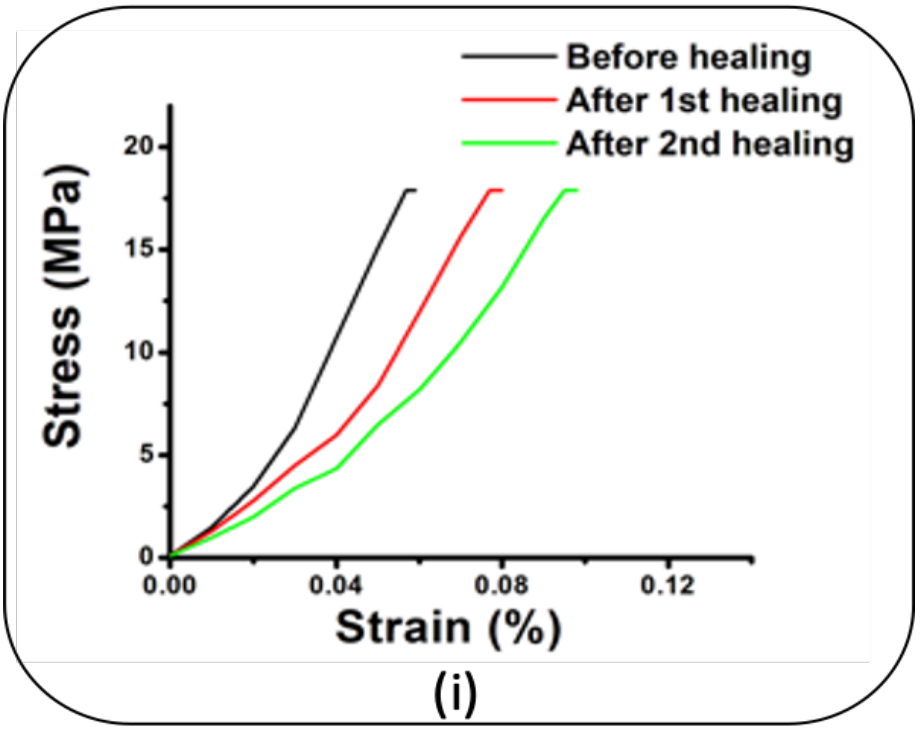

(i)

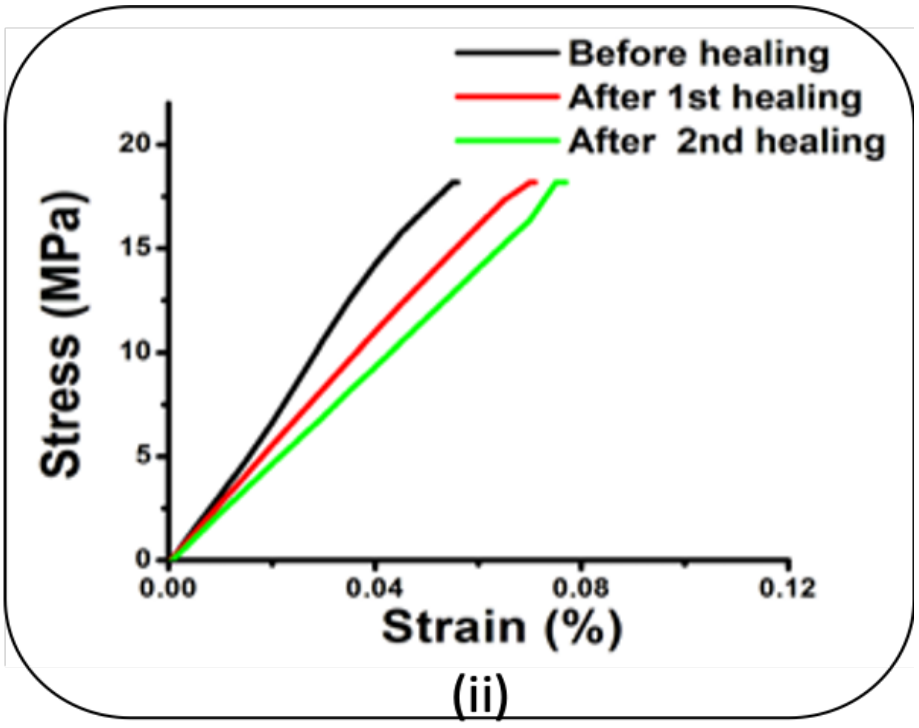

(ii)

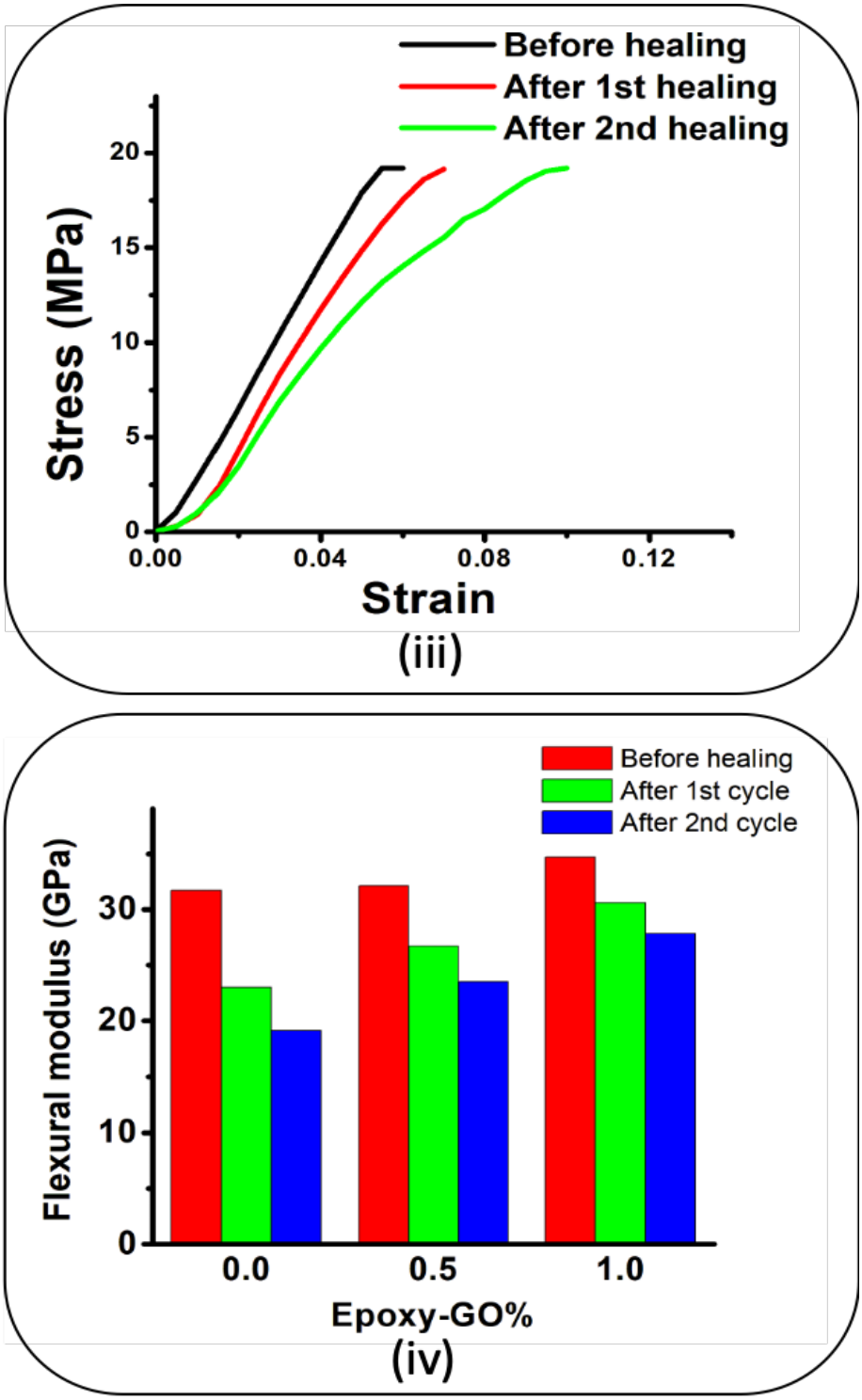

Figure 3.12: Healing represented stress-strain curves for i) EP-pristine ii) EP-0.5% and iii) EP-1% (iv) Flexural modulus changes after healing cycles for different samples

In this study, test specimen was cut into two pieces by razor blade and fractured samples were immediately put together for 5mins at 80 ^{0}C temperature

with the help of tweezer. The resulted healed samples efficiency was evaluated from flexural studies and two times healed samples stress-strain relationships had studied. Healing efficiency percentage was calculated through the equation 5, Where efficiency has been evaluated from their virgin ($K_{ICvirgin}$) specimen flexural modulus and healed specimen flexural modulus ($KI_{Chealed}$) [148].

$$\eta = K_{ICHealed}/K_{ICvirgin} \tag{5}$$

After healing no changes were observed in flexural strength, but flexural modulus was reduced intensively, due to their increased strain shown in Table 3.3.

Table 3.3: Flexural modulus changes after healing

EP-x%	Before healing (GPa)	After 1^{st} healing (GPa)	After 2^{nd} healing (GPa)	Shape memory (%)
EP-pristine	31.7	23.0	19.1	95
EP-0.5	32.1	26.7	23.5	100
EP-1	34.7	30.6	27.8	100

The reduction in crosslink density has been observed after each cycle of healing via flexural studies, where the material was elongated with respect to the applied stress. Consequently, the increment in elongation of the healed specimen has perceived due to the subtle entanglement of chain linkages [149].

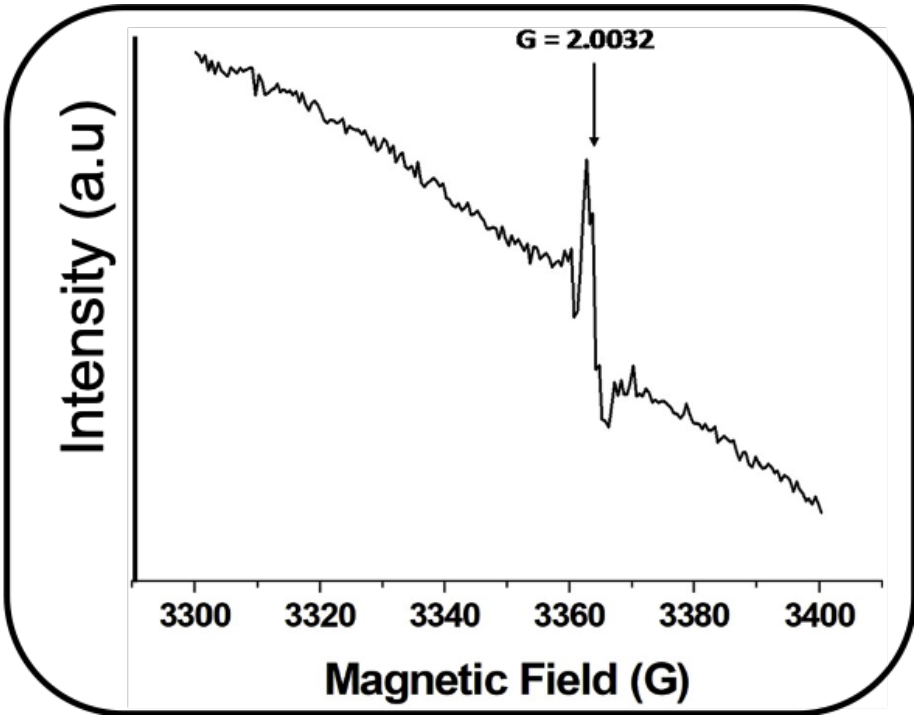

Figure 3.13: EPR spectrum of EP-1% sample at 70 ^{0}C

Thus, repeated healing of the material extends their healing region width, which is directly interacting to the stress; and helpful to enhance the specimen toughness [150]. Further, increased strain at break determines the limitation for entanglement of crosslinked chains and also pertained the crosslink density reduction [151]. After healing, EP-pristine, EP-0.5% and EP-1%were regained their flexural modulus as 73%, 83% and 88% and furthermore second healing cycle exhibited a 60%, 73% and 80% respectively (Figure 3.12).

Hence reported values were helpful to determine the prevailed healing efficiency, and it was postulated GO is beneficial to achieve the efficient healing. EPR spectroscopy was used for the confirmation of the radical-mediated exchange mechanism (Figure 3.13). The solid state EPR analysis assents the radical exchanges at healing temperature (70 ^{0}C), and attained isotropic EPR signal (g-value= 2.0032) confirms the disulfide exchange reaction [152] for the prepared vitrimaric materials, designed to achieve the self-healing behavior. Shape memory behavior was also observed for all the vitrimer samples, where deformation of the material changes their molecular chains conformation and entropy in presence of temperature and force [153]. Thus, material deformation attaining temperature was denoted as shape transition temperature (T_{trans}), which was higher than the T_g.

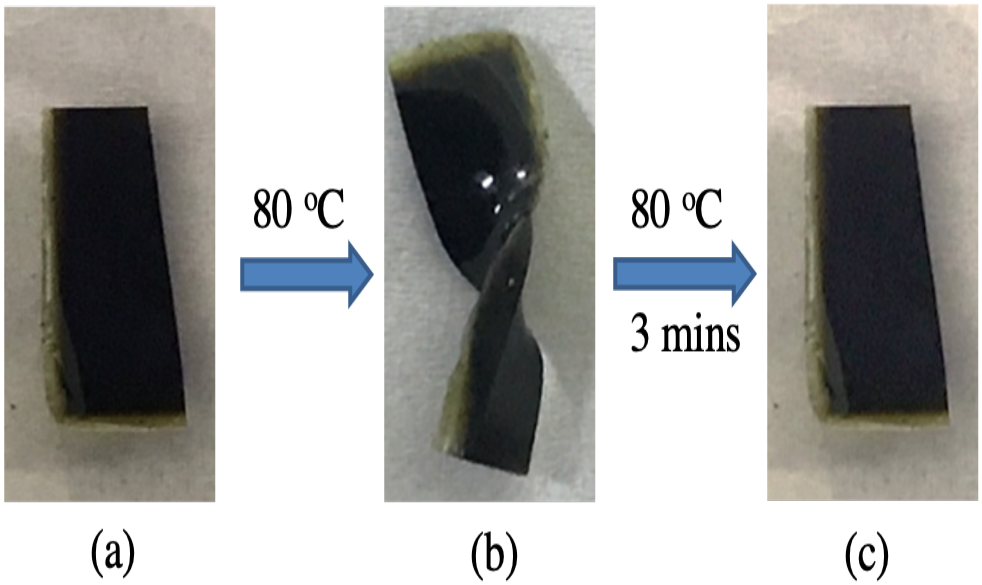

Figure 3.14: Shape recovery of EP-1%nanocomposite. (a) Flat specimen, (b) Deformed (θ_i) and (c) Recovered (θ_f) specimen

Here the material was heated at 80 ^{0}C(T_{trans}) to increase their molecular chain mobility and the prevail external force helps to deform the defined conformation

and entropy, whereas, cooling down the material below to T_{trans} has endured to fixed it in temporary shape with stabilized entropic energy. While reheating material above T_{trans} without force tends to activate molecular mobility and release their entropic energy to recover their permanent shape. The shape recovery ratio (R_r) has been calculated through equation 6.

$$R_r = (\theta_i - \theta_f)/\theta_i \tag{6}$$

Where, θ_i denoted a deformation angle, and θ_f stands for change of angle with respect to time [154]. Here flat specimens were deformed (θ_i) to 180^0 angle at 80 ^{0}C temperature, then it was allowed to be cooled down at room temperature to retain their temporary shape. After that, permanent shape of the specimen was regained with help of heating at 80 ^{0}C for 5 mins and change of angle (θ_f) was noted with respect of time. Based on the calculations (for details, see supporting information), EP-pristine retrieved their shape almost 95%, though incorporation of GO resulted 100% recovery (Table 3.3, Figure 3.14 (a-c)). Generally, carbon nanomaterials are having ability to store the entropy in polymeric matrix [155], and having the tendency to restore their entropy while reheating, so GO was extended that behavior effectively to achieve an efficient shape memory through their restoring entropy energy. And also, EP-1% shape memory was demonstrated at 60 ^{0}C, this low temperature shape memory has established due to their glass transition temperature, as described earlier.

Summary

The performed epoxy/grphene oxide (GO) based vitrimer has promoted their exchanges through disulfide exchanges, which was helpful to attain the self-healing, hence included GO has demonstrated low temperature self-healing (due to lower T_g) and prominent shape memory properties. The optimized results were addressed one percentage of nanofiller involved epoxy vitrimer (EP-1%) had resulted a 7.1% and 9.4% higher flexural strength and modulus than pristine epoxy vitrimer. Hence resulted a prominent self-healing and intact shape memory at 80 ^{0}C for 5 mins, whereas nanofiller involved epoxy vitrimer (EP-1%) demonstrated self-healing at 60 ^{0}C for 5mins and shape memory at 80 ^{0}C for 3 mins. The resulted self-healing efficiency was assessed through flexural studies, and EP-1% has demonstrated 88%and 80%healing after two consecutive healings respectively.

CHAPTER 4: DEVELOPMENT OF EPOXY/ POLYDIMTHYLSILOXANE/ GRAPHENE OXIDE VITRIMER NANOCOMPOSITE

4.1 Introduction

Catalyst free disulfide exchange promoted epoxy/PDMS/GO nanocomposite vitrimer materials with self-healing behavior was studied after epoxy/ GO nano compsite. The addition of PDMS should not only be helpful for achieving the low temperature self-healing, but would also be helpful to overcome the brittleness of epoxy matrix and improve its impact properties, including the resistance of crack propagation in. As covalently crosslinked pristine epoxy demonstrates a brittle failure, so the involvement of flexible epoxy terminated polydimethylsiloxane has effectuated to increase the toughness, and graphene oxide nanofiller were introduced to enhance the material strength.

The performed composite vitrimer material exhibits a reduction in glass transition temperature (T_g) and storage modulus including the enhancement in flexural strain. The mechanical strength was increased by the addition of graphene oxide nanofillers, and fine dispersion of PDMS and graphene oxide was evaluated through SEM and contact angle measurements. Furthermore, vitrimer behavior has observed through stress relaxation characteristics and Arrhenius plot, where the prepared material displays the self-healing at 80 ^{0}C for 5 mins, whereas a low temperature self-healing (60 ^{0}C) was observed for epoxy/PDMS/ GO nanocomposites.

4.2 Prepararion of epoxy-PDMS compsite

In round bottom flask, BADGE resin and epoxy terminated PDMS(800 g/mol; sigma-aldrich) was stirred at 130 ^{0}C for 7 hours, and later 2-Aminophenyl disulfide (2-AFD) was added and reaction mixture was continuously stirred at same temperature for 15 mins (Figure 4.1). Subsequently, reaction mixture was poured into mold and kept at 150 ^{0}C for 5 hours for curing.

Finally, attained specimen was used for further studies to evaluate the mechanical and self-healing properties. To optimize the PDMS effect in epoxy, different percentages of PDMS has involved in matrix and investigated effectively (shown in Table 4.1), and the samples were denoted as EP-x%(x = p (0), 1, 2, 3 and 5)(Table A2(a)). The similar procedure was followed for the preparation of nanocomposite, where different percentage of ethanol dispersed GO solution was added in the mixture (PDMS/epoxy) and continued stirring till ethanol evaporation(Table A2(b)). Finally, 2-AFD was added and stirred for another 15 min. The reaction mixture was poured in the mold and kept in oven at 150 ^{0}C for 5 h.

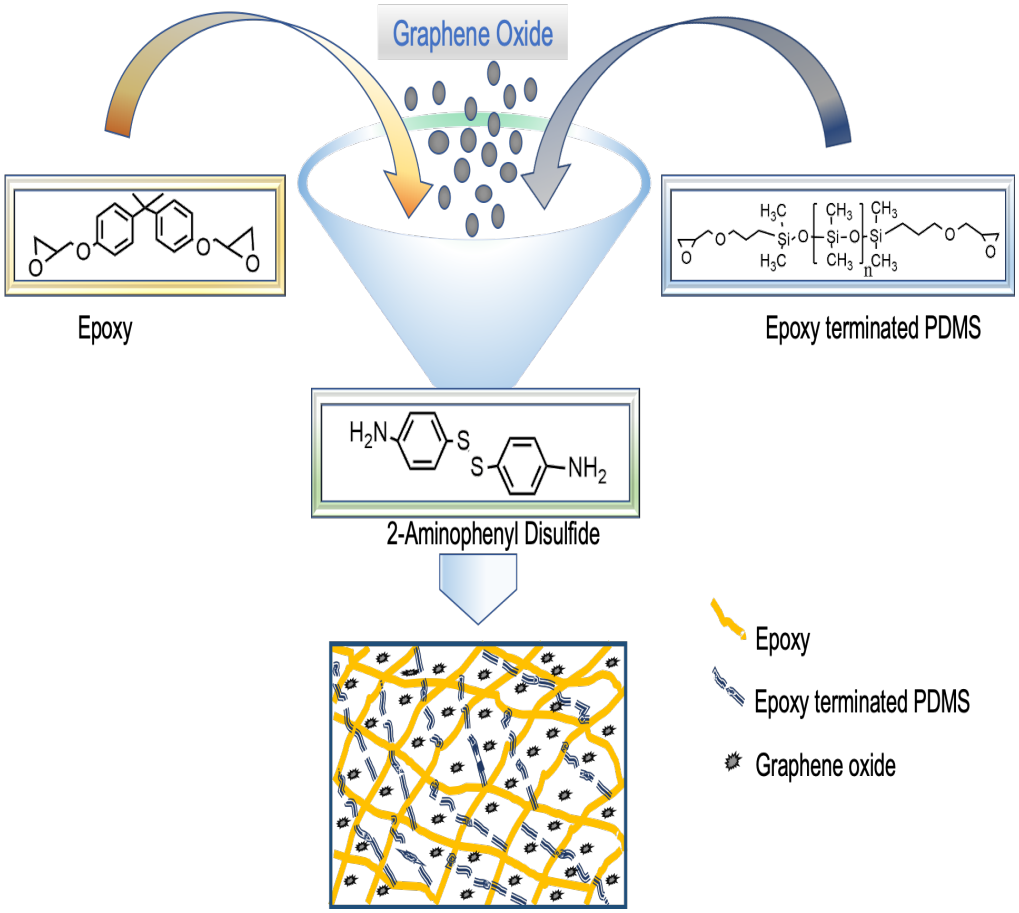

Figure 4.1: Synthesis route of epoxy-PDMS-GO nanocomposite

4.3 Material Characterization

Graphene oxide (GO) was prepared through Hummers method(Hummers and Offeman, 1958; Nia et al., 2014) (SI) from graphite flakes and obtained X-Ray Diffraction spectroscopy (XRD) (D8 ADVANCE ECO – Bruker) peak shift-

ing from 23 degree (graphite) to 12.3 degree assented the GO formation. And after the successful evaluation of contact angle measurements and DMA (TA-Q400em) analysis (T_g), different percentage of GO was included in good resulted EP-2 samples (Table 4.1), and hence performed sample names were denoted as EP-2-y% (y = 0.1, 0,2, 0.5, 1 and 2). FT-IR (Frontier FT-IR/FIR, Perkin Elmer) has been used to characterized and rectangular specimens (15*5*0.5 mm) were investigated by TA-Q400em three-point bending test (40 ^{0}C to 120 ^{0}C) to address the storage modulus and loss modulus (heat rate of 10 ^{0}C/min; 50mL/min nitrogen; 0.02N). Stress relaxation and stress-strain experiments have performed at 40 ^{0}C, with 1*10^{-3} N preload (1% strain) and 0.02N force respectively.

4.4 Results and discussions

The curing of epoxy had been examined over regular time intervals (hourly basis) with the help of FTIR analysis, eventually after 5 hours no declination (914 cm^{-1}) was observed (Figure 4.2) [95].

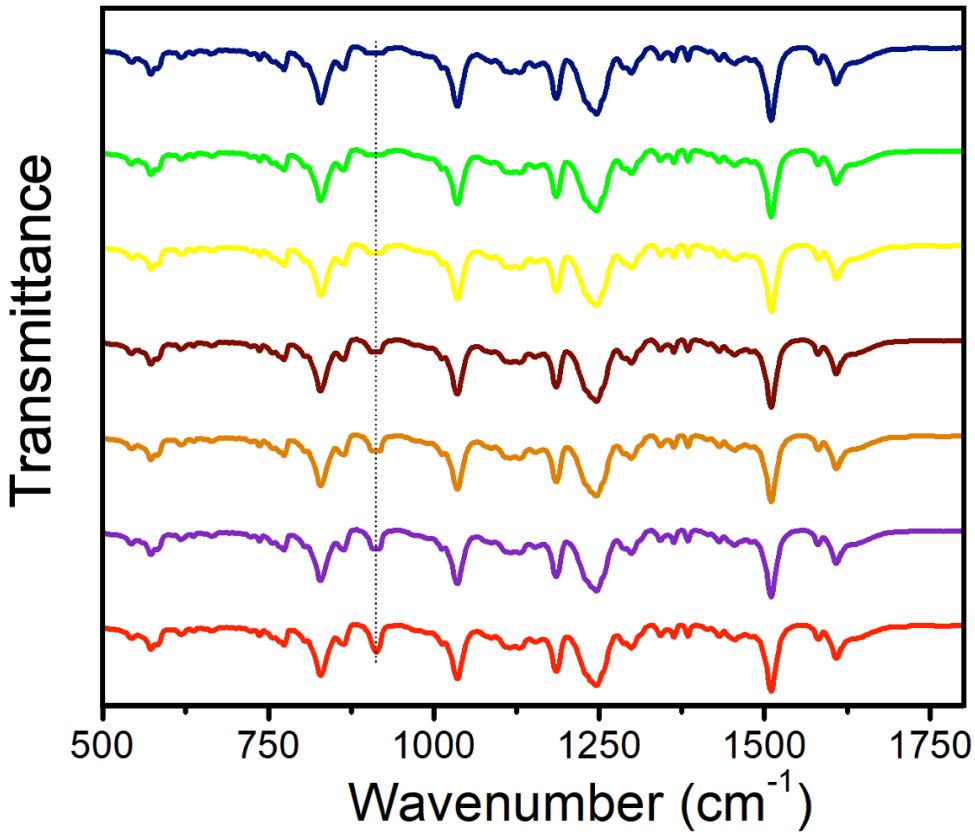

Figure 4.2: FTIR results for EP-pristine curing with respect to time

Furthermore, THF swelling test was performed to identify the complete curing, as uncured epoxy-PDMS composite has held unbonded covalent formations, which could not be retained under vigorous stirring(Figure 4.3).

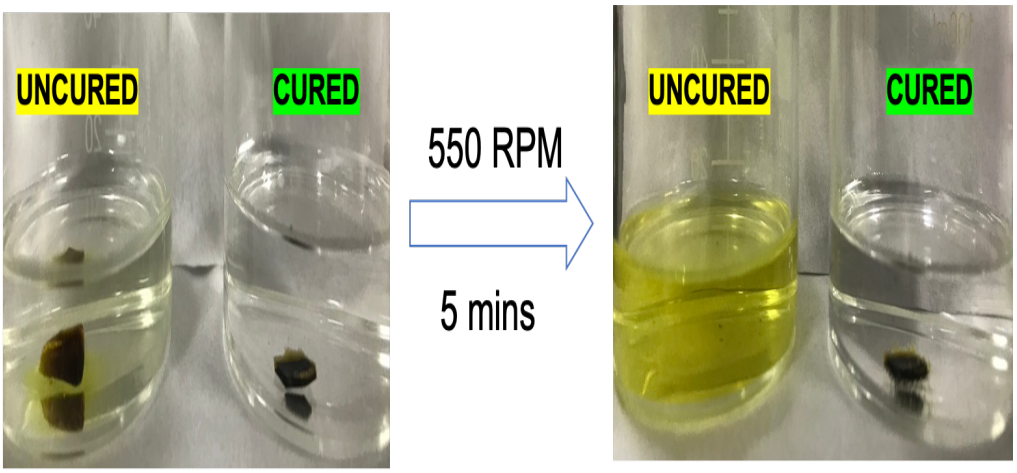

Figure 4.3: THF swelling test for EP-2-0.5

The dispersion of PDMS in epoxy was investigated through contact angle and SEM analysis. Initially, dispersion of the PDMS in epoxy was evaluated with hydrophobic changes, where enhancement in hydrophobicity was observed [sample EP-2], that could be due to a good dispersion of PDMS in epoxy matrix [151, 156]. However, with further addition of PDMS a gradual decrease in hydrophobicity was observed (Table 4.1) denotes PDMS dispersion failure in matrix [156]. A similar kind of behavior was observed for GO based composites, where hydrophobicity was increased with incorporation of GO [EP-2-0.5], whereas, a further increasing of GO incorporation decreases the hydrophobicity (Table 4.1).

Table 4.1: Glass transition temperature and contact angle values of different samples

Samples	Epoxy- PDMS (EP-x)					Epoxy-PDMS-GO (EP-2-y)				
	EP-p	EP-1	EP-2	EP-3	EP-5	EP-2-0.1	EP-2-0.2	EP-2-0.5	EP-2-1	EP-2-2
Glass transition temperature (T_g)	64	62	58	62	63	57	56	53	55	58
Contact angle (^{o})	85	88	97	94	89	98	99	101	97	97

The temperature dependent transition was noticed through DMA analysis and attained glass transition temperature of the epoxy vitrimer samples were tabulated in Table 4.1, and a resulted glass transition temperature was effectively assented that the incorporation of PDMS and GO is advantageous to reduce the T_g of the prepared composites(Figure A3). The observed change in T_g behavior could be owing to i) low T_g of PDMS [56] ii) fine dispersion of PDMS [151], however, after further addition of PDMS an increase in T_g was obtained.

To find out the impact of nanofillers, different percentage of GO were included in EP-2 samples, and the obtained results demonstrate a further decrease in T_g, where GO based nanofillers exhibit a free volume space between matrix and filler [142]. However, a further addition of GO increases the T_g of the composites [EP-2-1; EP-2-2], which might be again due to agglomeration of GO, thus makes poor interaction with epoxy-PDMS matrix. Based on these observations, further investigations have been carried out for EP-p, EP-2 and EP-2-0.5. The performed storage (E'), loss (E") modulus and tan δ data exhibits a temperature dependent viscoelastic behavior (Figure 4.4) for the prepared specimens and attained storage modulus of EP-p at 40 ^{0}C was much higher than the EP-2. The reduction in storage modulus could be due to the presence of PDMS, which demonstrates a lower in crosslinking density [151]. Furthermore, incorporated GO restrain the covalent formation of epoxy and thus promulgate the free volume space between filler and matrix.

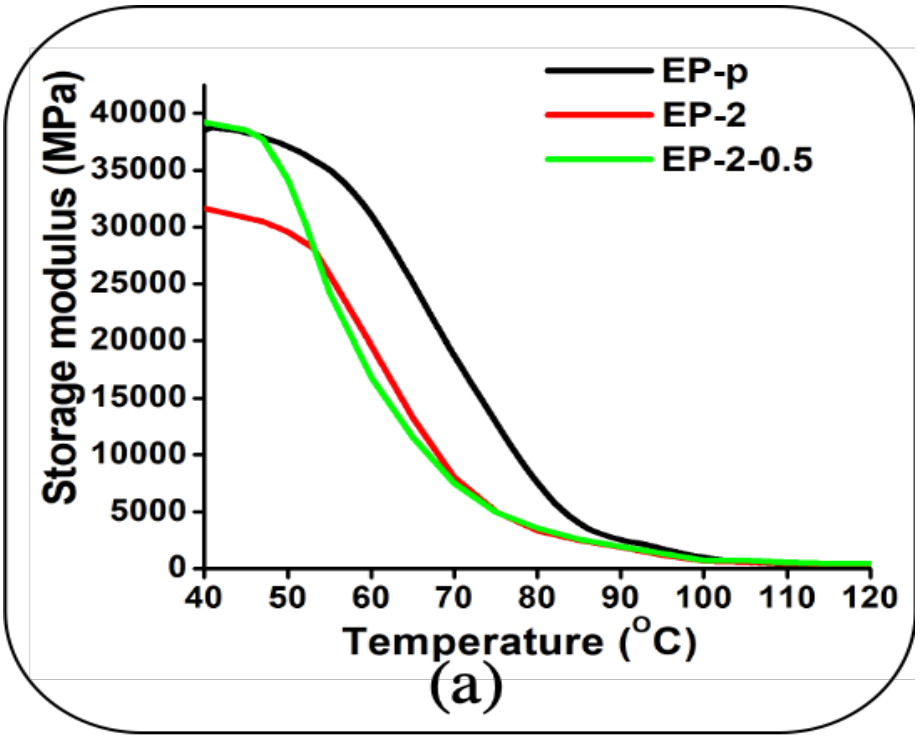

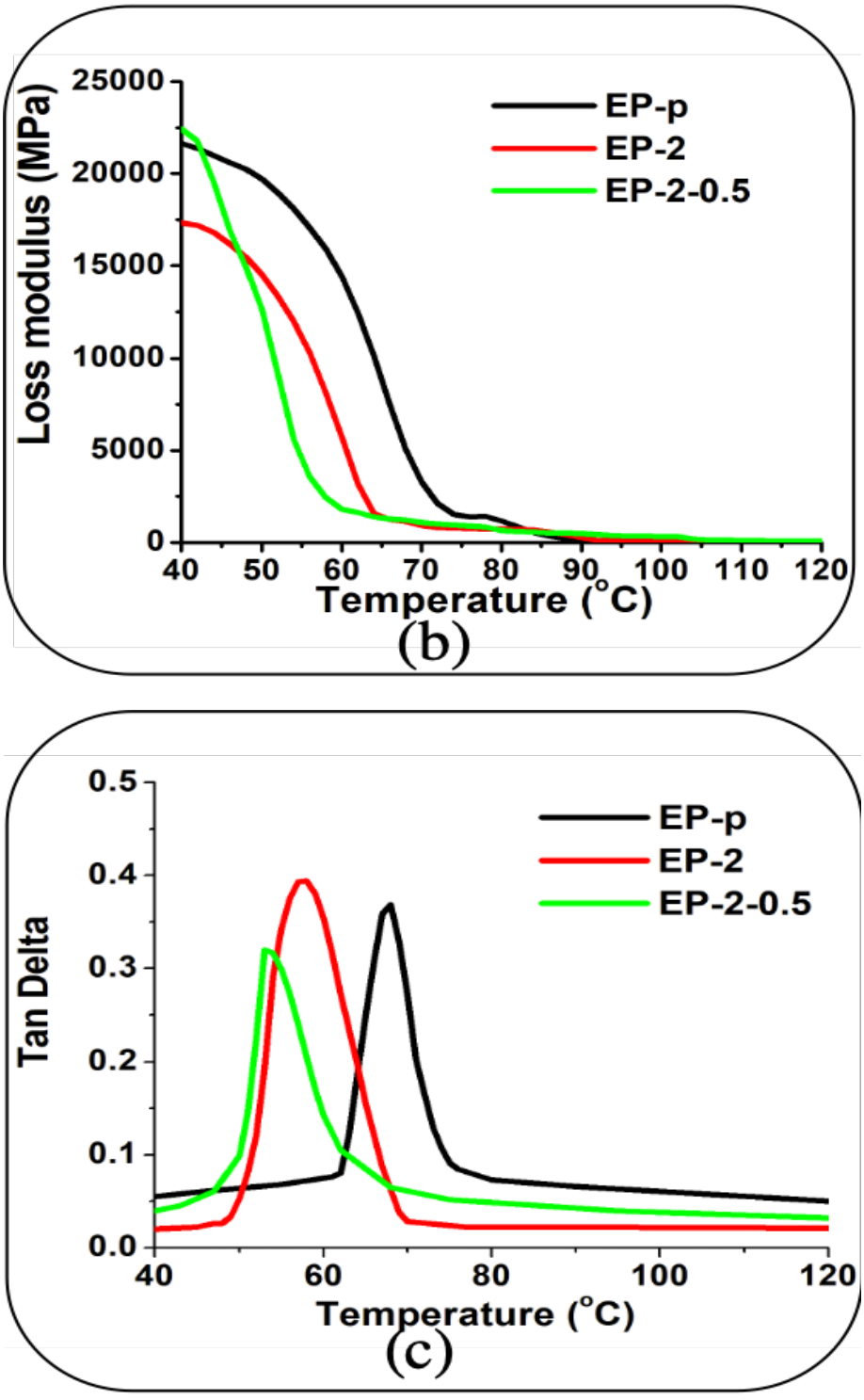

Figure 4.4: (a)Storage modulus (b) Loss modulus and (c) tan δ

The storage modulus of specimen EP-2-0.5 was higher than the EP-2 (Table 4.2), which could be due to the wavy topology of GO, enhances intercalate interlocking between matrix and nanofiller at low temperature [144]. Stress-strain curve shows that flexural strength (Figure 4.5) of EP-p (18 MPa) was

slightly lower than the EP-2 and EP-2-0.5 (18.1 MPa and 18.7 MPa, respectively), though EP-2 strain at break point was higher than the EP-p and EP-2-0.5 (Figure 4.5).

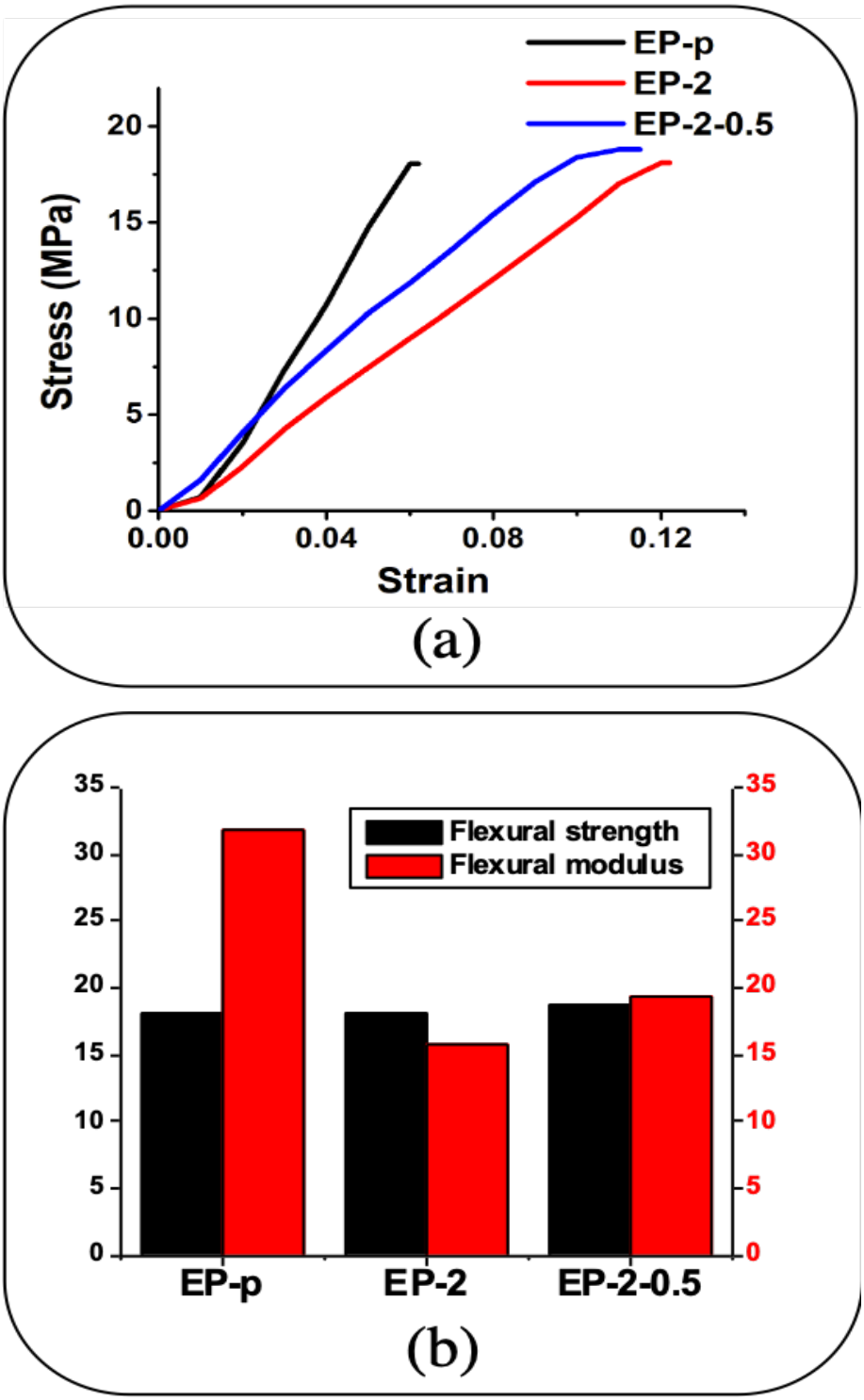

Figure 4.5: (a) Stress-strain(b)Bar diagram for flexural strength and modulus of different samples

The amelioration of EP-2 sample flexural strength was obtained, due to their homogenous addition and synergistic effect with epoxy [157]. Further, interfacial adhesion and thick interphase between the epoxy/PDMS and GO has increased the flexural strength of EP-2-0.5, where the material transfer stress from epoxy/PDMS to GO fillers. Also, this efficient interfacial interaction between the epoxy/PDMS/GO nanocomposite was demonstrated, due to the GO- hydroxyl group interaction, as well as mechanical interlock (owing to the wavy structure) with the epoxy [158, 159]. Significantly, the resulted EP-2 sample strain at break values have manifested the flexible (–Si–O–Si– linkages) PDMS in the epoxy network, which could be helpful to increase the toughness of the material [151]. However, the addition of GO filler (EP-2-0.5) has reduced the toughness/elongation has observed, due to their interfacial interaction and chain mobility restriction; although their free volume formation has rendered a higher elongation than the EP-p [160]. Also, the observed strain at break increment exemplified the flexural modulus decrement, and thus acquired due to the presence of PDMS which reduces the bending resistance/brittleness. Substantially, observed strain at break values of EP-2 and Ep-2-0.5 has increased two times (from 0.06 to 0.12) and 50%(0.06 to 0.09) than EP-p, respectively, whereas, obtained flexural modulus of EP-2 and EP-2-0.5 (15.7 GPa and 19.4 GPa, respectively) were lesser than EP-p flexural modulus (32.1 GPa) (shown in Table 4.2).

Table 4.2: Thermo-mechanical properties of EP-p, EP-2 and EP-2-0.5 samples

Samples	Storage modulus (GPa)	Flexural strength (MPa)	Flexural strain at break (mm/mm)	Flexural modulus (GPa)
EP-p	39.7	18.0	0.06	32.1
EP-2	31.6	18.1	0.12	15.7
EP-2-0.5	39.9	18.7	0.09	19.4

The SEM analysis was carried out to find the effect of PDMS in epoxy matrix. The fractured surfaces in Figure 3 (a,b) show that there is a homogeneous cured resins as could not obtained any phase domains. The dispersibility of the graphene oxide nanosheets was analyzed using TEM image (Figure 3(c)). The images show an excellent dispersion of GO nanosheets in epoxy vitrimer matrix (EP-2).

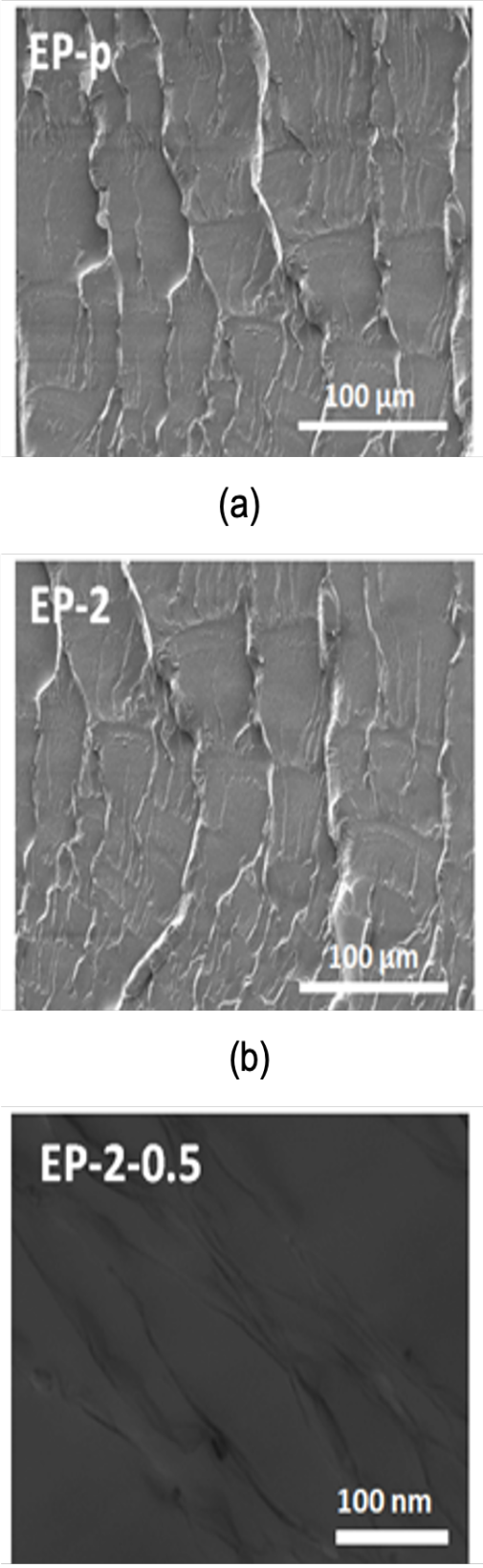

Figure 4.6: (a) SEM image of EP-p (b) SEM image of epoxy/PDMS (c) TEM image of Epoxy/PDMS/GO nanocomposite

For identifying the vitrimer behavior, stress relaxation behavior of the materials has been studied [95]. For an instance, a relaxation time 112.8s, 40.8s and 34s at 60 ^{0}C, 70 ^{0}C and 80 ^{0}C respectively, was observed for EP-p specimen (Figure 4.7(a)). However, in case of EP-2, a relaxation time 42.6s, 27.6s and 13.8s at 50 ^{0}C, 60 ^{0}C and 70^{0}C respectively was observed(Figure 4.7(b)).

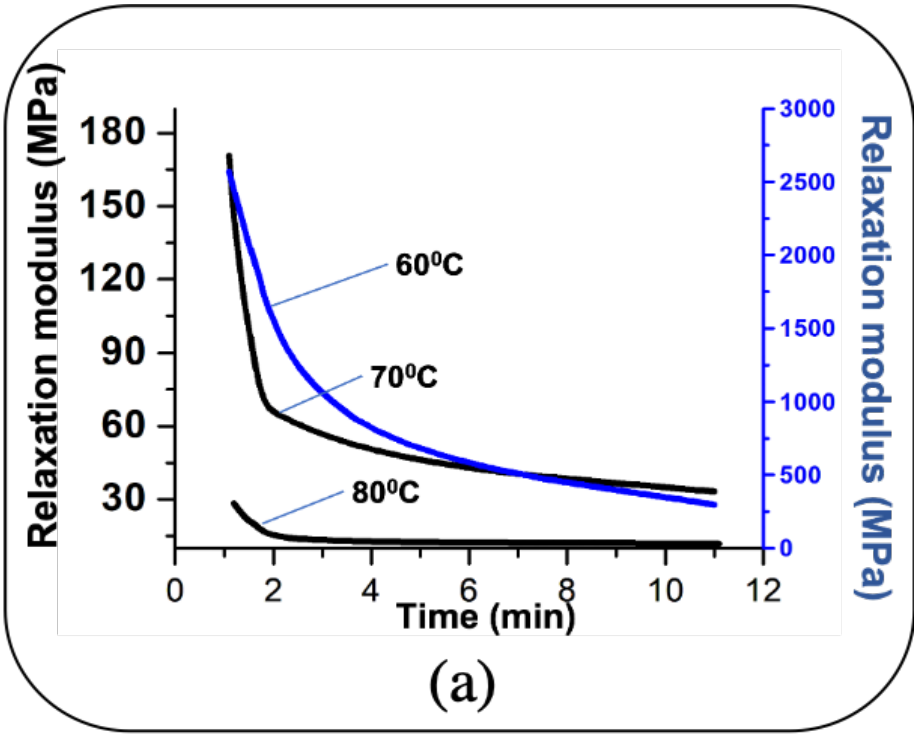

(a)

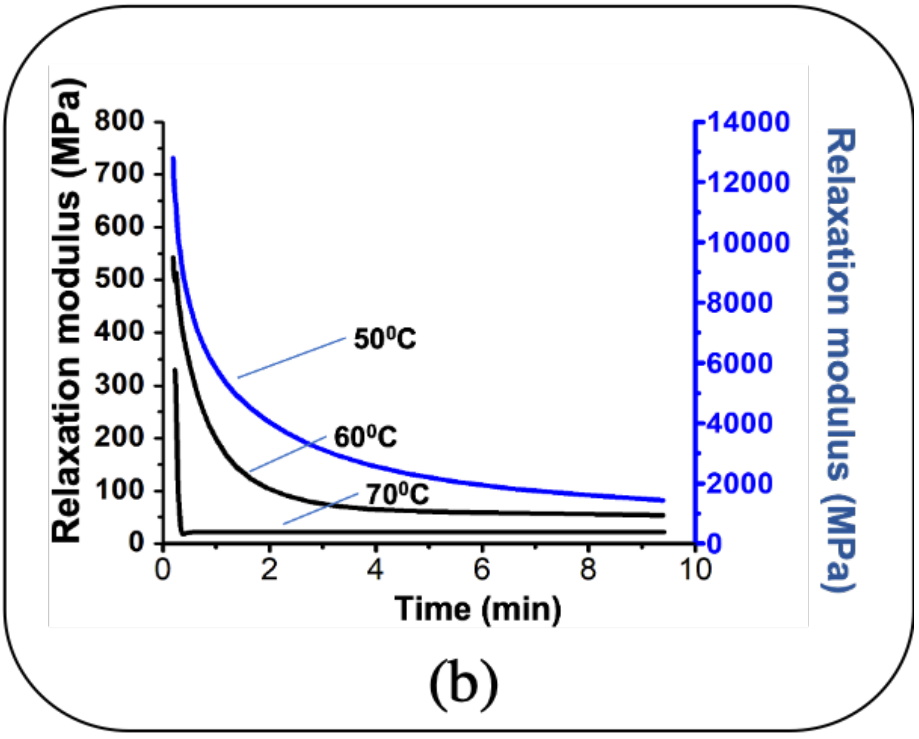

(b)

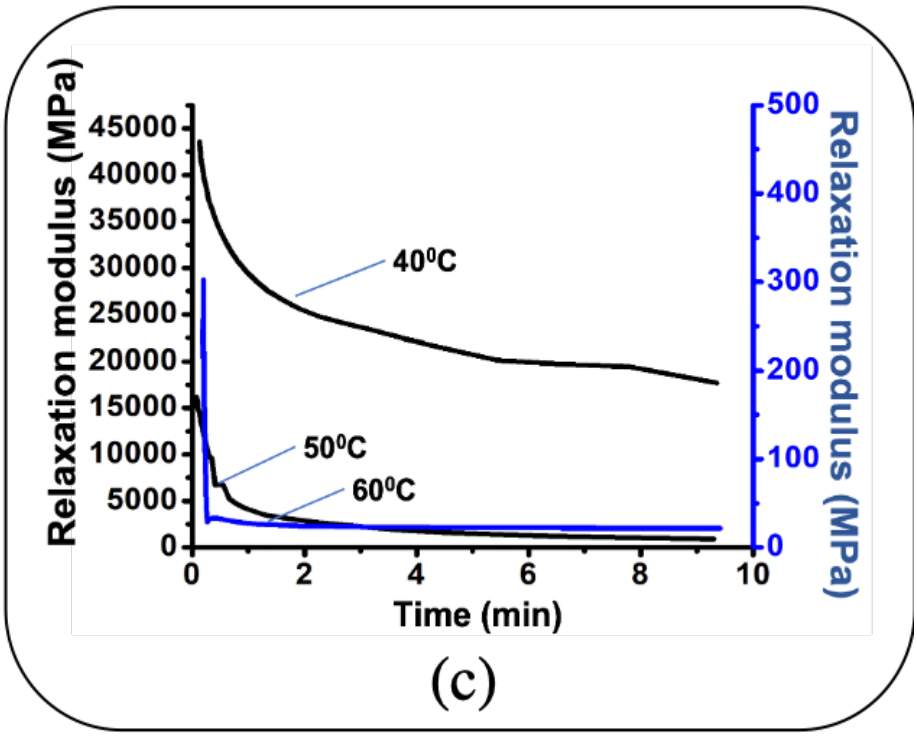

Figure 4.7: Stress relaxation analysis in different temperature for (a) EP-p (b) EP-2 and (c) EP-2-0.5

However, due to their faster relaxation after Tg, specimen EP-2-0.5 demonstrates 89.6 s, 16.8 s and 3s at 40 ^{0}C, 50 ^{0}C and 60 ^{0}C, respectively (Figure 4.7(c)). Thus, obtained relaxation times were plotted in graph to identify the Arrhenius equation, and from that equation activation energy (E_a) has been calculated (Table 4.3). The material T_v has been generally considered once their viscosity reaches 10^{12} Pa. s [161], hence this hypothesis T_v temperature range has been extrapolated based on literature [162] for EP-p sample. Subsequently, investigated low viscosity siloxanes contain PDMS involved EP-2 resulted a lower activation energy (E_a) [163] and T_v than the EP-p (Table 2; Calculation A1) [56, 164].

Table 4.3: Activavtion energy and topology tansition temperature

Samples	Activation energy (E_a) (KJ/mol)	Topology transition temperature (T_v) (^{0}C)
EP-p	59	19
EP-2	52	-1
EP-2-0.5	180	31

However, owing to the possession of GO, EP-2-0.5 exhibits a higher T_v and

$E_a$than EP-2 (not EP-p)(Calaculation A2), where GO nanofillers makes increment in viscosity and thus restricts the low temperature chain mobility [165], whereas assimilated free volumes has reduced the T_g [142]. Self-healing behavior of the EP-p was observed at 80 ^{0}C for 5mins, whereas, the performed EP-2 and EP-2-0.5 samples demonstrate efficient healing at 60 ^{0}C for 5mins, which could be due to their lower T_g. The obtained self-healing of the material was acquired through a disulfide exchanges, where sulfide radicals were accumulated at certain temperature (Figure 4.8).

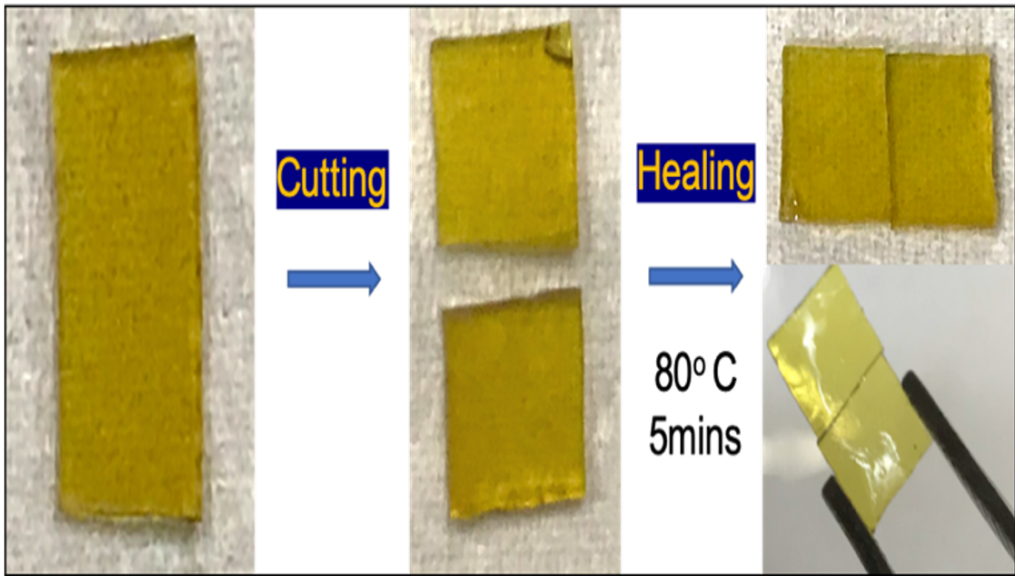

Figure 4.8: Healed sample EP-2

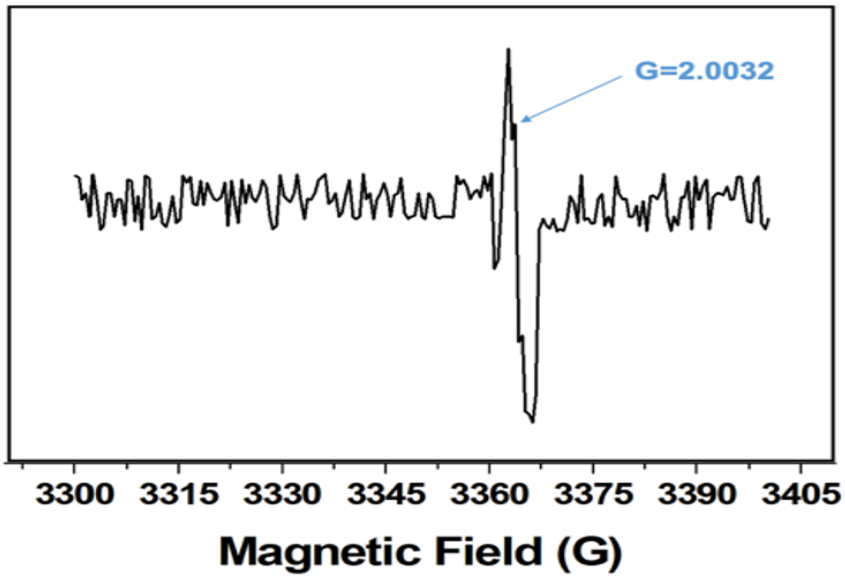

Figure 4.9: EPR analysis graph

The promulgated sulfide radical exchanges have identified through electro paramagnetic resonance (EPR) analysis (80 ^{0}C) and observed(g value=2.003) tweak confirms the radical formation in the material (Figure 4.9).

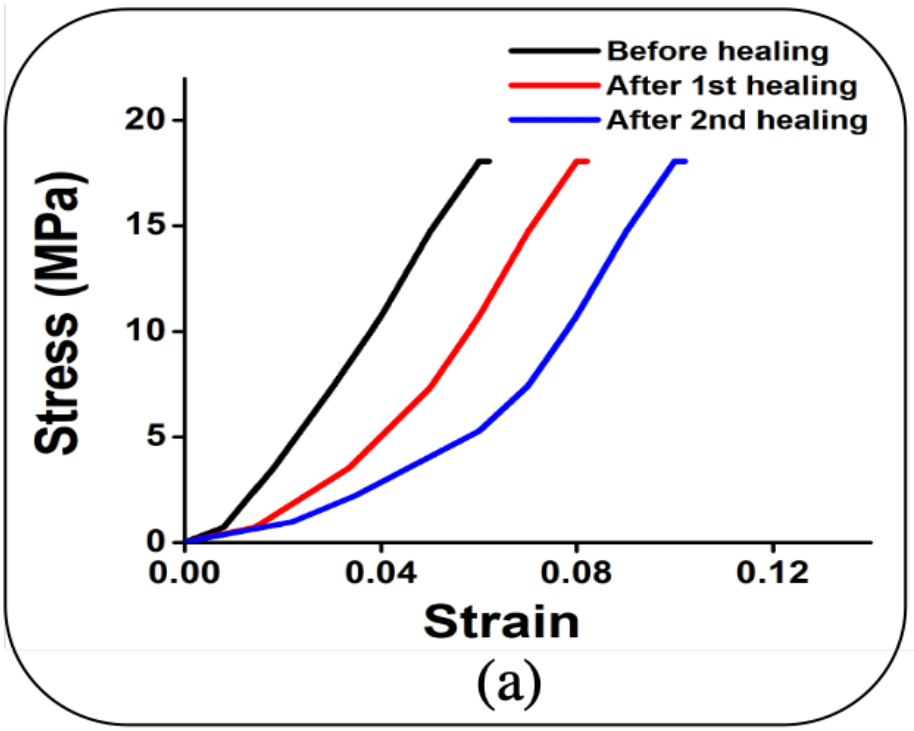

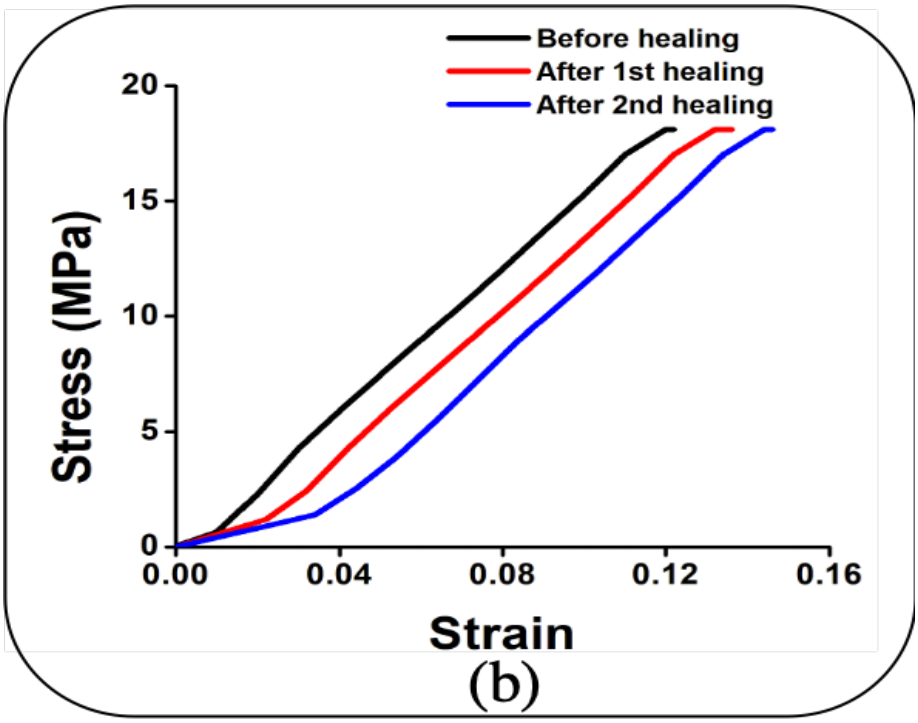

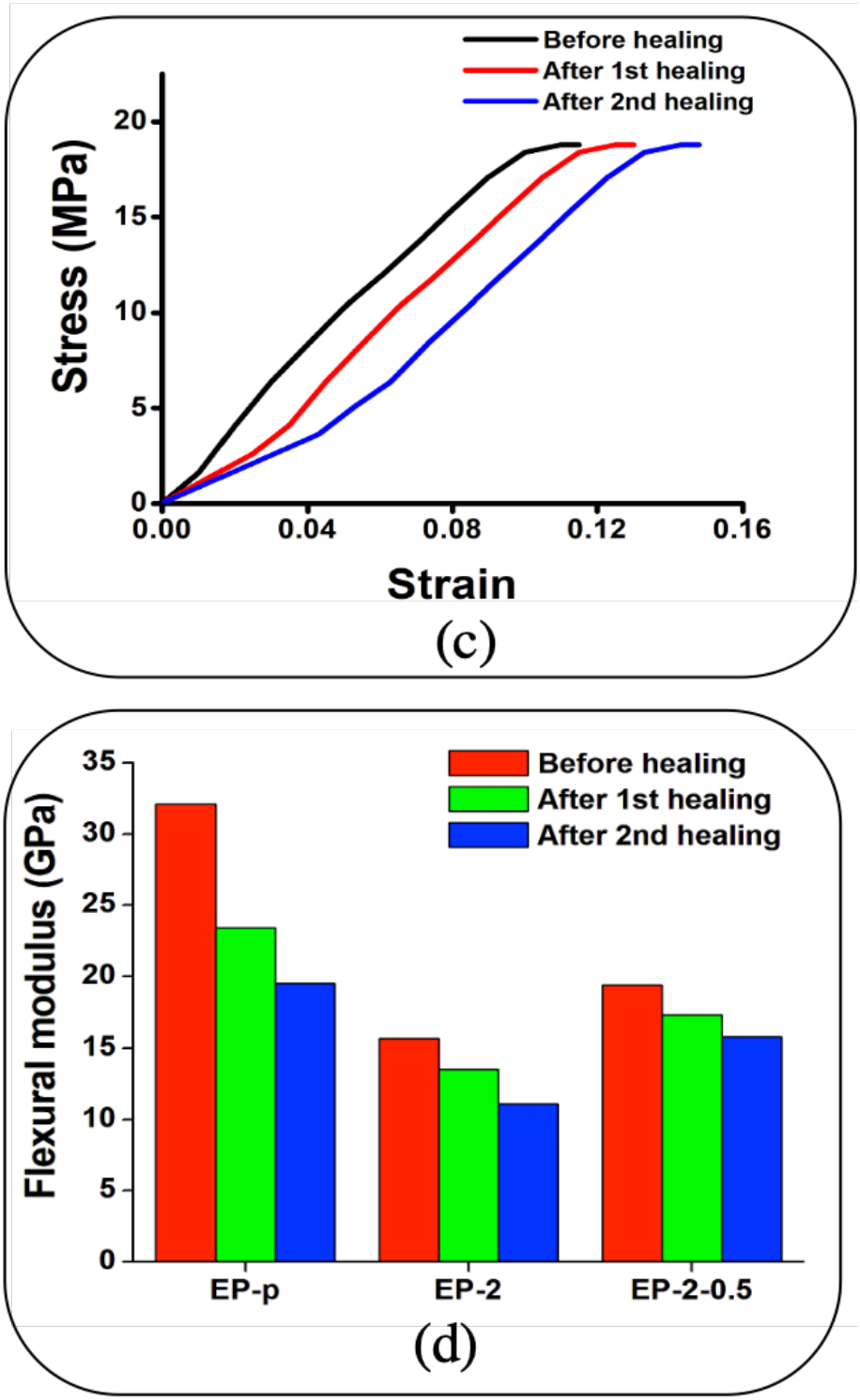

Figure 4.10: Stress- strain curve for (a) EP-p (b) EP-2 (c) EP-2-0.5 and (d) bar diagram for changes in flexural modulus after two healing cycles

Further, the self-healing efficiency was evaluated through flexural modulus, where the strength of the material was found almost similar after consecutive healing (Table 4.4). This reduction has not quantified the whole material brittle

failure reduction, instead its subject to mention the sag in cracked point chain rearrangements. Hence the reduction in crosslink density has observed after each cycle of healing via flexural studies, where the material was elongated with respect of applied stress. Consequently, the increment in elongation of the healed specimen has perceived due to the subtle entanglement of chain linkages [149]. Thus, repeated healing of the material extends their healing region width, which is directly interacting to the stress; and helpful to enhance the specimen toughness [150]. The observed healing efficiency of the material was addressed through flexural modulus changes, where healing efficiency of 72%; 85%; and 89% in first cycle and 60%; 77%; and 82% in second cycle were observed for EP-p, EP-2 and EP-2-0.5 specimen respectively (Figure 4.10).

Table 4.4: Activavtion energy and topology tansition temperature

Samples	Before healing (GPa)	After healing (GPa)	
		1 st	2 nd
EP-p	32.1	23.4	19.5
EP-2	15.7	13.5	12.1
EP-2-0.5	19.4	17.3	15.8

Summary

The pristine epoxy vitrimer demonstrated brittleness has reduced via an addition of PDMS, where performed epoxy-PDMS composite material exhibits a reduction in glass transition temperature without change of strength. Owing to this, GO nanofiller has introduced in vitrimer composite for better strength and EP-2-0.5 was described better properties. Furthermore, all the performed samples demonstrate a self -healing behavior at 80 ^{0}C for 5 min, hence also EP-2 and EP-2-0.5 resulted prevailed healing at 60 ^{0}C for 5 min. Then analyzed flexural modulus was helpful to quantify their mechanical properties and healing efficiency (EP-2-0.5) 89%and 82% after two successful healing.

CHAPTER 5: DEVELOPMENT OF EPOXY/ACTIVATED CARBON VITRIMER BIO COMPOSITE

5.1 Introduction

Bio derived monomers have been included in vitrimer studies to attain the sustainable self-healing vitrimer materials [76]. Diverse biobased vitrimers were demonstrated with different bio derivatives like lignin [166], fructose [76] and soybean oil [167]. However, obtained thermal/mechanical properties are comparatively lesser than the synthetically prepared vitrimer materials [71]. This kind of same drawbacks have been raised between synthetic and bio thermoset material, whereas it has been overcoming by addition of fillers in matrix (composite), specifically bio fillers incorporated synthetic matrix (bio composite) has resulted notable sustainability and thermal/mechanical properties [168]. Owing to this, unprecedented bio filler involvement in vitrimer has intrigued and sugarcane bagasse derived chemically activated carbon was involved in disulfide exchange promoted epoxy vitrimer matrix, where covalently adaptive network has demonstrated.

Hence it has optimized through different percentage of AC and their changes in glass transition temperature and mechanical properties are discussed. The self-healing efficiency has evaluated through flexural studies and AC dependent changes have been addressed eloquently. This work demonstrated epoxy vitrimer biocomposite has demonstrated the low temperature self-healing at 70 ^{0}C for 5 mins than the pristine epoxy (80 ^{0}C for 5mins), where healing was accomplished through disulfide exchanges. Further examined flexural studies for healing efficiency has described the 73% and 60% (epoxy) / 85%and 70%(biocomposite) recovery after two consecutive healings.

5.2 Preparation of epoxy vitrimer biocomposite

Activated carbon was prepared from sugarcane refuses, based on literature [169].

Sugarcane refuse was collected and put in dryer for moisture removal(110 ^{0}C for 3h), subsequently crushed into fine particles. The fine grinded powder was kept in 40 wt% Phosphoric acid for activation; hence carbonization has attained at 30 ^{0}C, 40 ^{0}C and 50 ^{0}C for every one-hour interval respectively. After carbonization, the material was allowed to cool, hence filtered and washed with hot water (around 90 ^{0}C) for adjust pH to 7. The prepared AC was dispersed in ethanol (150mg in 10mL) through an ultrasonication for 30 mins. Subsequently, finely dispersed activated carbon different loadings (EP-x%; x- 0(p-pristine), 0.1,0.2,0.5,1 and 2) were included in BADGE resin and heated at 80 ^{0}C under vacuum condition till ethanol evaporation(Table A3). Then after, stochiometric ratio of hardener AFD was added and stirred at same temperature for 15 mins. Finally, degassed mixture was kept in silicon mold and cured at 150 ^{0}C for 5 h(Figure 5.1).

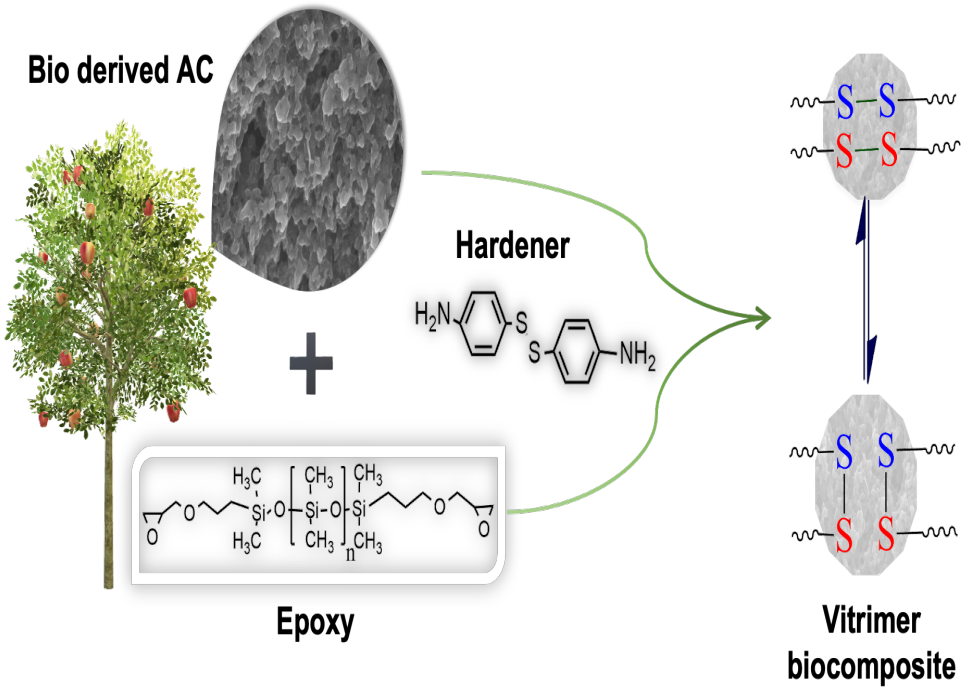

Figure 5.1: Preparation of AC involved epoxy vitrimer biocomposite

5.3 Material characterization

Biomass derived AC was investigated through XRD analysis to identify the formation AC from biomass (Figure 5.2).The observed peak 26.27^0 has determined graphite flakes like hexagonal structure, hence AC is also known as an assemblies of defective graphene layers [170]. Further performed SEM analysis explained the sugarcane bagasse derived carbon and activated carbon surface,

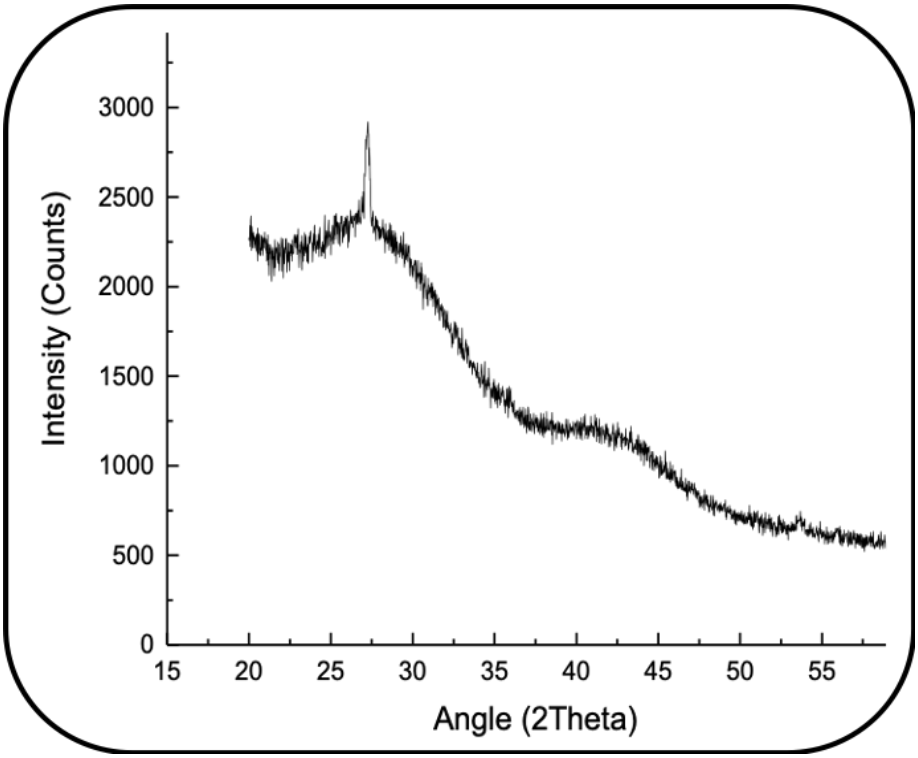

Figure 5.2: XRD graph of activated carbon

where chemically (phosphoric acid) activated carbon has depicted pores in their surface (Figure 5.3). This low volume pores have extended the surface area of chemical reactions and helpful to attain progressive chain exchanges.

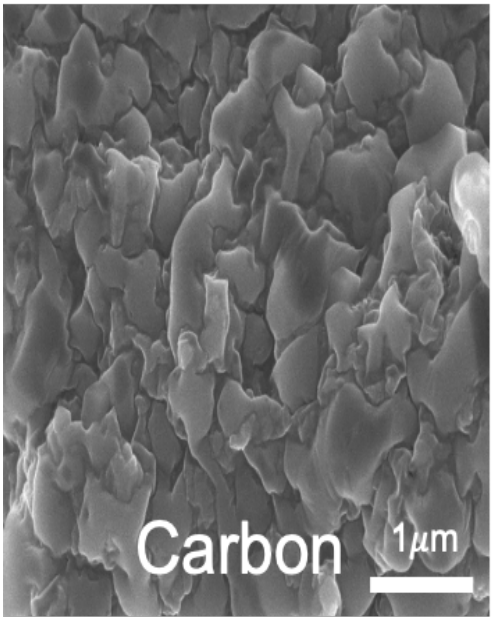

(i)

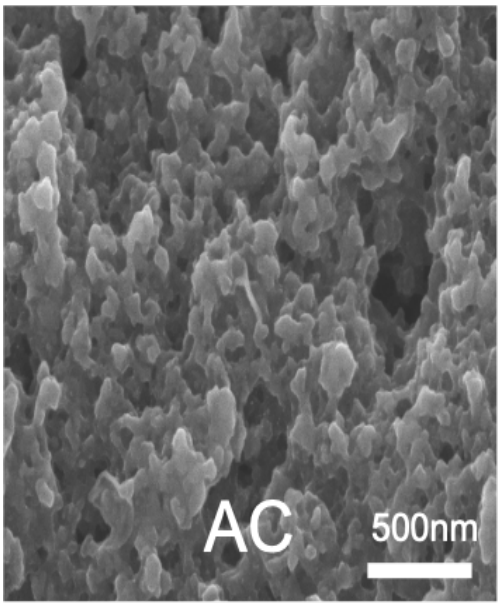

Figure 5.3: SEM images for biomass derived (i) Carbon and (ii) Activated carbon

Then epoxy vitrimer biocomposite curing was analyzed through FT-IR analysis, where the diminution of oxirane ring (914 cm^{-1}) was denoted the curing of epoxy. Hence curing was noted for each one hour through IR analysis, and after 5 hours curing was done completely. Further confirmation of curing was exhibited through tetrahydrofuran (THF) swelling test (5mins, 500 rpm), where uncured samples were dissolved.

5.4 Results and Discussions

After basic material characterizations, vitrimer biocomposite thermal and mechanical properties were investigated through thermomechanical analyzer, which could have been helped to find out the glass transition temperature and flexural strength of the material. Primarily, pristine epoxy vitrimer was investigated and

Table 5.1: Glass transition temperature of different samples

Samples	Epoxy- AC(EP-x)				
	EP-p	EP-1	EP-2	EP-3	EP-5
Glass transition temperature (T_g)	64	62	58	62	63

then after different percentage of AC fillers involved epoxy vitrimer biocomposite glass transition temperatures were analyzed and tabulated in Table 5.1. From the observed results, material EP-1 had denoted low glass transition temperature than the other investigated epoxy samples(Figure A4). The reduction in glass transition temperature was achieved due to the free volume space between matrix and nanofiller [142, 171]. The pristine and biocomposite vitrimer demonstrated stress-strain curves were exhibited a same flexural strength (Figure 5.4).

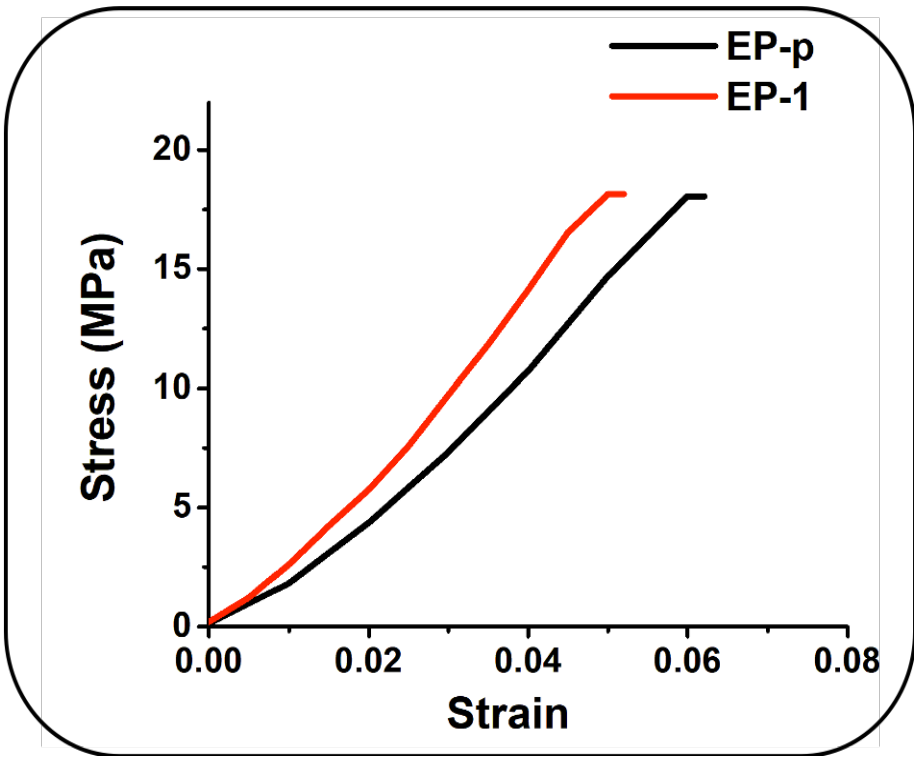

Figure 5.4: Flexural stress-strain curve for epoxy vitrimer

However, strain at break and flexural modulus of the material has reduced and increased respectively, where it denotes the stiffness increment as well as high bending resistance.

Table 5.2: Thermo-mechanical properties of epoxy vitrimer

Samples	Storage modulus (GPa)	Flexural strength (MPa)	Flexural strain at break (mm/mm)	Flexural modulus (GPa)
EP-p	39.7	18.0	0.06	32.1
EP-1	57.5	18.1	0.05	43.3

Storage modulus and loss modulus of the vitrimer and biocomposite were ob-

served to understand the temperature dependent viscoelasticity, whereas performed biocomposite exhibited a higher storage modulus than the EP-p.

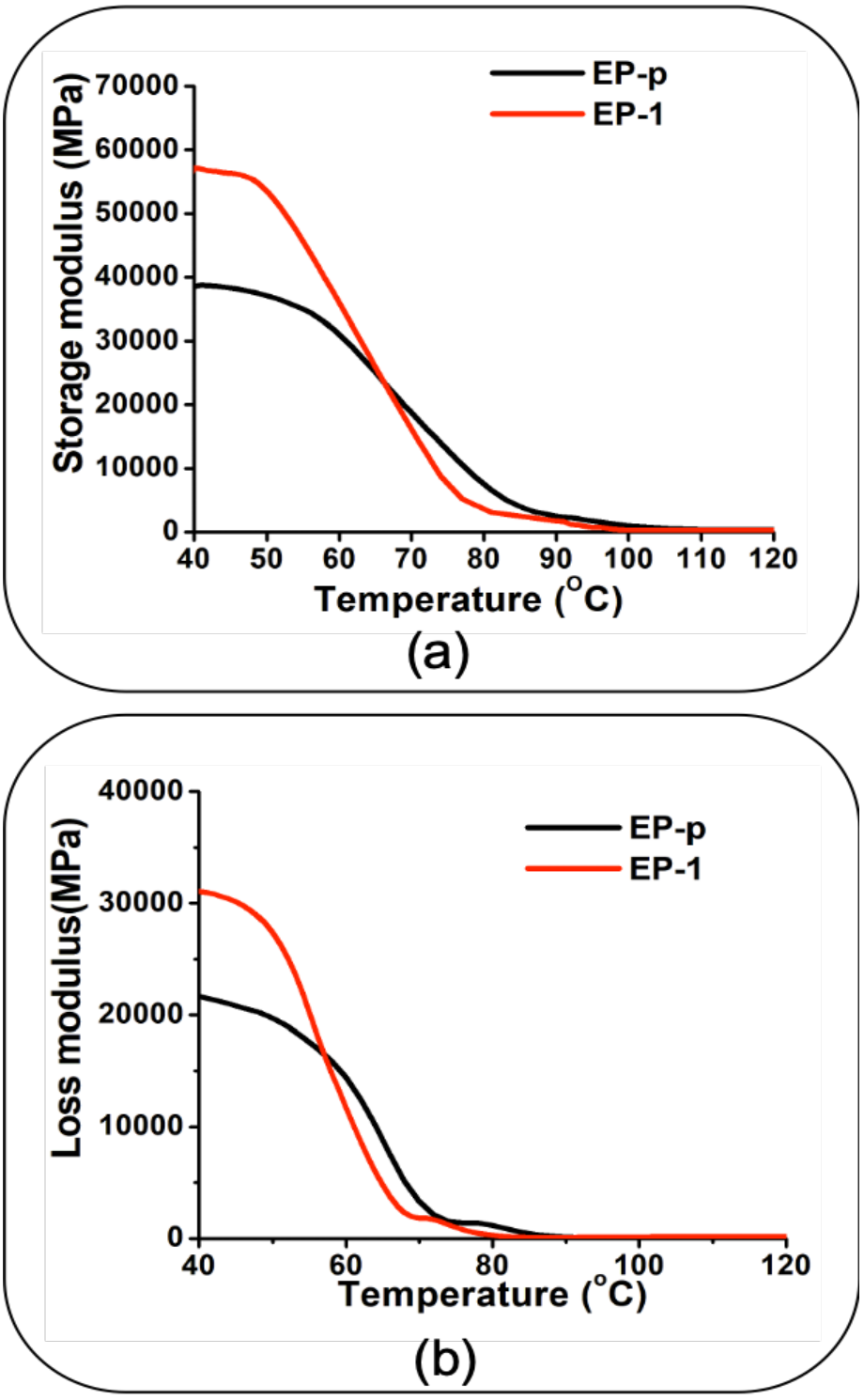

Figure 5.5: (a) Storage modulus (b)Loss modulus for epoxy vitrimer

The viscoelasticity behavior presented EP-1 has demonstrated higher storage modulus (Table 5.2) due to the presence of activated carbon, where matrix in-

terlocked fillers have restricted the chain exchanges in lower temperature. However, lower T_g of EP-1 has availed faster reduction in viscoelasticity (after glass transition temperature)(Figure 5.5). Stress relaxation experiments were performed for the EP-p and EP-1 at different temperatures (60 ^{0}C, 70 ^{0}C and 80 ^{0}C), hence resulted relaxation times (EP-p= 112.8 s, 40.8 s and 34 s; EP-1= 234s, 129.6s and 46.2s respectively)were plotted in Arrhenius equation to identify the activation energy and toplogy freezing point transition temperature of the vitrimer and their biocomposite (Table 5.3; Calaculation A3).

Table 5.3: Activation energy and topology transition temperature

Samples	Activation energy (E_a) (KJ/mol)	Topology transition temperature (T_v) (^{0}C)	Before healing (GPa)	After healing (GPa)	
				1^{st}	2^{nd}
EP-p	59	19	32.1	23.4	19.5
EP-1	79	43	43.3	36.9	33.7

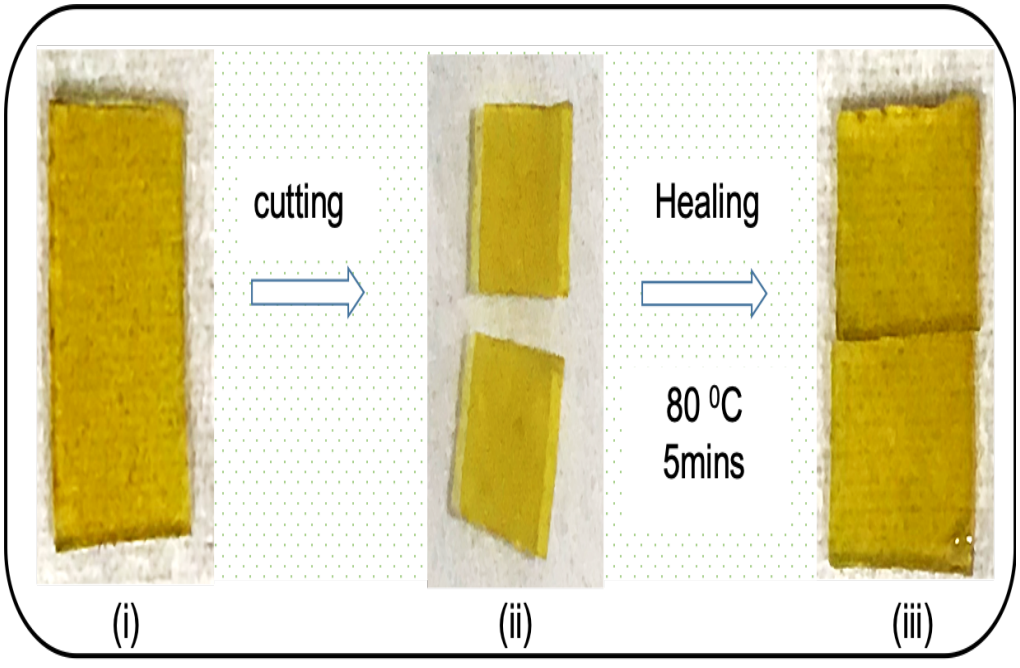

Figure 5.6: Self-healing of epoxy vitrimer: (i) pristine, (ii) cut into two pieces and (iii) rejoined

The investigated EP-p relaxation time has comparatively lower than the EP-1, this due to the presence of activated carbon, which has restricted the chain

mobility and increased the viscosity of epoxy vitrimer. However, free volume formation between filler and matrix were encouraged the glass transition temperature reduction [142].

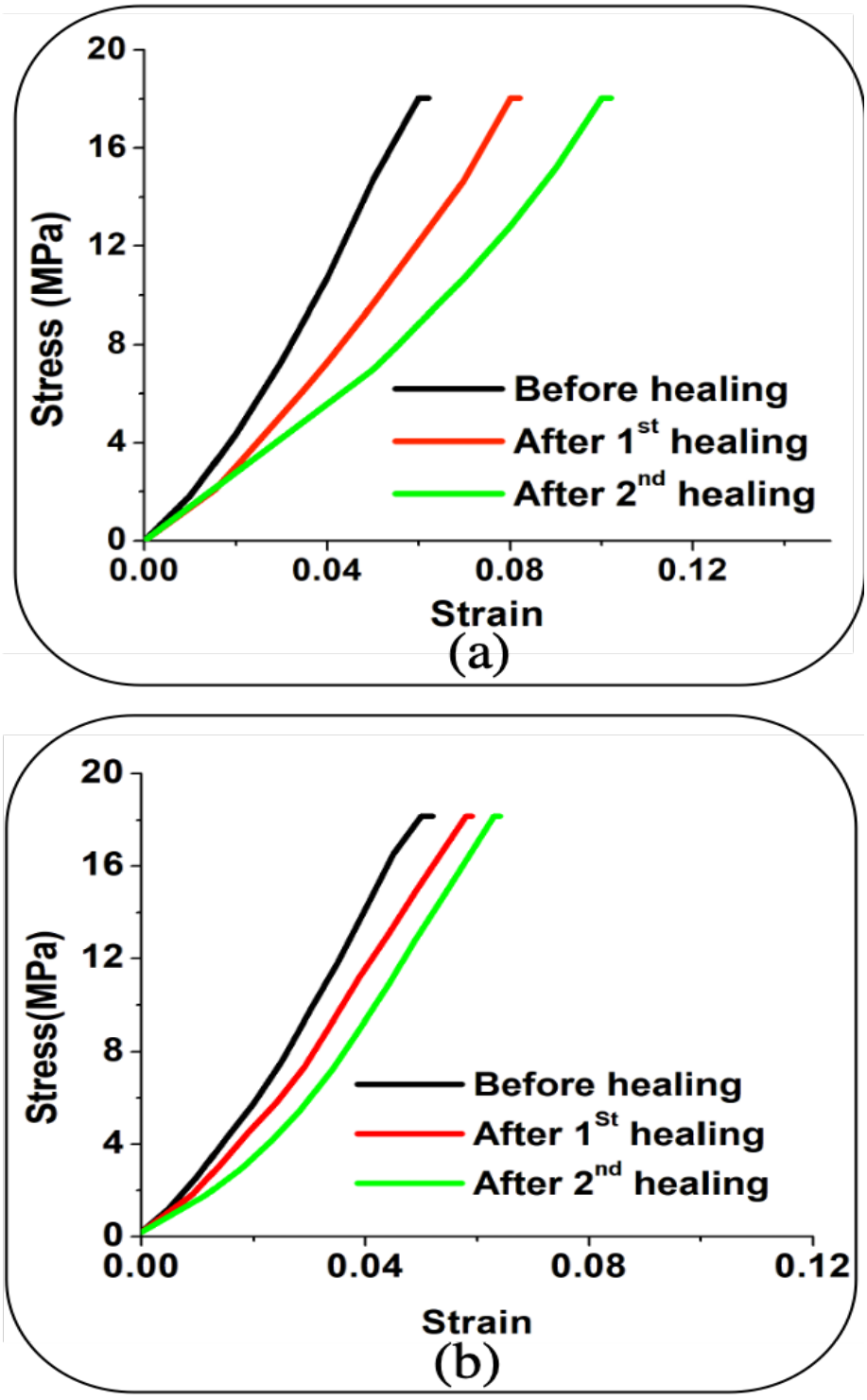

Figure 5.7: Healing efficiency of vitrimer was calculated via stress-strain relationship for (a) EP-p and (b) EP-1

The performed epoxy vitrimer and biocomposites had demonstrated efficient self-healing via disulfide exchanges at 80 ^{0}C for 5 mins(Figure 5.6), however, activated carbon involved EP-1 was exhibited self-healing at 70 ^{0}C for 5 mins, owing to their low glass transition temperature. Hence healing efficiency was evaluated through flexural studies,where healed epoxy vitrimer and biocomposites were demonstrated healing efficiency 73%and 85% respectively after first cycle. Then performed second healing was shown 60%and 78% healing from their unhealed samples, these results were determined the healing efficiency reduction an after each cycle (Figure 5.6). However, material flexural strength was same after every healing, whereas flexural modulus and strain at break has changed.

Summary

The sustainable self-healing vitrimer biocomposite was demonstrated via the presence of bagasse derived activated carbon (AC), owing to this addition, disulfide exchanges promoted temperature dependent self-healing vitrimer (at 80 ^{0}C for 5 mins) material had demonstrated low temperature self-healing at 70 ^{0}C for 5mins (low T_g). Hence flexural studies via evaluated healing efficiency was described the prominent recovery in EP-1, where 85% and 70% efficiency had demonstrated after two consecutive healings.

CHAPTER 6: CONCLUSION AND FUTURE SCOPE

In summary, we have discussed the impact of nanofillers on self-healing properties of synthesized intrinsic materials. Epoxy/GO based vitrimer nanocomposites with self-healing and shape memory properties were prepared. The exchanges in the epoxy vitrimer network was carried out through disulfide exchanges, whereas, GO promoted low glass transition temperature was helpful to achieve a low temperature self-healing and shape memory properties. As prepared nanocomposite EP-1% (containing 1 wt% GO) demonstrates a 7.1% and 9.4% higher flexural strength and modulus compared to pristine epoxy vitrimers. To overcome brittleness failure of vitrimer, epoxy terminated PDMS was involved and resulted epoxy-PDMS composite material exhibits a prominent reduction in glass transition temperature and decrement in their bending resistance effectively, however strength of the material has unchanged. The better strength contains EP-2-0.5 was identified through optimization.

After an addition of PDMS and GO nanofiller in epoxy vitrimer, stipulated mechanical properties were investigated through flexural studies and obtained results assented a difference in mechanical strength, strain at break and modulus. Furthermore, all the performed samples demonstrate a self -healing behavior at 80 ^{0}C for 5 min, hence also EP-2 (Epoxy with 2% PDMS) and EP-2-0.5 (Epoxy with 2% PDMS and 0.5% GO) resulted prevailed healing at 60 ^{0}C for 5 min. Then analyzed flexural modulus was helpful to quantify their mechanical properties and healing efficiency after successful healing, the reduction in flexural modulus was observed with each healing cycle. However, the flexural strength of the material has not been changed after two successful healing.

To attain sustainable self-healing vitrimer materials, epoxy vitrimer network was demonstrated with activated carbon (sugarcane bagasse derived), which could be an effective filler to achieve sustainable epoxy vitrimer biocomposite. Hence disulfide exchanges promoted temperature dependent self-healing vitrimer (at 80 ^{0}C for 5 mins) material had demonstrated low temperature self-healing at 70 ^{0}C for 5mins after an addition of activated carbon (low T_g). However, more addition of AC had not resulted a better result like EP-1, due to

their agglomeration in epoxy matrix. Flexural studies via evaluated healing efficiency was described the prominent recovery in EP-AC-1, where 85% and 70% efficiency had demonstrated after two consecutive healings. Overall, admirable healing and shape memory properties of the vitrimers were observed, together with the competitive material strength within technologically useful boundaries. This will provide an important contribution to improve durability and recyclability of thermoset-systems, although there still is a long way to place these materials in the technical environment, due to the constrain of involved mechanisms and service temperature ranges.

In the future, nanocomposite and biocomposite vitrimer study would be helpful to envisage an efficient smart materials for real time application with sustainable properties in the fields like soft electronics, solid electrolytes, etc. Although at the present stage more investigations are required to achieve lower temperature self-healing and reprocessing of these materials, some of the concepts will appear in technology soon, revolutionizing the self-healing and recycling of thermost-systems widely used in industry. Future needs for increased life-cycle times and a more careful look on the CO_2 -profile of all used materials, whether in automotive, engineering, or insulation- materials will speed up the need for vitrimer-thermoset-materials.

REFERENCES

[1] Z. P. Zhang, Y. Lu, M. Z. Rong, and M. Q. Zhang, "A thermally remendable and reprocessable crosslinked methyl methacrylate polymer based on oxygen insensitive dynamic reversible C–ON bonds," *RSC Adv.*, vol. 6, no. 8, pp. 6350–6357, 2016.

[2] J. Ye, W. Liu, J. Cai, S. Chen, X. Zhao, H. Zhou, and L. Qi, "Nanoporous Anatase TiO 2 Mesocrystals: Additive-Free Synthesis, Remarkable Crystalline-Phase Stability, and Improved Lithium Insertion Behavior," *Journal of the American Chemical Society*, vol. 133, pp. 933–940, feb 2011.

[3] S. Chen, N. Mahmood, M. Beiner, and W. H. Binder, "Self-Healing Materials from V- and H-Shaped Supramolecular Architectures," *Angewandte Chemie International Edition*, vol. 54, pp. 10188–10192, aug 2015.

[4] D. Döhler, H. Peterlik, and W. H. Binder, "A dual crosslinked self-healing system: Supramolecular and covalent network formation of four-arm star polymers," *Polymer*, vol. 69, pp. 264–273, jul 2015.

[5] J.-M. Lehn, "Dynamers: dynamic molecular and supramolecular polymers," *Progress in polymer science*, vol. 30, no. 8-9, pp. 814–831, 2005.

[6] Y. Hong and M. Su, "Multifunctional self-healing and self-reporting polymer composite with integrated conductive microwire networks," *ACS applied materials & interfaces*, vol. 4, no. 7, pp. 3759–3764, 2012.

[7] T. Garrison, A. Murawski, and R. Quirino, "Bio-Based Polymers with Potential for Biodegradability," *Polymers*, vol. 8, p. 262, jul 2016.

[8] B. J. Blaiszik, M. M. Caruso, D. A. McIlroy, J. S. Moore, S. R. White, and N. R. Sottos, "Microcapsules filled with reactive solutions for self-healing materials," *Polymer*, vol. 50, no. 4, pp. 990–997, 2009.

[9] S. H. Cho, H. M. Andersson, S. R. White, N. R. Sottos, and P. V. Braun, "Polydiniethylsiloxane-based self-healing materials," *Advanced Materials*, vol. 18, no. 8, pp. 997–1000, 2006.

[10] M. W. Keller, S. R. White, and N. R. Sottos, "A self-healing poly (dimethyl siloxane) elastomer," *Advanced Functional Materials*, vol. 17, no. 14, pp. 2399–2404, 2007.

[11] G. Lanzara, Y. Yoon, H. Liu, S. Peng, and W. I. Lee, "Carbon nanotube reservoirs for self-healing materials," *Nanotechnology*, vol. 20, no. 33, p. 335704, 2009.

[12] Y. C. Yuan, T. Yin, M. Z. Rong, and M. Q. Zhang, "Self healing in polymers and polymer composites. Concepts, realization and outlook: A review," *Express Polymer Letters*, vol. 2, no. 4, pp. 238–250, 2008.

[13] H. Wei, S. Du, Y. Liu, H. Zhao, C. Chen, Z. Li, J. Lin, Y. Zhang, J. Zhang, and X. Wan, "Tunable, luminescent, and self-healing hybrid hydrogels of polyoxometalates and triblock copolymers based on electrostatic assembly," *Chemical Communications*, vol. 50, no. 12, pp. 1447–1450, 2014.

[14] X. Yu, L. Chen, M. Zhang, and T. Yi, "Low-molecular-mass gels responding to ultrasound and mechanical stress: towards self-healing materials," *Chemical Society Reviews*, vol. 43, no. 15, pp. 5346–5371, 2014.

[15] K. S. Toohey, N. R. Sottos, J. A. Lewis, J. S. Moore, and S. R. White, "Self-healing materials with microvascular networks," *Nature materials*, vol. 6, no. 8, p. 581, 2007.

[16] Y. Bai, Y. Chen, Q. Wang, and T. Wang, "Poly (vinyl butyral) based polymer networks with dual-responsive shape memory and self-healing properties," *Journal of Materials Chemistry A*, vol. 2, no. 24, pp. 9169–9177, 2014.

[17] B. J. Adzima, C. J. Kloxin, and C. N. Bowman, "Externally triggered healing of a thermoreversible covalent network via self-limited hysteresis heating," *Advanced Materials*, vol. 22, no. 25, pp. 2784–2787, 2010.

[18] M. Capelot, M. M. Unterlass, F. Tournilhac, and L. Leibler, "Catalytic Control of the Vitrimer Glass Transition," *ACS Macro Letters*, vol. 1, pp. 789–792, jul 2012.

[19] X. Chen, M. A. Dam, K. Ono, A. Mal, H. Shen, S. R. Nutt, K. Sheran, and F. Wudl, "A thermally re-mendable cross-linked polymeric material," *Science*, vol. 295, no. 5560, pp. 1698–1702, 2002.

[20] B. Ghosh and M. W. Urban, "Self-repairing oxetane-substituted chitosan polyurethane networks," *Science*, vol. 323, no. 5920, pp. 1458–1460, 2009.

[21] K. Imato, M. Nishihara, T. Kanehara, Y. Amamoto, A. Takahara, and H. Otsuka, "Self-healing of chemical gels cross-linked by diarylbibenzofuranone-based trigger-free dynamic covalent bonds at room temperature," *Angewandte Chemie*, vol. 124, no. 5, pp. 1164–1168, 2012.

[22] H. Ying, Y. Zhang, and J. Cheng, "Dynamic urea bond for the design of reversible and self-healing polymers," *Nature communications*, vol. 5, p. 3218, 2014.

[23] H. Fischer, "Self-repairing material systems - a dream or a reality ?," *Natural Science*, vol. 2, no. 8, pp. 873–901, 2010.

[24] V. K. Thakur and M. R. Kessler, "Self-healing polymer nanocomposite materials: A review," *Polymer*, vol. 69, pp. 369–383, jul 2015.

[25] H. L. James Darnell and D. Baltimore, "Molecular cell biology," *Gamete Research*, vol. 17, pp. 95–95, may 1987.

[26] T. Smith, "Physical chemistry," in *Fundamentals of Anaesthesia* (C. Pinnock, T. Lin, and T. Smith, eds.), pp. 537–549, Cambridge: Cambridge University Press, 4 ed., 2016.

[27] T. Kaiser, "Highly crosslinked polymers," *Progress in Polymer Science*, vol. 14, pp. 373–450, jan 1989.

[28] J.-M. Raquez, M. Deléglise, M.-F. Lacrampe, and P. Krawczak, "Thermosetting (bio)materials derived from renewable resources: A critical review," *Progress in Polymer Science*, vol. 35, pp. 487–509, apr 2010.

[29] B. H. Rutz and J. C. Berg, "A review of the feasibility of lightening structural polymeric composites with voids without compromising mechanical properties," *Advances in Colloid and Interface Science*, vol. 160, pp. 56–75, oct 2010.

[30] A. Shiota and C. K. Ober, "Rigid rod and liquid crystalline thermosets," *Progress in Polymer Science*, vol. 22, pp. 975–1000, jan 1997.

[31] J. P. Jensen and K. Skelton, "Wind turbine blade recycling: Experiences, challenges and possibilities in a circular economy," *Renewable and Sustainable Energy Reviews*, vol. 97, pp. 165–176, 2018.

[32] A. Pourrajabian, M. Dehghan, A. Javed, and D. Wood, "Choosing an appropriate timber for a small wind turbine blade: A comparative study," *Renewable and Sustainable Energy Reviews*, vol. 100, pp. 1–8, 2019.

[33] K. Senthilkumar, N. Saba, N. Rajini, M. Chandrasekar, M. Jawaid, S. Siengchin, and O. Y. Alotman, "Mechanical properties evaluation of sisal fibre reinforced polymer composites: A review," *Construction and Building Materials*, vol. 174, pp. 713–729, 2018.

[34] A. Campanella, D. Döhler, and W. H. Binder, "Self-Healing in Supramolecular Polymers," *Macromolecular Rapid Communications*, vol. 39, no. 17, p. 1700739, 2018.

[35] D. Döhler, P. Michael, and W. H. Binder, "CuAAC-Based Click Chemistry in Self-Healing Polymers," *Accounts of Chemical Research*, vol. 50, no. 10, pp. 2610–2620, 2017.

[36] F. Herbst, D. Döhler, P. Michael, and W. H. Binder, "Self-healing polymers via supramolecular forces," *Macromolecular Rapid Communications*, vol. 34, no. 3, pp. 203–220, 2013.

[37] C. Soutis, "Fibre reinforced composites in aircraft construction," *Progress in Aerospace Sciences*, vol. 41, no. 2, pp. 143–151, 2005.

[38] A. B. M. Supian, S. M. Sapuan, M. Y. M. Zuhri, E. S. Zainudin, and H. H. Ya, "Hybrid reinforced thermoset polymer composite in energy ab-

sorption tube application: A review," *Defence Technology*, vol. 14, no. 4, pp. 291–305, 2018.

[39] I. Azcune and I. Odriozola, "Aromatic disulfide crosslinks in polymer systems: Self-healing, reprocessability, recyclability and more," *European Polymer Journal*, vol. 84, pp. 147–160, 2016.

[40] E. Tsangouri, D. Aggelis, and D. V. Hemelrijck, "Quantifying thermoset polymers healing efficiency: A systematic review of mechanical testing," *Progress in Polymer Science*, vol. 49-50, pp. 154–174, 2015.

[41] K. Urdl, A. Kandelbauer, W. Kern, U. Müller, M. Thebault, and E. Zikulnig-Rusch, "Self-healing of densely crosslinked thermoset polymers—a critical review," *Progress in Organic Coatings*, vol. 104, pp. 232–249, 2017.

[42] P. Zhang and G. Li, "Advances in healing-on-demand polymers and polymer composites," *Progress in Polymer Science*, vol. 57, pp. 32–63, 2016.

[43] F. JD, "Viscoelastic properties of polymers," *John wiley &sons*, 1980.

[44] S. R. White, B. J. Blaiszik, S. L. B. Kramer, S. C. Olugebefola, J. S. Moore, and N. R. Sottos, "Self-healing polymers and composites," *American Scientist*, vol. 99, no. 5, pp. 392–399, 2011.

[45] A. G. Fallis, "Thermosetting Polymer," *Journal of Chemical Information and Modeling*, vol. 53, no. 9, pp. 1689–1699, 2013.

[46] A. Voznyi, V. Kosyak, P. Onufrijevs, L. Grase, J. Vecstaudža, A. Opanasyuk, and A. Medvid, "Ac Sc," *Journal of Alloys and Compounds*, 2016.

[47] R. Long, H. J. Qi, and M. L. Dunn, "Modeling the mechanics of covalently adaptable polymer networks with temperature-dependent bond exchange reactions," *Soft Matter*, vol. 9, no. 15, pp. 4083–4096, 2013.

[48] L. Guadagno, L. Vertuccio, C. Naddeo, E. Calabrese, G. Barra, M. Raimondo, A. Sorrentino, W. H. Binder, P. Michael, and S. Rana, "Re-

versible Self-Healing Carbon-Based Nanocomposites for Structural Applications," *Polymers*, vol. 11, p. 903, may 2019.

[49] C. N. Bowman and C. J. Kloxin, "Covalent adaptable networks: Reversible bond structures incorporated in polymer networks," *Angewandte Chemie - International Edition*, vol. 51, no. 18, pp. 4272–4274, 2012.

[50] B. C. N. Kloxin CJ, "Covalent adaptable networks: smart, reconfigurable and responsive network systems," *Chem Soc Rev*, 2013.

[51] P. Chakma and D. Konkolewicz, "Dynamic Covalent Bonds in Polymeric Materials," *Angewandte Chemie International Edition*, vol. 58, pp. 9682–9695, jul 2019.

[52] W. Denissen, G. Rivero, R. Nicolaÿ, L. Leibler, J. M. Winne, and F. E. Du Prez, "Vinylogous urethane vitrimers," *Advanced Functional Materials*, vol. 25, no. 16, pp. 2451–2457, 2015.

[53] A. Jurowska and K. Jurowski, "Vitrimers – the miracle polymer materials combining the properties of glass and plastic?," *Chemik*, vol. 69, no. 7, pp. 389–394, 2015.

[54] S. D. Bergman and F. Wudl, "Mendable polymers," *Journal of Materials Chemistry*, vol. 18, no. 1, pp. 41–62, 2008.

[55] C. M. Chung, Y. S. Roh, S. Y. Cho, and J. G. Kim, "Crack healing in polymeric materials via photochemical [2+2] cycloaddition," *Chemistry of Materials*, vol. 16, no. 21, pp. 3982–3984, 2004.

[56] M. Capelot, D. Montarnal, F. Tournilhac, and L. Leibler, "Metal-Catalyzed Transesterification for Healing and Assembling of Thermosets," *Journal of the American Chemical Society*, vol. 134, pp. 7664–7667, may 2012.

[57] T. F. Scott, A. D. Schneider, W. D. Cook, and C. N. Bowman, "Chemistry: Photoinduced plasticity in cross-linked polymers," *Science*, vol. 308, no. 5728, pp. 1615–1617, 2005.

[58] D. A. Kissounko, P. Taynton, and C. Kaffer, "New material: vitrimers promise to impact composites," *Reinforced Plastics*, vol. 62, no. 3, pp. 162–166, 2018.

[59] J. P. Brutman, P. A. Delgado, and M. A. Hillmyer, "Polylactide Vitrimers," *ACS Macro Letters*, vol. 3, pp. 607–610, jul 2014.

[60] G. B. Lyon, L. M. Cox, J. T. Goodrich, A. D. Baranek, Y. Ding, and C. N. Bowman, "Remoldable Thiol–Ene Vitrimers for Photopatterning and Nanoimprint Lithography," *Macromolecules*, vol. 49, pp. 8905–8913, dec 2016.

[61] F. Smallenburg, L. Leibler, and F. Sciortino, "Patchy Particle Model for Vitrimers," *Physical Review Letters*, vol. 111, p. 188002, oct 2013.

[62] L. Rovigatti, G. Nava, T. Bellini, and F. Sciortino, "Self-Dynamics and Collective Swap-Driven Dynamics in a Particle Model for Vitrimers," *Macromolecules*, vol. 51, pp. 1232–1241, feb 2018.

[63] W. Denissen, M. Droesbeke, R. Nicolaÿ, L. Leibler, J. M. Winne, and F. E. Du Prez, "Chemical control of the viscoelastic properties of vinylogous urethane vitrimers," *Nature Communications*, vol. 8, p. 14857, mar 2017.

[64] J. C. Dyre, "Colloquium : The glass transition and elastic models of glass-forming liquids," *Reviews of Modern Physics*, vol. 78, pp. 953–972, sep 2006.

[65] M. D. Ediger, C. A. Angell, and S. R. Nagel, "Supercooled Liquids and Glasses," *The Journal of Physical Chemistry*, vol. 100, pp. 13200–13212, jan 1996.

[66] K. J. Laidler, "The development of the Arrhenius equation," *Journal of Chemical Education*, vol. 61, p. 494, jun 1984.

[67] M. Guerre, C. Taplan, R. Nicolaÿ, J. M. Winne, and F. E. Du Prez, "Fluorinated Vitrimer Elastomers with a Dual Temperature Response," *Journal of the American Chemical Society*, vol. 140, pp. 13272–13284, oct 2018.

[68] H. Han and X. Xu, "Poly(methyl methacrylate)-epoxy vitrimer composites," *Journal of Applied Polymer Science*, vol. 135, p. 46307, jun 2018.

[69] Y. Yang, Z. Pei, Z. Li, Y. Wei, and Y. Ji, "Making and Remaking Dynamic 3D Structures by Shining Light on Flat Liquid Crystalline Vitrimer Films without a Mold," *Journal of the American Chemical Society*, vol. 138, no. 7, pp. 2118–2121, 2016.

[70] D. J. Fortman, J. P. Brutman, C. J. Cramer, M. A. Hillmyer, and W. R. Dichtel, "Mechanically Activated, Catalyst-Free Polyhydroxyurethane Vitrimers," *Journal of the American Chemical Society*, vol. 137, no. 44, pp. 14019–14022, 2015.

[71] Z. Ma, Y. Wang, J. Zhu, J. Yu, and Z. Hu, "Bio-based epoxy vitrimers: Reprocessibility, controllable shape memory, and degradability," *Journal of Polymer Science, Part A: Polymer Chemistry*, vol. 55, no. 10, pp. 1790–1799, 2017.

[72] A. Ruiz De Luzuriaga, J. M. Matxain, F. Ruipérez, R. Martin, J. M. Asua, G. Cabañero, and I. Odriozola, "Transient mechanochromism in epoxy vitrimer composites containing aromatic disulfide crosslinks," *Journal of Materials Chemistry C*, vol. 4, no. 26, pp. 6220–6223, 2016.

[73] R. L. Snyder, D. J. Fortman, G. X. De Hoe, M. A. Hillmyer, and W. R. Dichtel, "Reprocessable Acid-Degradable Polycarbonate Vitrimers," *Macromolecules*, vol. 51, no. 2, pp. 389–397, 2018.

[74] W. Denissen, J. M. Winne, and F. E. Du Prez, "Vitrimers: permanent organic networks with glass-like fluidity," *Chemical Science*, vol. 7, no. 1, pp. 30–38, 2016.

[75] G. Urbain, Y. Bottinga, and P. Richet, "Viscosity of liquid silica, silicates and alumino-silicates," *Geochimica et Cosmochimica Acta*, vol. 46, no. 6, pp. 1061–1072, 1982.

[76] S. Dhers, G. Vantomme, and L. Avérous, "A fully bio-based polyimine vitrimer derived from fructose," *Green Chemistry*, vol. 21, no. 7, pp. 1596–1601, 2019.

[77] Y. Yang, S. Zhang, X. Zhang, L. Gao, Y. Wei, and Y. Ji, "Detecting topology freezing transition temperature of vitrimers by AIE luminogens," *Nature Communications*, vol. 10, no. 1, pp. 1–8, 2019.

[78] J. Otera, "Transesterification," *Chemical Reviews*, vol. 93, pp. 1449–1470, jun 1993.

[79] A. Legrand and C. Soulié-Ziakovic, "Silica-Epoxy Vitrimer Nanocomposites," *Macromolecules*, vol. 49, no. 16, pp. 5893–5902, 2016.

[80] J. Liu, X. Zhang, X. Chen, L. Qu, L. Zhang, W. Li, and A. Zhang, "Stimuli-responsive dendronized polymeric hydrogels through Schiff-base chemistry showing remarkable topological effects," *Polymer Chemistry*, vol. 9, no. 3, pp. 378–387, 2018.

[81] F. I. Altuna, C. E. Hoppe, and R. J. Williams, "Epoxy vitrimers with a covalently bonded tertiary amine as catalyst of the transesterification reaction," *European Polymer Journal*, vol. 113, pp. 297–304, apr 2019.

[82] C. Zhang, P.-L. Show, and S.-H. Ho, "Progress and perspective on algal plastics – A critical review," *Bioresource Technology*, vol. 289, p. 121700, oct 2019.

[83] Y. Spiesschaert, M. Guerre, L. Imbernon, J. M. Winne, and F. Du Prez, "Filler reinforced polydimethylsiloxane-based vitrimers," *Polymer*, vol. 172, pp. 239–246, 2019.

[84] J. Han, T. Liu, C. Hao, S. Zhang, B. Guo, and J. Zhang, "A Catalyst-Free Epoxy Vitrimer System Based on Multifunctional Hyperbranched Polymer," *Macromolecules*, vol. 51, pp. 6789–6799, sep 2018.

[85] Y. Amamoto, H. Otsuka, A. Takahara, and K. Matyjaszewski, "Self-healing of covalently cross-linked polymers by reshuffling thiuram disulfide moieties in air under visible light," *Advanced Materials*, vol. 24, no. 29, pp. 3975–3980, 2012.

[86] J. Canadell, H. Goossens, and B. Klumperman, "Self-healing materials based on disulfide links," *Macromolecules*, vol. 44, no. 8, pp. 2536–2541, 2011.

[87] U. Lafont, H. van Zeijl, and S. van der Zwaag, "Influence of Cross-linkers on the Cohesive and Adhesive Self-Healing Ability of Polysulfide-Based Thermosets," *ACS Applied Materials & Interfaces*, vol. 4, pp. 6280–6288, nov 2012.

[88] B. T. Michal, C. A. Jaye, E. J. Spencer, and S. J. Rowan, "Inherently Photohealable and Thermal Shape-Memory Polydisulfide Networks," *ACS Macro Letters*, vol. 2, pp. 694–699, aug 2013.

[89] G. D. T. Owen, W. J. MacKnight, and A. V. Tobolsky, "Urethane Elastomers Containing Disulfide and Tetrasulfide Linkages," *The Journal of Physical Chemistry*, vol. 68, no. 4, pp. 784–786, 1964.

[90] M. Pepels, I. Filot, B. Klumperman, and H. Goossens, "Self-healing systems based on disulfide–thiol exchange reactions," *Polymer Chemistry*, vol. 4, no. 18, pp. 4955–4965, 2013.

[91] A. Rekondo, R. Martin, A. Ruiz de Luzuriaga, G. Cabañero, H. J. Grande, and I. Odriozola, "Catalyst-free room-temperature self-healing elastomers based on aromatic disulfide metathesis," *Mater. Horiz.*, vol. 1, no. 2, pp. 237–240, 2014.

[92] C. Xu, L. Cao, B. Lin, X. Liang, and Y. Chen, "Design of Self-Healing Supramolecular Rubbers by Introducing Ionic Cross-Links into Natural Rubber via a Controlled Vulcanization," *ACS Applied Materials and Interfaces*, vol. 8, no. 27, pp. 17728–17737, 2016.

[93] P. A. Pratama, A. M. Peterson, and G. R. Palmese, "The role of maleimide structure in the healing of furan-functionalized epoxy–amine thermosets," *Polymer Chemistry*, vol. 4, no. 18, p. 5000, 2013.

[94] D. J. Fortman, R. L. Snyder, D. T. Sheppard, and W. R. Dichtel, "Rapidly Reprocessable Cross-Linked Polyhydroxyurethanes Based on Disulfide Exchange," *ACS Macro Letters*, vol. 7, pp. 1226–1231, oct 2018.

[95] B. Krishnakumar, R. Prasanna Sanka, W. H. Binder, C. Park, J. Jung, V. Parthasarthy, S. Rana, and G. J. Yun, "Catalyst free self-healable vit-

rimer/graphene oxide nanocomposites," *Composites Part B: Engineering*, vol. 184, p. 107647, mar 2020.

[96] M. M. Obadia, B. P. Mudraboyina, A. Serghei, D. Montarnal, and E. Drockenmuller, "Reprocessing and Recycling of Highly Cross-Linked Ion-Conducting Networks through Transalkylation Exchanges of C-N Bonds," *Journal of the American Chemical Society*, vol. 137, no. 18, pp. 6078–6083, 2015.

[97] M. M. Obadia, A. Jourdain, P. Cassagnau, D. Montarnal, and E. Drockenmuller, "Tuning the Viscosity Profile of Ionic Vitrimers Incorporating 1,2,3-Triazolium Cross-Links," *Advanced Functional Materials*, vol. 27, no. 45, pp. 1–10, 2017.

[98] B. Hendriks, J. Waelkens, J. M. Winne, and F. E. Du Prez, "Poly(thioether) Vitrimers via Transalkylation of Trialkylsulfonium Salts," *ACS Macro Letters*, vol. 6, pp. 930–934, sep 2017.

[99] D. J. Fortman, J. P. Brutman, M. A. Hillmyer, and W. R. Dichtel, "Structural effects on the reprocessability and stress relaxation of crosslinked polyhydroxyurethanes," *Journal of Applied Polymer Science*, vol. 134, p. 44984, dec 2017.

[100] A. Chao, I. Negulescu, and D. Zhang, "Dynamic Covalent Polymer Networks Based on Degenerative Imine Bond Exchange: Tuning the Malleability and Self-Healing Properties by Solvent," *Macromolecules*, vol. 49, pp. 6277–6284, sep 2016.

[101] Z. Feng, B. Yu, J. Hu, H. Zuo, J. Li, H. Sun, N. Ning, M. Tian, and L. Zhang, "Multifunctional Vitrimer-Like Polydimethylsiloxane (PDMS): Recyclable, Self-Healable, and Water-Driven Malleable Covalent Networks Based on Dynamic Imine Bond," *Industrial & Engineering Chemistry Research*, vol. 58, pp. 1212–1221, jan 2019.

[102] P. Taynton, C. Zhu, S. Loob, R. Shoemaker, J. Pritchard, Y. Jin, and W. Zhang, "Re-healable polyimine thermosets: polymer composition and moisture sensitivity," *Polymer Chemistry*, vol. 7, no. 46, pp. 7052–7056, 2016.

[103] S. Wang, S. Ma, Q. Li, W. Yuan, B. Wang, and J. Zhu, "Robust, Fire-Safe, Monomer-Recovery, Highly Malleable Thermosets from Renewable Bioresources," *Macromolecules*, vol. 51, pp. 8001–8012, oct 2018.

[104] H. Zhang, D. Wang, W. Liu, P. Li, J. Liu, C. Liu, J. Zhang, N. Zhao, and J. Xu, "Recyclable polybutadiene elastomer based on dynamic imine bond," *Journal of Polymer Science Part A: Polymer Chemistry*, vol. 55, pp. 2011–2018, jun 2017.

[105] Y. Zhang, C. Dai, S. Zhou, and B. Liu, "Enabling shape memory and healable effects in a conjugated polymer by incorporating siloxane via dynamic imine bond," *Chemical Communications*, vol. 54, no. 72, pp. 10092–10095, 2018.

[106] H. Zheng, Q. Liu, X. Lei, Y. Chen, B. Zhang, and Q. Zhang, "A conjugation polyimine vitrimer: Fabrication and performance," *Journal of Polymer Science Part A: Polymer Chemistry*, vol. 56, pp. 2531–2538, nov 2018.

[107] P. Taynton, K. Yu, R. K. Shoemaker, Y. Jin, H. J. Qi, and W. Zhang, "Heat- or water-driven malleability in a highly recyclable covalent network polymer," *Advanced Materials*, vol. 26, no. 23, pp. 3938–3942, 2014.

[108] H. Zheng, Q. Liu, X. Lei, Y. Chen, B. Zhang, and Q. Zhang, "Performance-modified polyimine vitrimers: flexibility, thermal stability and easy reprocessing," *Journal of Materials Science*, vol. 54, no. 3, pp. 2690–2698, 2019.

[109] S. Chen, F. Tang, L. Tang, and L. Li, "Synthesis of Cu-Nanoparticle Hydrogel with Self-Healing and Photothermal Properties," *Applied Materials & Interfaces*, vol. 9, no. 24, pp. 20895–20903, 2017.

[110] S. Chen and W. H. Binder, "Dynamic Ordering and Phase Segregation in Hydrogen-Bonded Polymers," *Accounts of Chemical Research*, vol. 49, pp. 1409–1420, jul 2016.

[111] Y. Yang, Z. Pei, X. Zhang, L. Tao, Y. Wei, and Y. Ji, "Chemical Science and effi cient photo-welding of epoxy," *Chemical Science*, vol. 5, pp. 3486–3492, 2014.

[112] T. Liu, C. Hao, S. Zhang, X. Yang, L. Wang, J. Han, Y. Li, J. Xin, and J. Zhang, "A Self-Healable High Glass Transition Temperature Bioepoxy Material Based on Vitrimer Chemistry," *Macromolecules*, vol. 51, pp. 5577–5585, aug 2018.

[113] L. Cao, J. Fan, J. Huang, and Y. Chen, "A robust and stretchable cross-linked rubber network with recyclable and self-healable capabilities based on dynamic covalent bonds," *J. Mater. Chem. A*, vol. 7, no. 9, pp. 4922–4933, 2019.

[114] Z. Wang, Z. Li, Y. Wei, and Y. Ji, "Gold nanospheres dispersed light responsive epoxy vitrimers," *Polymers*, vol. 10, no. 1, pp. 1–2, 2018.

[115] Z. Huang, Y. Wang, J. Zhu, J. Yu, and Z. Hu, "Surface engineering of nanosilica for vitrimer composites," *Composites Science and Technology*, vol. 154, pp. 18–27, jan 2018.

[116] Z. Yang, Q. Wang, and T. Wang, "Dual-Triggered and Thermally Reconfigurable Shape Memory Graphene-Vitrimer Composites," *ACS Applied Materials and Interfaces*, vol. 8, no. 33, pp. 21691–21699, 2016.

[117] A. Li, J. Fan, and G. Li, "Recyclable thermoset shape memory polymers with high stress and energy output via facile UV-curing," *J. Mater. Chem. A*, vol. 6, no. 24, pp. 11479–11487, 2018.

[118] Z. Pei, Y. Yang, Q. Chen, E. M. Terentjev, Y. Wei, and Y. Ji, "Mouldable liquid-crystalline elastomer actuators with exchangeable covalent bonds," *Nature Materials*, vol. 13, no. 1, pp. 36–41, 2014.

[119] D. W. Hanzon, N. A. Traugutt, M. K. McBride, C. N. Bowman, C. M. Yakacki, and K. Yu, "Adaptable liquid crystal elastomers with transesterification-based bond exchange reactions," *Soft Matter*, vol. 14, no. 6, pp. 951–960, 2018.

[120] L. L. Wang, J. N. Sloand, A. C. Gaffey, C. M. Venkataraman, Z. Wang, A. Trubelja, D. A. Hammer, P. Atluri, and J. A. Burdick, "Injectable, Guest–Host Assembled Polyethylenimine Hydrogel for siRNA Delivery," *Biomacromolecules*, vol. 18, pp. 77–86, jan 2017.

[121] Q. Chen, Y. Wei, and Y. Ji, "Photo-responsive liquid crystalline vitrimer containing oligoanilines," *Chinese Chemical Letters*, vol. 28, pp. 2139–2142, nov 2017.

[122] Z. Wang, Z. Li, Y. Wei, and Y. Ji, "Gold Nanospheres Dispersed Light Responsive Epoxy Vitrimers," *Polymers*, vol. 10, p. 65, jan 2018.

[123] A. Ruiz de Luzuriaga, R. Martin, N. Markaide, A. Rekondo, G. Cabañero, J. Rodríguez, and I. Odriozola, "Epoxy resin with exchangeable disulfide crosslinks to obtain reprocessable, repairable and recyclable fiber-reinforced thermoset composites," *Materials Horizons*, vol. 3, no. 3, pp. 241–247, 2016.

[124] A. Buonerba, V. Speranza, C. Capacchione, S. Milione, and A. Grassi, "Improvement of tensile properties, self-healing and recycle of thermoset styrene/2-vinylfuran copolymers via thermal triggered rearrangement of covalent crosslink," *European Polymer Journal*, vol. 99, pp. 368–377, 2018.

[125] Y.-L. L. Chuo and Tsai-Wei, "Self-healing polymers based on thermally reversible Diels–Alder chemistry," *Polymer Chemistry*, vol. 4, no. 7, pp. 2194–2205, 2013.

[126] P. Du, M. Wu, X. Liu, Z. Zheng, X. Wang, T. Joncheray, and Y. Zhang, "Diels-Alder-based crosslinked self-healing polyurethane/urea from polymeric methylene diphenyl diisocyanate," *Journal of Applied Polymer Science*, vol. 131, no. 9, pp. 1–7, 2014.

[127] M. Capelot, D. Montarnal, F. Tournilhac, and L. Leibler, "Metal-Catalyzed Transesterification for Healing and Assembling of Thermosets," *Journal of the American Chemical Society*, vol. 134, pp. 7664–7667, may 2012.

[128] B. Hendriks, J. Waelkens, J. M. Winne, and F. E. Du Prez, "Poly(thioether) Vitrimers via Transalkylation of Trialkylsulfonium Salts," *ACS Macro Letters*, vol. 6, pp. 930–934, sep 2017.

[129] J. Canadell, H. Goossens, and B. Klumperman, "Self-Healing Materials Based on Disulfide Links," *Macromolecules*, vol. 44, no. 8, pp. 2536–2541, 2011.

[130] Z. Ma, Y. Wang, J. Zhu, J. Yu, and Z. Hu, "Bio-based epoxy vitrimers: Reprocessibility, controllable shape memory, and degradability," *Journal of Polymer Science, Part A: Polymer Chemistry*, vol. 55, no. 10, pp. 1790–1799, 2017.

[131] A. Ruiz De Luzuriaga, J. M. Matxain, F. Ruipérez, R. Martin, J. M. Asua, G. Cabañero, and I. Odriozola, "Transient mechanochromism in epoxy vitrimer composites containing aromatic disulfide crosslinks," *Journal of Materials Chemistry C*, vol. 4, no. 26, pp. 6220–6223, 2016.

[132] Y. Yang, Z. Pei, X. Zhang, L. Tao, Y. Wei, and Y. Ji, "Correction: Carbon nanotube-vitrimer composite for facile and efficient photowelding of epoxy (Chemical Science (2014) 5 (3486–3492) DOI: 10.1039/C4SC00543K)," *Chemical Science*, vol. 8, no. 3, p. 2464, 2017.

[133] D. R. Bortz, E. G. Heras, and I. Martin-Gullon, "Impressive fatigue life and fracture toughness improvements in graphene oxide/epoxy composites," *Macromolecules*, vol. 45, no. 1, pp. 238–245, 2012.

[134] J. Luo, S. Yang, L. Lei, J. Zhao, and Z. Tong, "Toughening, synergistic fire retardation and water resistance of polydimethylsiloxane grafted graphene oxide to epoxy nanocomposites with trace phosphorus," *Composites Part A: Applied Science and Manufacturing*, vol. 100, pp. 275–284, 2017.

[135] G. Watson, K. Starost, P. Bari, N. Faisal, S. Mishra, and J. Njuguna, "Tensile and Flexural Properties of Hybrid Graphene Oxide / Epoxy Carbon Fibre Reinforced Composites," *IOP Conference Series: Materials Science and Engineering*, vol. 195, no. 1, 2017.

[136] W. S. Hummers and R. E. Offeman, "Preparation of Graphitic Oxide," *Journal of the American Chemical Society*, vol. 80, p. 1339, mar 1958.

[137] M. J. A. Fernández-garcia and Rodriguez, "Metal Oxide Nanoparticles," *Nanomaterials: Inorganic and Bioinorganic Perspectives*, no. October, p. 60, 2007.

[138] S. Rana, D. Döhler, A. S. Nia, M. Nasir, M. Beiner, and W. H. Binder, ""Click"-Triggered Self-Healing Graphene Nanocomposites," *Macromolecular Rapid Communications*, vol. 37, no. 21, pp. 1715–1722, 2016.

[139] B. A. Aragaw, "Reduced graphene oxide-intercalated graphene oxide nano-hybrid for enhanced photoelectrochemical water reduction," *Journal of Nanostructure in Chemistry*, vol. 10, no. 1, pp. 9–18, 2020.

[140] G. B. Olowojoba, S. Kopsidas, S. Eslava, E. S. Gutierrez, A. J. Kinloch, C. Mattevi, V. G. Rocha, and A. C. Taylor, "A facile way to produce epoxy nanocomposites having excellent thermal conductivity with low contents of reduced graphene oxide," *Journal of Materials Science*, vol. 52, no. 12, pp. 7323–7344, 2017.

[141] O. Vryonis, S. T. H. Virtanen, T. Andritsch, A. S. Vaughan, and P. L. Lewin, "Understanding the cross-linking reactions in highly oxidized graphene/epoxy nanocomposite systems," *Journal of Materials Science*, vol. 54, pp. 3035–3051, feb 2019.

[142] C. Park, J. Jung, and G. J. Yun, "Thermomechanical properties of mineralized nitrogen-doped carbon nanotube/polymer nanocomposites by molecular dynamics simulations," *Composites Part B: Engineering*, vol. 161, pp. 639–650, 2019.

[143] J. Glaum, M.-A. Einarsrud, A. Dalod, M. Balci, and M. Adnan, "In Situ Synthesis of Hybrid Inorganic–Polymer Nanocomposites," *Polymers*, vol. 10, no. 10, p. 1129, 2018.

[144] G. B. Olowojoba, S. Kopsidas, S. Eslava, E. S. Gutierrez, A. J. Kinloch, C. Mattevi, V. G. Rocha, and A. C. Taylor, "A facile way to produce epoxy nanocomposites having excellent thermal conductivity with

low contents of reduced graphene oxide," *Journal of Materials Science*, vol. 52, pp. 7323–7344, jun 2017.

[145] S. Ebnesajjad and A. H. Landrock, "Chapter 5 - Characteristics of Adhesive Materials," in *Adhesives Technology Handbook (Third Edition)* (S. Ebnesajjad and A. H. Landrock, eds.), pp. 84–159, Boston: William Andrew Publishing, third edit ed., 2015.

[146] W. A. Ogden and Z. Guan, "Recyclable, Strong, and Highly Malleable Thermosets Based on Boroxine Networks," *Journal of the American Chemical Society*, vol. 140, pp. 6217–6220, may 2018.

[147] R. L. Snyder, D. J. Fortman, G. X. De Hoe, M. A. Hillmyer, and W. R. Dichtel, "Reprocessable Acid-Degradable Polycarbonate Vitrimers," *Macromolecules*, vol. 51, pp. 389–397, jan 2018.

[148] Guadagno, Liberata, Vertuccio, Luigi, Naddeo, Carlo, Calabrese, Elisa, Barra, Giuseppina, Raimondo, Marialuigia, Sorrentino, Andrea, Binder, Wolfgang H., Michael, Philipp, and Rana, Sravendra, "Development of aeronautical epoxy nanocomposites having an integrated selfhealing ability," *MATEC Web Conf.*, vol. 233, p. 21, 2018.

[149] J. Zhao, P. Yu, and S. Dong, "The influence of crosslink density on the failure behavior in amorphous polymers by molecular dynamics simulations," *Materials*, vol. 9, no. 4, 2016.

[150] T. Osada, A. Watabe, J. Yamamoto, J. C. Brouwer, C. Kwakernaak, S. Ozaki, S. van der Zwaag, and W. G. Sloof, "Full strength and toughness recovery after repeated cracking and healing in bone-like high temperature ceramics," *Scientific Reports*, vol. 10, no. 1, p. 18990, 2020.

[151] N. M. Florea, A. Lungu, P. Badica, L. Craciun, M. Enculescu, D. G. Ghita, C. Ionescu, R. G. Zgirian, and H. Iovu, "Novel nanocomposites based on epoxy resin / epoxy-functionalized polydimethylsiloxane reinforced with POSS," *Composites Part B*, vol. 75, pp. 226–234, 2015.

[152] S. Nevejans, N. Ballard, J. I. Miranda, B. Reck, and J. M. Asua, "The underlying mechanisms for self-healing of poly(disulfide)s," *Phys. Chem. Chem. Phys.*, vol. 18, no. 39, pp. 27577–27583, 2016.

[153] L. Ling, J. Li, G. Zhang, R. Sun, and C.-P. Wong, "Self-Healing and Shape Memory Linear Polyurethane Based on Disulfide Linkages with Excellent Mechanical Property," *Macromolecular Research*, vol. 26, pp. 365–373, apr 2018.

[154] H. Du, X. Liu, Y. Yu, Y. Xu, Y. Wang, and Z. Liang, "Microwave-Induced Poly(ionic liquid)/Poly(vinyl alcohol) Shape Memory Composites," *Macromolecular Chemistry and Physics*, vol. 217, pp. 2626–2634, dec 2016.

[155] S. Rana, N. Karak, J. W. Cho, and Y. H. Kim, "Enhanced dispersion of carbon nanotubes in hyperbranched polyurethane and properties of nanocomposites," *Nanotechnology*, vol. 19, no. 49, p. 495707, 2008.

[156] A. Romo-Uribe, J. A. Arcos-Casarrubias, A. Reyes-Mayer, and R. Guardian-Tapia, "PDMS Nanodomains in DGEBA Epoxy Induce High Flexibility and Toughness," *Polymer - Plastics Technology and Engineering*, vol. 56, no. 1, pp. 96–107, 2017.

[157] A. Selvaganapathi, M. Alagar, and P. Gnanasundaram, "Studies on synthesis and characterization of hydroxyl-terminated polydimethylsiloxane-modified epoxy bismaleimide matrices," *High Performance Polymers*, vol. 25, no. 6, pp. 622–633, 2013.

[158] Y. Wu, B. Tang, K. Liu, X. Zeng, J. Lu, T. Zhang, and X. Shen, "Enhanced flexural properties of aramid fiber/epoxy composites by graphene oxide," *Nanotechnology Reviews*, vol. 8, pp. 484–492, dec 2019.

[159] A. K. Srivastava, V. Gupta, C. S. Yerramalli, and A. Singh, "Flexural strength enhancement in carbon-fiber epoxy composites through graphene nano-platelets coating on fibers," *Composites Part B: Engineering*, vol. 179, p. 107539, 2019.

[160] S. Verma, S. Mohanty, and S. K. Nayak, "Preparation of hydrophobic epoxy-polydimethylsiloxane-graphene oxide nanocomposite coatings for antifouling application," *Soft Matter*, vol. 16, no. 5, pp. 1211–1226, 2020.

[161] D. Montarnal, M. Capelot, F. Tournilhac, and L. Leibler, "Silica-Like Malleable Materials from Permanent Organic Networks," *Science*, vol. 334, pp. 965–968, nov 2011.

[162] B. Krishnakumar, R. V. S. P. Sanka, W. H. Binder, V. Parthasarthy, S. Rana, and N. Karak, "Vitrimers: Associative Dynamic Covalent Adaptive Networks in Thermoset Polymers," *Chemical Engineering Journal*, p. 123820, 2019.

[163] F. E. Swallow, "Viscosity of polydimethylsiloxane gum: Shear and temperature dependence from dynamic and capillary rheometry," *Journal of Applied Polymer Science*, vol. 84, no. 13, pp. 2533–2540, 2002.

[164] C. Taplan, M. Guerre, J. M. Winne, and F. E. Du Prez, "Fast processing of highly crosslinked, low-viscosity vitrimers," *Materials Horizons*, 2020.

[165] M. Castelaín, P. S. Shuttleworth, C. Marco, G. Ellis, and H. J. Salavagione, "Comparative study of the covalent diazotization of graphene and carbon nanotubes using thermogravimetric and spectroscopic techniques," *Phys. Chem. Chem. Phys.*, vol. 15, no. 39, pp. 16806–16811, 2013.

[166] S. Zhang, T. Liu, C. Hao, L. Wang, J. Han, H. Liu, and J. Zhang, "Preparation of a lignin-based vitrimer material and its potential use for recoverable adhesives," *Green Chemistry*, vol. 20, no. 13, pp. 2995–3000, 2018.

[167] F. I. Altuna, V. Pettarin, and R. J. J. Williams, "Self-healable polymer networks based on the cross-linking of epoxidised soybean oil by an aqueous citric acid solution," *Green Chemistry*, vol. 15, no. 12, pp. 3360–3366, 2013.

[168] A. K. Mohanty, M. Misra, and L. T. Drzal, *Natural Fibers, Biopolymers, and Biocomposites*. CRC Press, apr 2005.

[169] D. Bose, S. Sridharan, H. Dhawan, P. Vijay, and M. Gopinath, "Biomass derived activated carbon cathode performance for sustainable power generation from Microbial Fuel Cells," *Fuel*, vol. 236, pp. 325–337, 2019.

[170] X. Hu, M. Fan, B. F. Towler, M. Radosz, D. A. Bell, and O. A. Plumb, "Hydrogen Adsorption and Storage," in *Coal Gasification and Its Applications*, pp. 157–245, Elsevier Inc., 2011.

[171] B. Krishnakumar, M. Singh, V. Parthasarthy, C. Park, N. G. Sahoo, G. J. Yun, and S. Rana, "Disulfide exchange assisted self-healing epoxy/PDMS/graphene oxide nanocomposites," *Nanoscale Advances*, pp. –, 2020.

APPENDIX

Table A1. Different nanocomposite percentage prepared with an addition of dispersed solution

EP-x%	Graphene oxide dispersed solution (mL)
EP-pristine	0
EP-0.1%	0.04
EP-0.2%	0.08
EP-0.5%	0.20
EP-1%	0.041
EP-3%	1.25

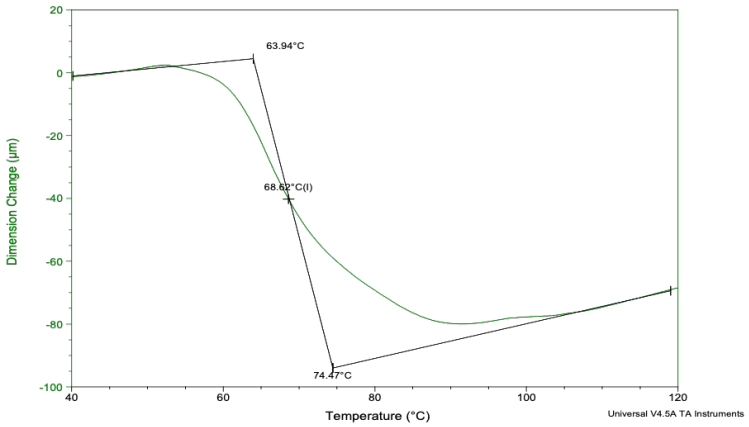

(a) EP-pristine

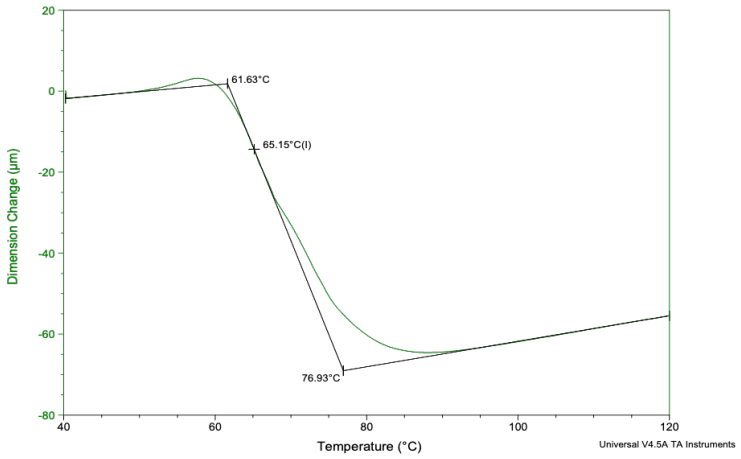

(b) EP-0.1

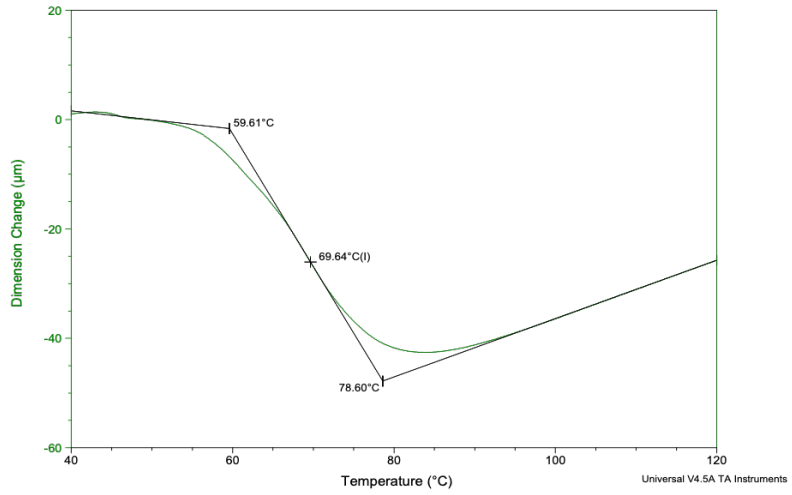

(c) EP-0.2

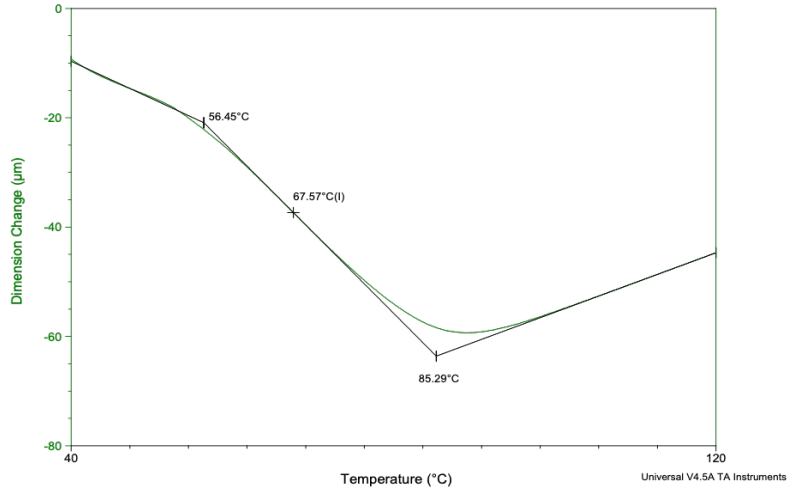

(d) EP-0.5

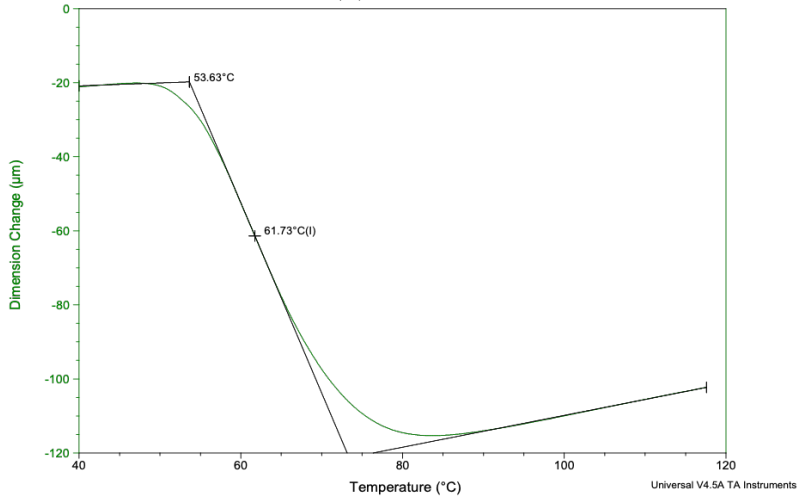

(e) EP-1

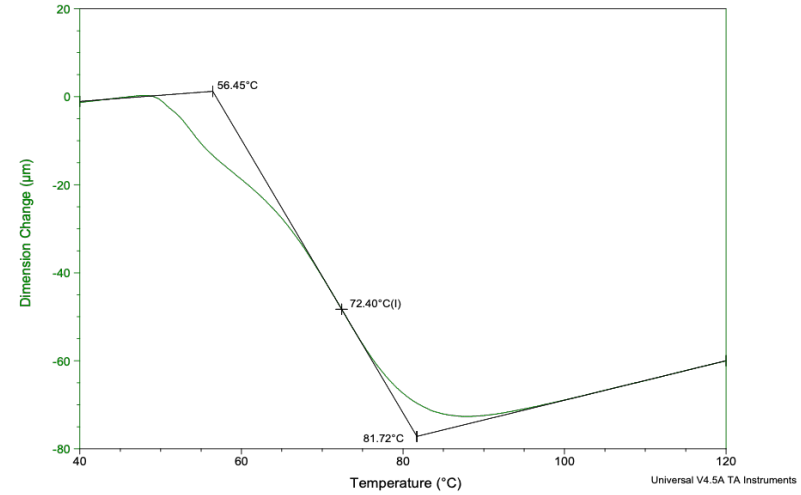

(f) EP-3

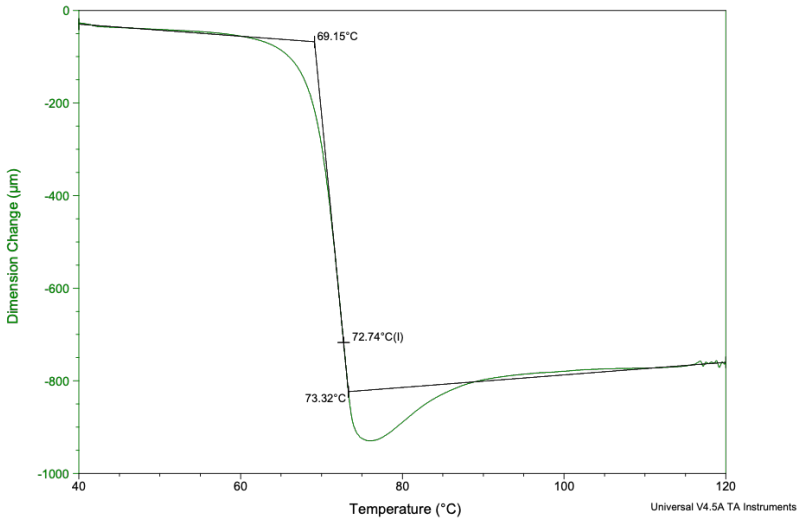

(g) R-Epoxy

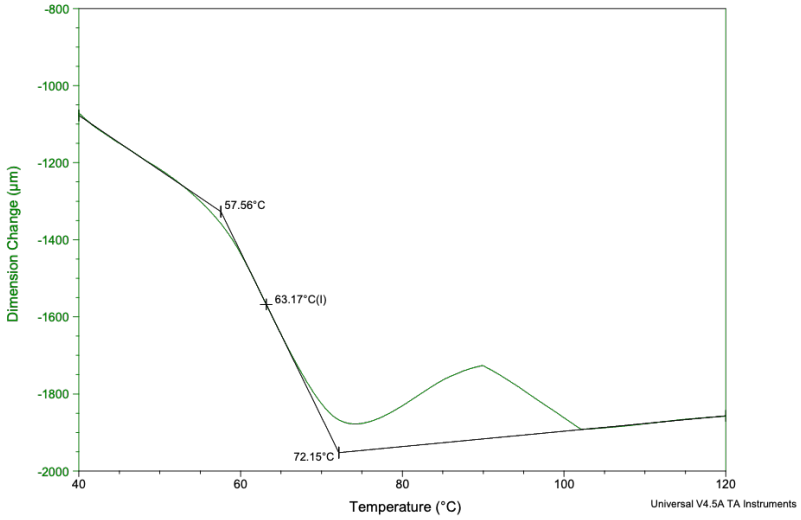

(h) R-Epoxy-1

Figure A1. Glass transition Temperature of Epoxy-GO vitrimers

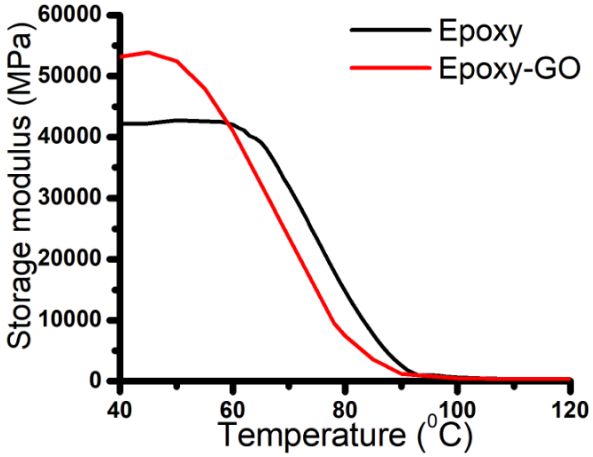

(a)

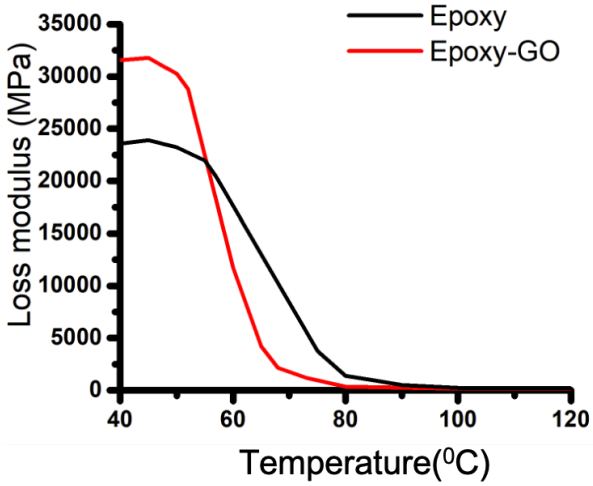

(b)

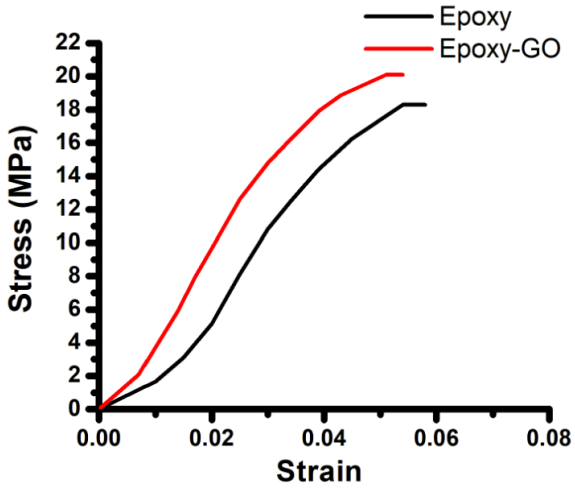

(c)

Figure A2. (a) Storage (b) Loss modulus and (c) Stress-strain curve for reference epoxy samples

Table A2. Different (a) epoxy composite and (b) epoxy nanocomposite

(a)

EP-PDMS	Epoxy (mg)	DG-PDMS (mg)
EP-pristine	500	0
EP-1%	500	5
EP-2%	500	10
EP-3%	500	15
EP-5%	500	25

(b)

Epoxy-2-GO (EP-2-y)	Epoxy (mg)	DG-PDMS (mg)	Graphene oxide (mg)	Graphene oxide dispersed solution (mL)
EP-2-0.1	600	12	0.6	0.04
EP-2-0.2	600	12	1.2	0.08
EP-2-0.5	600	12	3	0.2
EP-2-1	600	12	6	0.4
EP-2-2	600	12	12	0.8

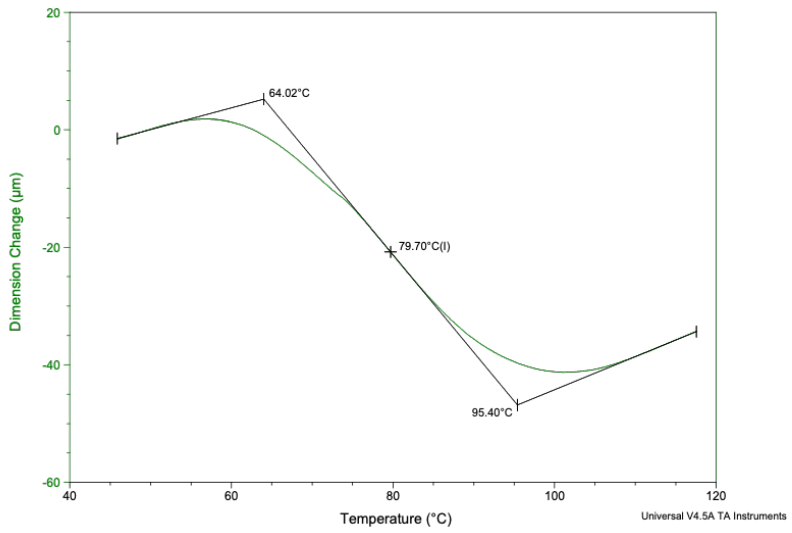

(a) EP-pristine

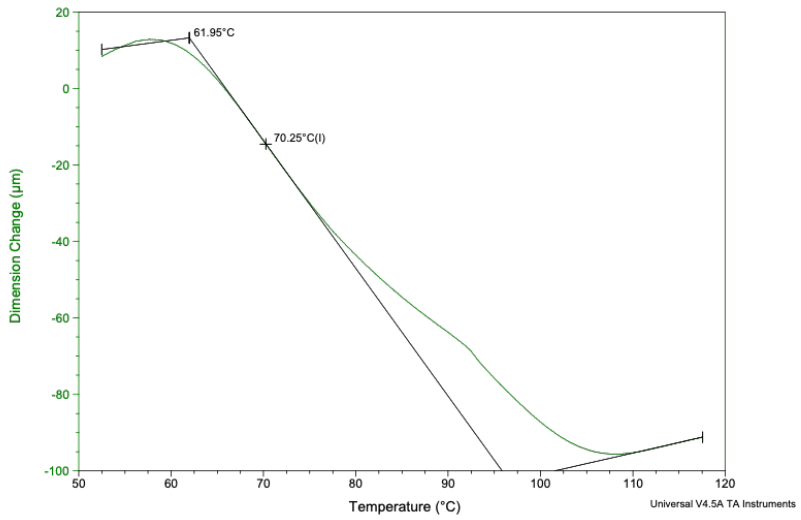

(b) EP-1

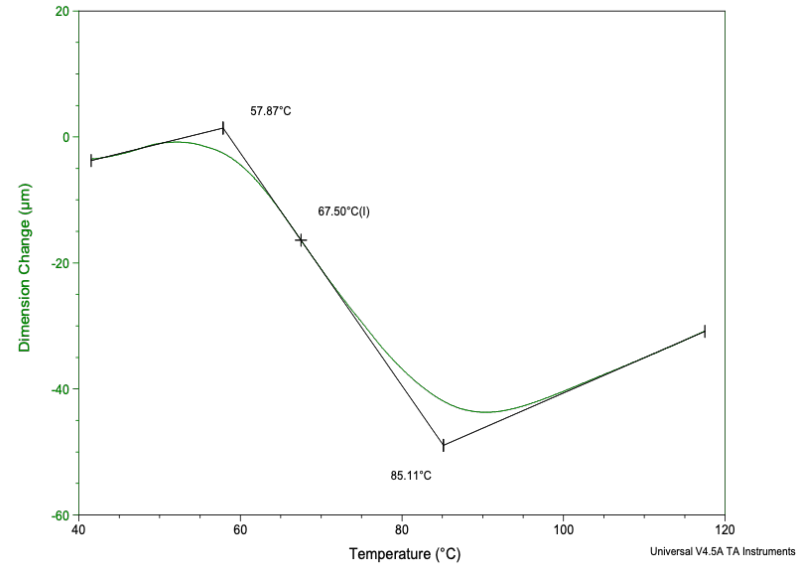

(c) EP-2

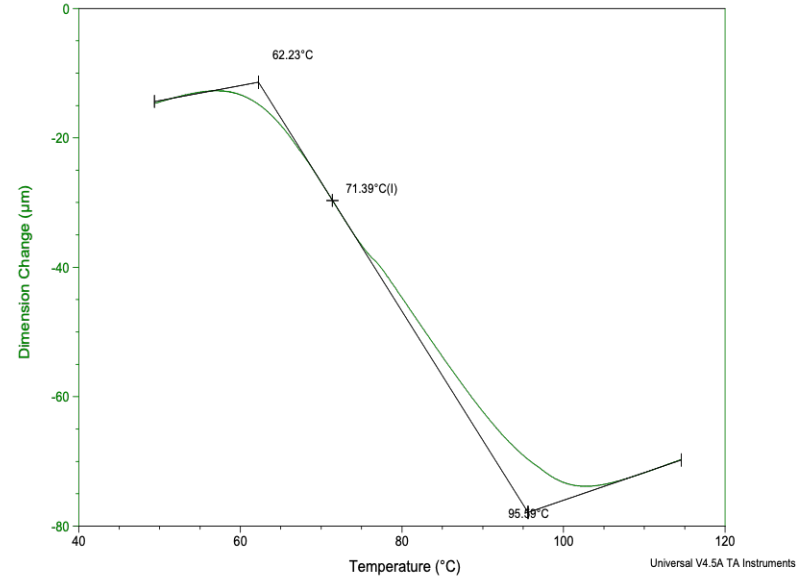

(d) EP-3

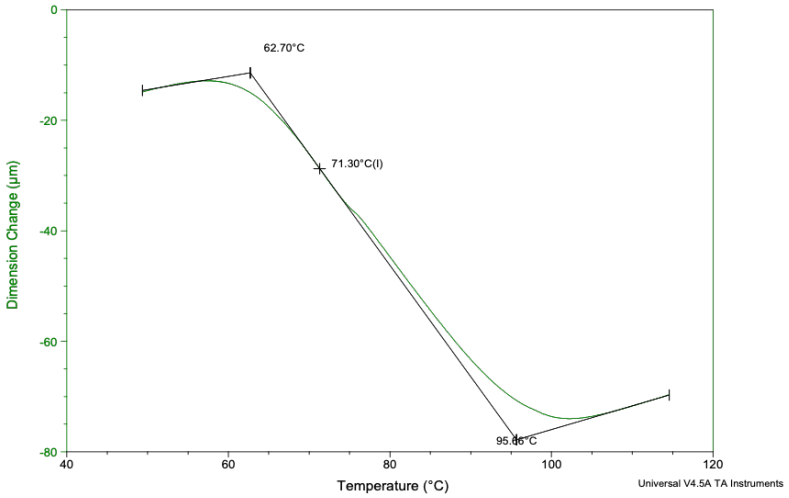

(e) EP-5

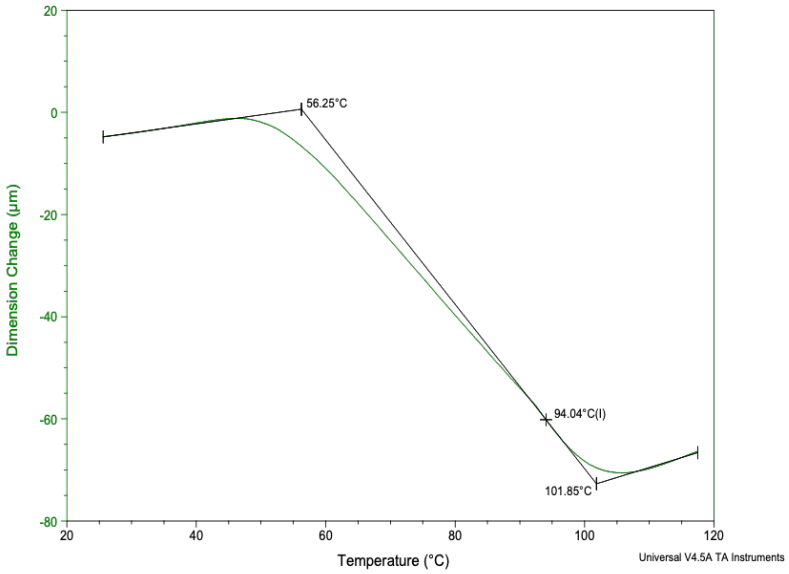

(f) EP-2-0.1

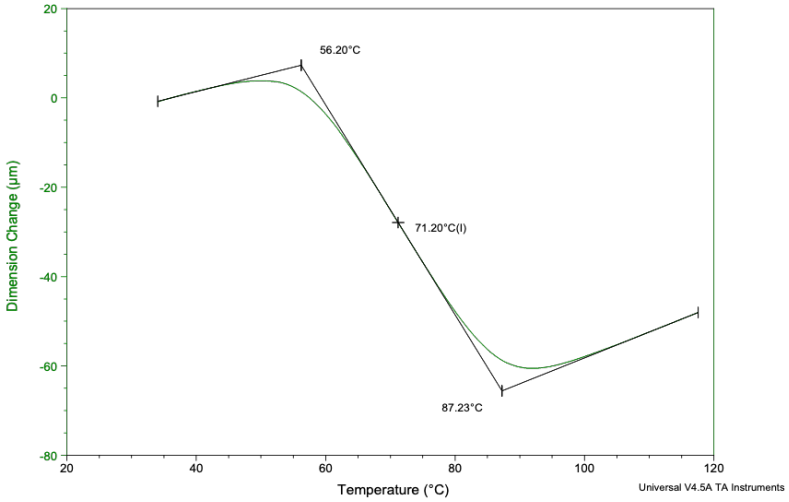

(g) EP-2-0.2

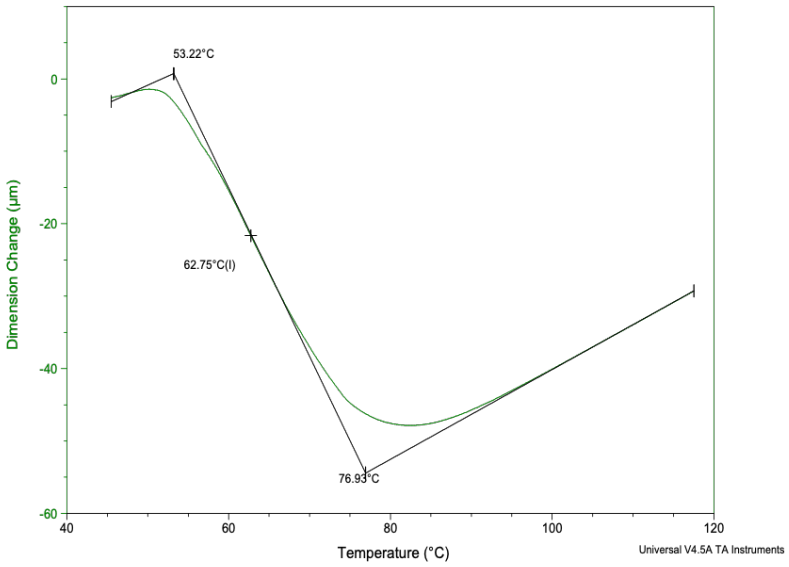

(h) EP-2-0.5

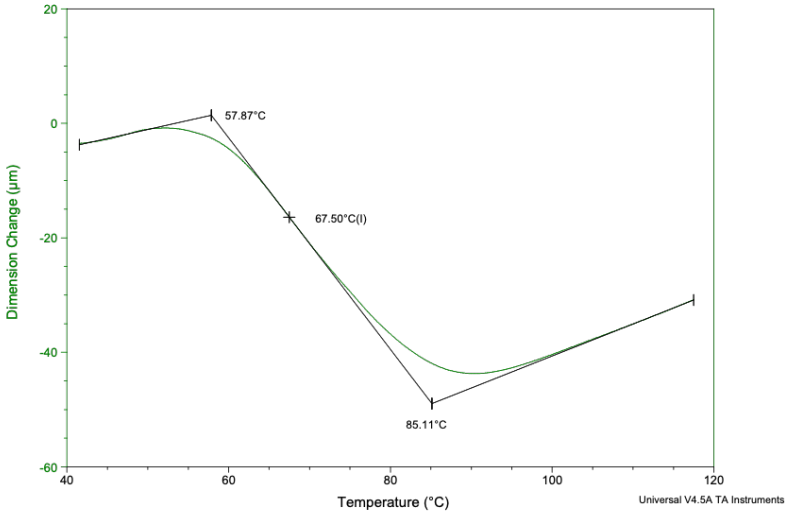

(i) EP-2-1

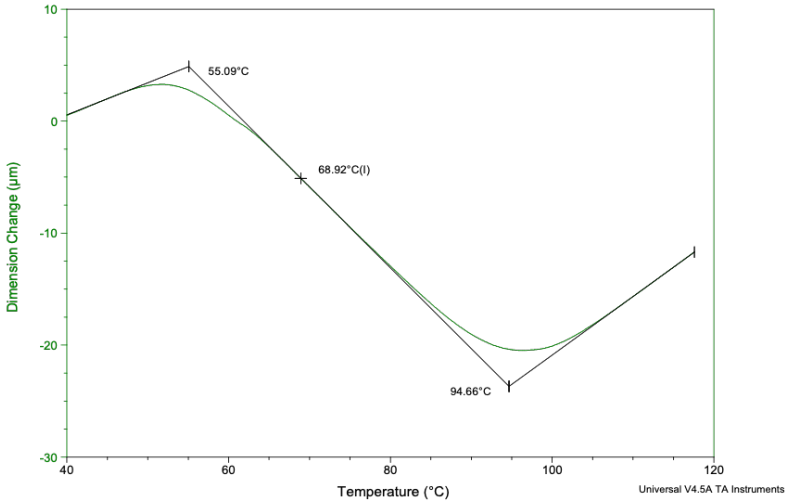

(j) EP-2-2

Figure A3. Glass transition Temperature of Epoxy/PDMS and Epoxy/PDMS/GO vitrimers

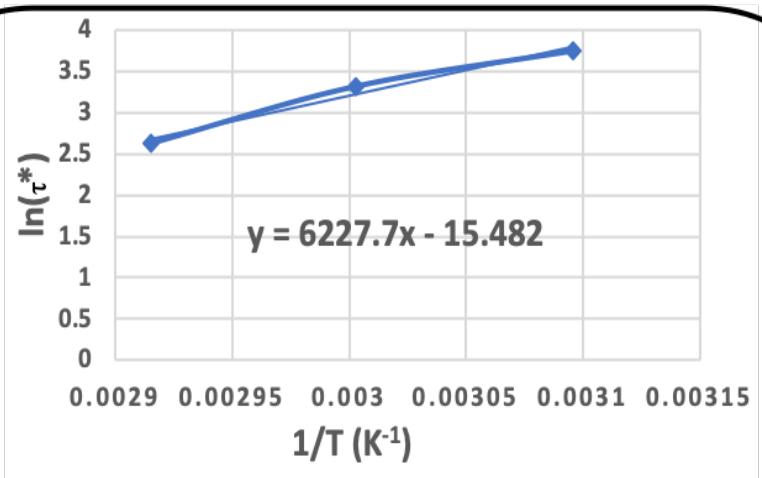

$y = 6227.7x - 15.482$

Which corresponds to : $\ln(\tau^*) = E_a/R\ (1/T) + \ln(\tau_0)$

$\ln(\tau^*) = 6227.7 * 1/T - 15.482$

$E_a/R = 6227.7$

$E_a = 6227.7 * 8.314 = 51.7$ kJ/mol

$\eta = G.\ \tau^*$

G- Shear viscosity modulus;

Relation between shear modulus and tensile modulus,

$G = E'/2(1+\upsilon)$

Generally, υ- Poisson's ratio is 0.5 for rubbery materials.

So , $G=1795/3= 598.3$ MPa (or) $598.3*10^6$ Pa

$\tau^*= 10^{12}/(598.3*10^6) = 1671.42$ s.

$\ln(\tau^*) = \ln(1671.42) = 7.42$

Equation obtained from Arrhenius law: $\ln(\tau^*) = 6227.7x - 15.482$

$x=1/T= (\ln(\tau^*)+15.482)/6227.7 =0.003677$

So, $T= 1/0.003677$

T_v=272 K (or) -1^{0}C

Calculation A1. Epoxy/PDMS activation energy and topology freezing transition temperature

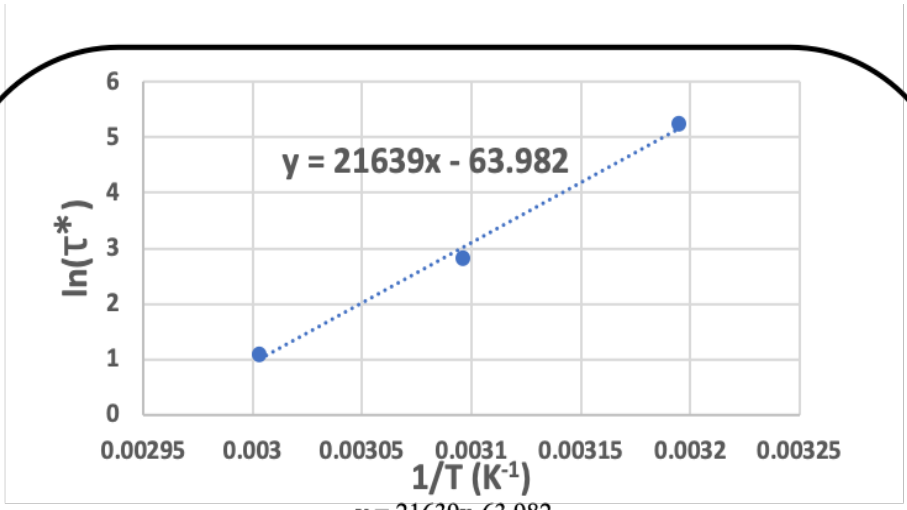

y = 21639x-63.982

Which corresponds to : $\ln(\tau^*) = E_a/R\ (1/T) + \ln(\tau_0)$

$\ln(\tau^*) = 21639 * 1/T - 63.982$

$E_a/R = 21639$

E_a = 21639 * 8.314 = 179.9 kJ/mol

$\eta = G.\ \tau^*$

G- Shear viscosity modulus;

Relation between shear modulus and tensile modulus,

$G = E'/\ 2(1+\upsilon)$

Generally, υ- Poisson's ratio is 0.5 for rubbery materials.

So , G=2452/3= 817.3 MPa (or) $817.3*10^6$ Pa

$\tau^* = 10^{12}/(817.3*10^6) = 1223.5$ s.

$\ln(\tau^*) = \ln(1223.5) = 7.1$

Equation obtained from Arrhenius law: $\ln(\tau^*) = 21639x - 63.982$

$x=1/T= (\ln(\tau^*)+63.982)/21639 =0.00328$

So, T= 1/0.00328

T_v=304 K (or) 31 ^{0}C

Calculation A2. Epoxy/PDMS/GO activation energy and topology freezing transition temperature

Table A3. Different composite percentage prepared with an addition of dispersed solution

EP-x%	Activated carbon dispersed solution (mL)
EP-pristine	0
EP-0.1%	0.04
EP-0.2%	0.08
EP-0.5%	0.20
EP-1%	0.041
EP-3%	1.25

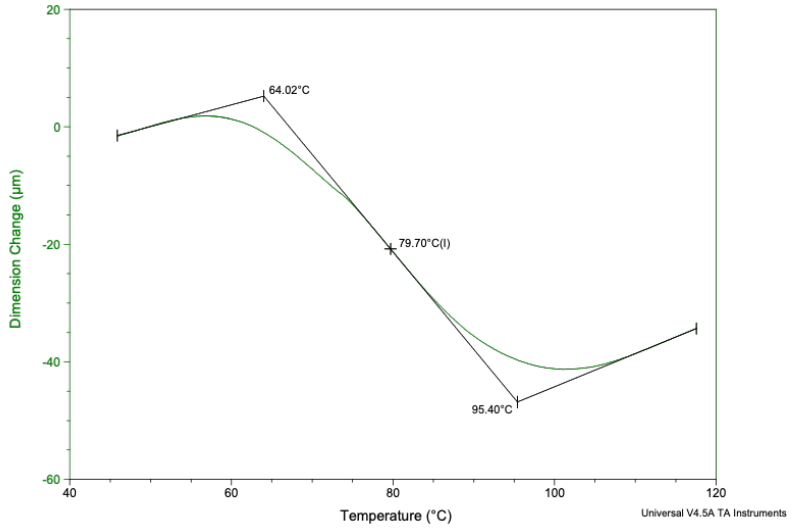

(a) EP-pristine

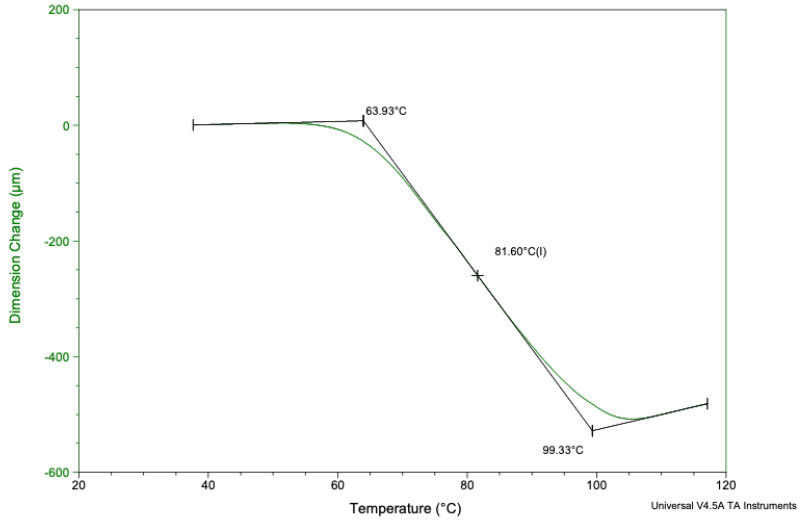

(b) EP-0.1

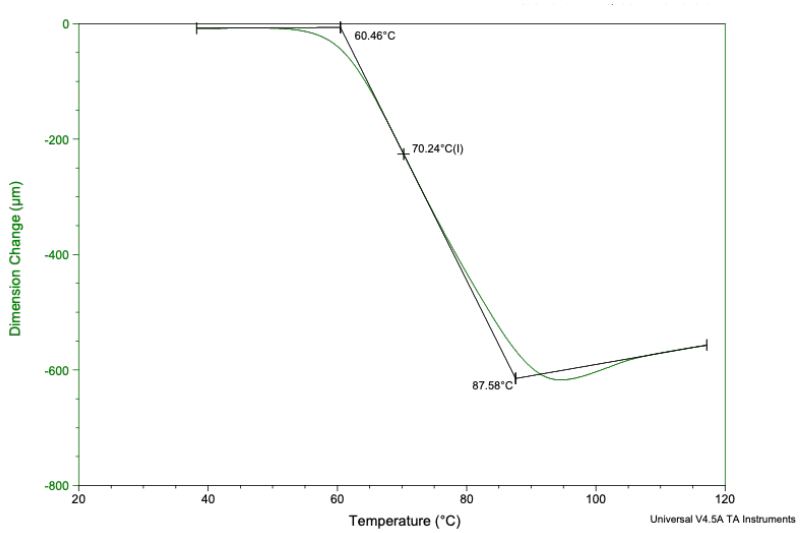

(c) EP-0.2

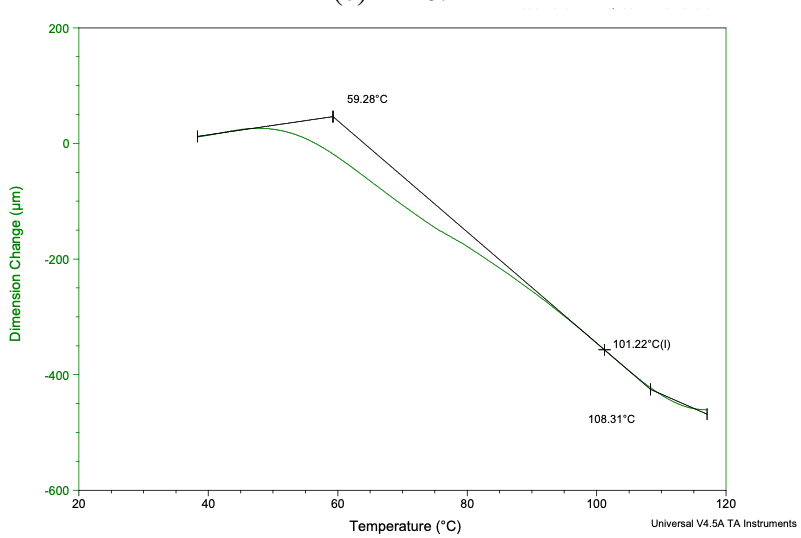

(d) EP-0.5

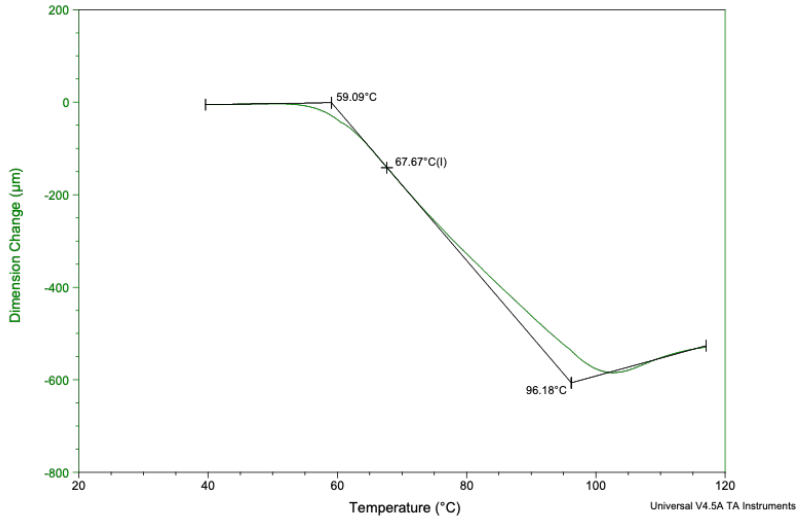

(e) EP-1

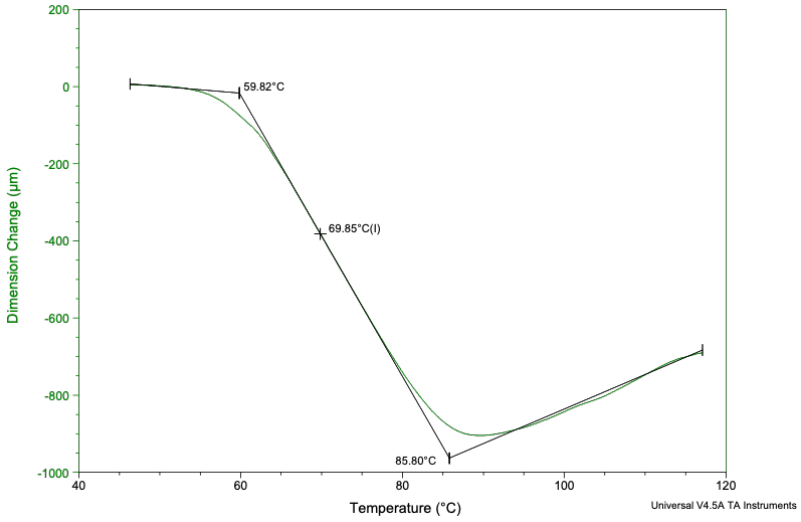

(f) EP-2

Figure A4. Glass transition Temperature of Epoxy/AC vitrimers

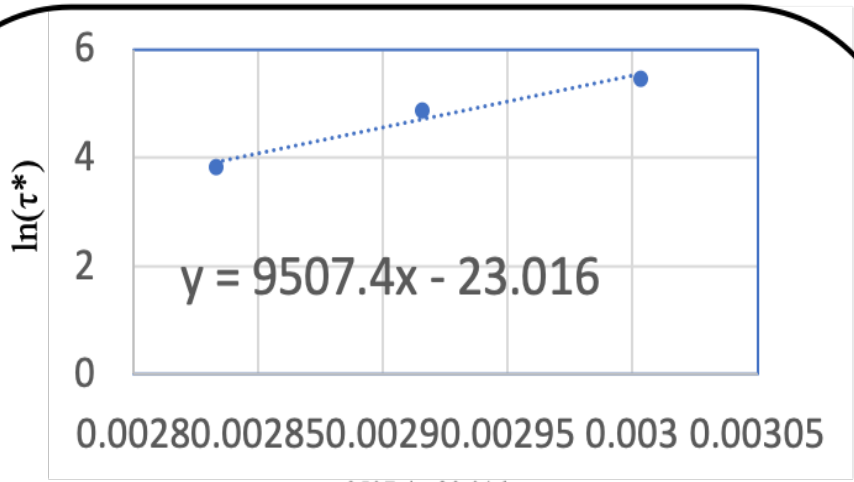

$y = 9507.4x - 23.016$

Which corresponds to : $\ln(\tau^*) = E_a/R\ (1/T) + \ln(\tau_0)$

$\ln(\tau^*) = 9507.4 * 1/T - 23.016$

$E_a/R = 9507.4$

$E_a = 9507.4 * 8.314 = 79$ kJ/mol

$\eta = G.\ \tau^*$

G- Shear viscosity modulus;

Relation between shear modulus and tensile modulus,

$G = E'/\ 2(1+\upsilon)$

Generally, υ- Poisson's ratio is 0.5 for rubbery materials.

So , $G=2705/3= 901.6$ MPa (or) $901.6*10^6$ Pa

$\tau^*= 10^{12}/(901.6*10^6) = 1109.1$ s.

$\ln(\tau^*) = \ln(1109.1) = 7.01$

Equation obtained from Arrhenius law: $\ln(\tau^*) = 9507.4x - 23.016$

$x=1/T= (\ln(\tau^*)+23.016)/9507.4 =0.00316$

So, $T= 1/0.00316$

T_v=316 K (or) 43^0C

Calculation A3. Epoxy/AC activation energy and topology freezing transition temperature

Balaji.K

EDUCATION

2015-2017	M.Tech in Polymer Science and Engineering, College of Engineering Guindy, Anna University, Tamilnadu
2010-2014	BE in Electrical and Electronics Engineering, PSNACET, Anna University, Tamilnadu

JOURNAL PUBLICATIONS

Articles

1. Balaji Krishnakumar, R. V. S. Prasanna Sanka, Wolfgang H. Binder, Vijay Parthasarthy, Sravendra Rana, * Niranjan Karak*. “Vitrimers: Associative Dynamic Covalent Adaptive Network in Thermoset Polymers”. Chem. Eng. J., 2019, 123820.

2. Balaji Krishnakumar, R. V. Siva Prasanna Sanka, Wolfgang H. Binder, Chanwook Park, Jiwon Jung, Vijay Parthasarthy, Sravendra Rana* and Gun Jin Yun*. “Catalyst free self-healable vitrimer/graphene oxide nanocomposites”. Compos. Part B Eng., 2019, 107647.

3. Sanka, RV Siva Prasanna, K. Balaji, Yves Leterrier, Shyam Pandey, Monika Srivastava, Anurag Srivastava, Wolfgang H. Binder, Sravendra Rana, and Véronique Michaud. "Nitrogen-doped graphene stabilized copper nanoparticles for Huisgen [3+ 2] cycloaddition “click” chemisty." Chemical Comm., 2019, 6249-6252.

4. Sanka RVS Prasanna, Balaji Krishnakumar, Yves Leterrier, Sravendra Rana* and Veronique Michaud*. “Soft Self-healing Nanocomposites: A Review”. Front. Mater. 2019, 6, 137.

5. Balaji Krishnakumar, S. Rana. “COVID 19 in INDIA: Strategies to combat from combination threat of life and livelihood,” J. Microbiol. Immunol. Infect., 2020.

6. Balaji Krishnakumar, B. K, M. Singh, V. Pathasarthy, C. Park, N.G. Sahoo,

G.J. Yun, S. Rana. “Disulfide Exchange Assisted Self-healing Epoxy/ PDMS/ Graphene Oxide Nanocomposites”, Nanoscale Adv., 2020.

7. Chanwook Park, Geonwoo Kim, Jiwon Jung, Balaji Krishnakumar, Sravendra Rana, and Gun Jin Yun. “Enhanced Self-Healing Performance of Graphene Oxide/Vitrimer Nanocomposites: A Molecular Dynamics Simulations Study”, polymer, 2020.

8. Debajyoti Bose, Mahula Santra, RV Siva Prasanna Sanka, Balaji Krishnakumar. “Bioremediation Analysis of s-MFCs for Energy Recovery from Microbial Activity in Soil”, International Journal of Energy Research, 2020.

9. Balaji Krishnakumar, Debajyoti Bose, Manjeet Singh, R. V. Siva Prasanna Sanka, Gurunadh Velidi, Shailey Singhal, Vijay Parthasarthy, Liberata Guadagno, Poornima Vijayan P, Sabu Thomas and Sravendra Rana. “Sugarcane bagasse derived activated carbon (AC)-epoxy vitrimer biocomposite: Thermomechanical and self-healing performance”. (Under Review: International Journal of Polymer Science; 2021)

Book Chapters

1. Prasanna, SRV Siva, K. Balaji, Shyam Pandey, and Sravendra Rana. "Metal Oxide Based Nanomaterials and Their Polymer Nanocomposites." In Nanomaterials and Polymer Nanocomposites, pp. 123-144. Elsevier, 2019.

Conference Publications

1. “International Conference on Nanotechnology: Ideas, Innovation & Initiatives-2017 (ICN:31-2017)”, being held at Indian Institute of Technology Roorkee (IITR) on December 06-08, 2017. “Click triggered self-healing graphene nano composites”, Sravendra Rana*, S. R. V. Siva Prasanna, Balaji K

2. “International Conference on Science and Engineering of Materials-ICSEM 2018” being held at Sharda University on January 06-08, 2018, as an Invited Speaker. “Carbon nanofillers based self-healing composite materials”, S. R. V. Siva Prasanna, Balaji K, Sravendra Rana*

3. “Third International Conference on Recent Advances in Material chemistry-ICRAMC 2019” being held at SRM Institute of Science and Technology with Alternative Energies and Atomic Energy Commission (CEA) on February 13-15, 2019. “Click Chemistry Promoted by Graphene Immobilized Copper Nano particles”, Balaji K, SRV Siva Prasanna, Sravendra Rana*.

4. “Sixth International Conference on Recent Advances in Composite Materials” being held at IIT Banaras on February 25-28, 2019. “Graphene reinforced self-repairing nanocomposites”, Balaji K, SRV Siva Prasanna, Sravendra Rana*.

5. “Second International Conference on Energy, Functional materials and Nanotechnology and Sustainable Environmental Management” being held at Kumaun University on May 24-26, 2019. “Room temperature self-healing composites for structural applications”, Sravendra Rana*, Balaji K, SRV Siva Prasanna.

6. “International Conference on Advances in Chemical Engineering (ADCHE-2020)” being held at UPES, Dehradun on 05-07-Feb, 2020. “Graphene based self-healing vitrimer nanocomposite”, Sravendra Rana*, Balaji K, Sanka, R.V.Siva Prassanna. (Best paper award).

7. “International Conference on Advances in Chemical Engineering (ADCHE-2020)” being held at UPES, Dehradun on 05-07-Feb, 2020. “Self-healing epoxy graphene oxide vitrimer nanocomposite with disulfide exchanges”, Balaji K, Sanka, R.V.Siva Prassanna, Vijay Parthasarthy, Sravendra Rana*.